

# eScholarship@UMassChan

## Mechanistic Role of the Calcium Channel TRPC6 in Driving Aggressive Traits in Triple-Negative Breast Cancer

Item Type	Doctoral Dissertation
Authors	Mukhopadhyay, Dimpi
DOI	<a href="https://doi.org/10.13028/704b-zp91">10.13028/704b-zp91</a>
Publisher	UMass Chan Medical School
Rights	Copyright © 2024 Dimpi Mukhopadhyay
Download date	2026-06-17 07:51:06
Item License	<a href="https://creativecommons.org/licenses/by/4.0/">https://creativecommons.org/licenses/by/4.0/</a>
Link to Item	<a href="https://hdl.handle.net/20.500.14038/53329">https://hdl.handle.net/20.500.14038/53329</a>

MECHANISTIC ROLE OF THE CALCIUM CHANNEL TRPC6 IN DRIVING  
AGGRESSIVE TRAITS IN TRIPLE-NEGATIVE BREAST CANCER

A Dissertation Presented

By

Dimpi Mukhopadhyay

Submitted to the Faculty of the

University of Massachusetts Graduate School of Biomedical Sciences, Worcester

in partial fulfillment of the requirements for the degree of

DOCTOR OF PHILOSOPHY

March 26<sup>th</sup>, 2024

(PhD, Cancer Biology)

MECHANISTIC ROLE OF THE CALCIUM CHANNEL TRPC6 IN DRIVING  
AGGRESSIVE TRAITS IN TRIPLE-NEGATIVE BREAST CANCER

A Dissertation Presented

By

Dimpi Mukhopadhyay

This work was undertaken in the Graduate School of Biomedical Sciences

(PhD, Cancer Biology)

Under the mentorship of

Arthur M. Mercurio, PhD, Thesis Advisor

Leslie Shaw, PhD, Chair of Committee

Dannel Mccollum, PhD, Member of Committee

Dohoon Kim, PhD, Member of Committee

Andreas Bergmann, PhD, Member of Committee

Xaralobos Varelas, PhD, External Member of Committee

Mary Ellen Lane, PhD,

Dean of the Graduate School of Biomedical Sciences

March 26<sup>th</sup>, 2024

## ACKNOWLEDGMENT

As I reflect on my PhD journey, I am truly grateful for the guidance and expertise of my thesis advisor, Dr. Arthur Mercurio. His support and the professional opportunities he offered, such as conference attendance and seminar participation, have been crucial in building my research skills and self-assurance. Dr. Mercurio's dedication to creating a supportive and collaborative lab environment that values both scientific excellence and a healthy dose of humor has made a positive impact on all of us in the lab. Thank you for your mentorship and the professional relationship we have developed. I want to specially thank Dr. Hira Lal Goel whose insights and meticulous attention to detail have significantly enhanced my research skills including manuscript preparation and presentations.

This thesis was completed with significant contributions from the Mercurio lab members. Their technical skills and support were crucial. The lab team collaborates effectively, sharing knowledge and investing in each other's work. I am grateful for the mentoring from post-doctoral scholars, especially Mandy Wang, and Caitlin Brown, who guided my initial work on ferroptosis. The graduate students are central to the lab's dynamic, consistently helping one another. I value the teamwork and assistance from my peers Emmet Karner, Ayush Kumar, Melanie Walker, and Ameer Elaimy, as well as the essential support from our lab technicians, John Amante, Peter Chhoy, Christi Wisniewski, and Choua Xiong. Choua Xiong made significant contributions to this thesis and her insights and attention to details in figure making for manuscript was indispensable. I am also thankful to have had the opportunity to work with Dr. Melanie Walker, who was always ready to engage in detailed discussions about my ideas and experiments over at the white board.

I express my sincere thanks to my TRAC and DEC members, especially to Dr. Leslie Shaw, my Chair, for the insightful conversations and unwavering support. A heartfelt thanks to Drs. Dannel McCollum, Dohoon Kim, Andreas Bergmann, and Yang Xiang for their invaluable feedback and for challenging me to excel. I am very grateful to all the members of my TRAC committee and my mentor for supporting me and sending letters of recommendation for my Post-Doc applications. I owe them my success in this process and hope to do justice to their confidence in me. I would also like to thank Dr. Jason Pitaressi who gave me valuable feedback during my thesis project and while writing the thesis manuscript. I am also grateful to Dr. Xaralabos Varelas for serving as the external examiner for my defense and for his thorough review of my dissertation.

My journey at the University of Massachusetts Medical School has been greatly enriched by the Department of Molecular, Cell and Cancer Biology and my peers, especially those

in the Shaw lab and my PhD cohort. My rotations during my first year has also made significant contributions towards my training as a scientist and experience of graduate school, especially my time in Guertin lab. I had the greatest opportunity to work with the Post-doctoral scholar Dr. Su Myung Jung who taught me experimental designing and stressed on being rigorous and have robust approaches.

I extend a heartfelt thank you to Tasfia Rakib, Mohona Gupta, Silviana Lee, Ceasar Bautista Sotelo, Mihir Doshi, Michael Lero, Claire Tocheny, Namgyu Lee, Khushali Gupta, and my PhD cohort for their assistance with research protocols, engaging in scientific discussions, and above all, for their valued friendship.

To my family, whose enduring love and support have been the bedrock of my aspirations—I am forever grateful. My parents, Bandana and Subrata Mukhopadhyay, have always supported me and urged me to pursue my true interests. To my brother Dr. Subhadeep Mukhopadhyay who has been my idol, inspiration and taught me the values of hard work and boundless dreaming. My friends who were my pillars of emotional support during this journey, Aritree Mitra, Anindita Chakraborty, Diya Dutta, Ayonika Mukherjee, Neha Manjari Akella, Caroline Rajiv, and Manasa Challa. A special mention to Dr. Neha Manjari Akella who, as my very first mentor, patiently taught me many valuable technical skills and prepared me for grad school. My time working with her in the Reginato lab in Drexel was instrumental in my interest to pursue a PhD.

Lastly, I owe deep thanks to my partner, Samyukta Ramnath, for her unwavering presence during both the best and toughest times of this journey including making the trip from Arizona to Worcester frequently. Her support has been a pillar of strength and patience, and I look forward to the future adventures with our dog, Mabel that we will share next in Boston.

## ABSTRACT

Despite advances in the diagnosis and therapy of breast cancer, issues continue to drive morbidity and mortality, especially tumor cells that persist after chemotherapy and contribute to recurrence and metastasis. The presence of such persister cells is particularly relevant for triple negative breast cancer (TNBC) because it harbors a relatively high frequency of cells with properties of cancer stem cells (CSCs) that resist standard-of-care therapies. My interest is understanding the nature of persister cells in TNBC and identifying novel mechanisms that contribute to persistence and stemness that can be exploited to improve therapy. In my first project, I identified a calcium channel TRPC6 that is enriched specifically in CSCs, including cells that are quiescent and persist after chemotherapy, and that has a causal role in promoting resistance. The mechanism by which it functions in this capacity involves its ability to regulate integrin  $\alpha 6$  mRNA splicing. Specifically, TRPC6-mediated  $\text{Ca}^{2+}$  entry represses the epithelial splicing factor epithelial splicing regulatory protein 1 (ESRP1), which enables expression of the integrin  $\alpha 6\text{B}$  splice variant. This integrin splice variant has been implicated in sustaining breast CSCs. TRPC6 and  $\alpha 6\text{B}$  function in tandem to facilitate stemness and persistence by activating TAZ and, consequently, repressing Myc. Therapeutic targeting of TRPC6 using a specific chemical inhibitor sensitizes TNBC cells, organoids, and patient-derived xenografts (PDX) to chemotherapy by impeding the splicing of  $\alpha 6$  integrin mRNA and inducing Myc. These data revealed a  $\text{Ca}^{2+}$ -dependent mechanism of chemotherapy-induced persistence, which is amenable to therapy, that involves integrin mRNA splicing.

In my second project, I extended my investigation of TRPC6 to cell metabolism based on my observation that TRPC6 inhibition sensitized TNBC cell lines and organoids to ferroptosis, a

form of cell death that involves iron-dependent lipid peroxidation of cell membranes. This observation piqued my interest because there is evidence that the ability to resist ferroptosis facilitates metastasis. In pursuit of the mechanism by which TRPC6 promotes ferroptosis resistance, I discovered that it maintains a level of reduced glutathione (GSH) that is sufficient to buffer oxidative stress. More specifically, I observed that the TRPC6-driven quiescent population has a low biosynthetic demand that enables GSH levels to be maintained by intracellular cysteine biosynthesis without relying on extracellular uptake through the xCT amino acid transporter. Based on these data, I propose that TRPC6 facilitates metastasis by enabling metastatic cells to resist ferroptosis.

In summary, this thesis details how a specific calcium channel (TRPC6) contributes to the function of persister/CSCs in TNBC to promote therapy resistance and metastasis, and that it can be targeted *in vivo* to improve the therapy of TNBC.

## Table of Contents

<b>CHAPTER I: INTRODUCTION .....</b>	<b>15</b>
<b>Overview.....</b>	<b>15</b>
<b>Breast cancer subtypes.....</b>	<b>16</b>
<b>Cancer stem cells.....</b>	<b>19</b>
<b>Triple Negative Breast Cancer and Cancer Stem Cell.....</b>	<b>22</b>
<b>Overview: Calcium signalling .....</b>	<b>22</b>
Calcium signaling in cancer .....	27
<b>Overview: Ferroptosis.....</b>	<b>29</b>
Ferroptosis in cancer .....	30
<b>Rationale for thesis work .....</b>	<b>32</b>
<b>CHAPTER II: <i>The Calcium Channel TRPC6 Promotes Chemotherapy-Induced Persistence by Regulating Integrin <math>\alpha 6</math> mRNA Splicing.....</i></b>	<b>34</b>
<b>Introduction.....</b>	<b>35</b>
<b>Results .....</b>	<b>36</b>
<b>Discussion .....</b>	<b>68</b>
<b>Materials and Methods .....</b>	<b>71</b>
<b>Chapter III: <i>Inducing ferroptosis to impede metastasis .....</i></b>	<b>85</b>
<b>Introduction.....</b>	<b>85</b>
<b>Results .....</b>	<b>87</b>
<b>Discussion .....</b>	<b>102</b>
<b>Materials and Methods .....</b>	<b>105</b>
<b>CHAPTER IV: DISCUSSION.....</b>	<b>108</b>
<b>Overview.....</b>	<b>108</b>
<b>TRPC6 and calcium signaling in breast cancer .....</b>	<b>110</b>
<b>Splicing: Developmental mechanism to generate transcriptomic heterogeneity .....</b>	<b>111</b>
<b>Therapy persister cells: Nature and Mechanisms.....</b>	<b>115</b>
<b>Metabolic adaptations during tumorigenesis.....</b>	<b>118</b>
<b>Oxidative stress and ROS: Is it good or bad for tumor progression? .....</b>	<b>124</b>
<b>Metastatic cascade and the metabolic challenges.....</b>	<b>125</b>
<b>Novel methods of targeting aggressive traits of breast cancer .....</b>	<b>126</b>

**Concluding Remarks.....130**  
***Bibliography ..... 148***

**LIST OF ABBREVIATIONS:****Table 1**

TNBC	Triple negative breast cancer
CSC	Cancer stem cell
ESRP1	Epithelial splicing regulatory protein 1
PDX	Patient derived xenograft
GSH	Glutathione
BCSC	Breast cancer stem cell
TLDU	Terminal ductal lobular units
HER2	Epidermal growth factor receptor 2
TRPC6	Transient receptor potential channel 6
ER	Estrogen receptor
PR	Progesterone receptor
IHC	Immunohistochemistry
BL1 and 2	Basal-like 1 and 2
IM	Immunomodulatory
M	Mesenchymal
MSL	Mesenchymal stem-like
LAR	Luminal androgen receptor
sc-RNA-Seq	Single cell-RNA Sequencing
MLCK	Myosin light chain kinase
CaMK	Calmodulin kinases
NCKX	Na <sup>+</sup> /Ca <sup>2+</sup> -K <sup>+</sup> exchangers
NCX	Na <sup>+</sup> /Ca <sup>2+</sup> exchangers
SERCA	Sarcoendoplasmic reticulum calcium atpase pump
TRP	Transient receptor potential
PLC	Phospholipase C

GPCR	G protein-coupled receptor
TKR	Tyrosine-kinase receptors
SOCE	Store-operated calcium entry
PMCA	Plasma membrane Ca <sup>2+</sup> atpase
NFAT	Nuclear factor of activated T cells
CREB	Camp Response Element-Binding Protein
SPCA2	Secretory Pathway Ca <sup>2+</sup> atpase
EMT	Epithelial to mesenchymal transition
CoQ	Coenzyme Q10
ROS	Reactive oxygen species
NRF2	Nuclear factor erythroid 2-related factor 2
FSP1	Ferroptosis suppressor protein
FACS	Fluorescence-activated cell sorting
PTX	Paclitaxel
KD	Knock-down
CaMKIV	Ca <sup>2+</sup> -calmodulin dependent kinase IV
GPX4	Glutathione peroxidase 4
IKE	Imidazole ketone erastin
Fer-1	Ferrostatin-1
BI	BI-749327
FM	Full media
FM-CM	Full media-Cystine free media
Cys-Free	Cystine free media
CBS	Cystathione betasynthetase
i.p	Intra-peritoneal
MUFA	Mono-unsaturated fatty acid
PUFA	Poly-unsaturated fatty acid

IVIS	In vivo imaging system
HCC	Hepatocellular carcinoma
LoF	Loss-of-Function
hnRNPs	Heterogeneous nuclear ribonucleoproteins
SF3B1	Splicing factor 3b subunit 1
SRSF1 and 2	Serine and arginine rich splicing factor 1 and 2
DVL2	Dishevelled segment polarity protein 2
RBFOX2	RNA binding fox-1 homolog 2
E/M	Epithelial/mesenchymal
PAD2	Protein arginine deiminase 2
ATAC-Seq	Assay for transposase-accessible chromatin with sequencing
TCA	Tricarboxylic acid
PPP	Pentose phosphate pathway
PI3K	Phosphatidylinositol 3-kinase
SREBP	Sterol regulatory element binding protein
MS	Mass spectrometry
NMR	Nuclear magnetic resonance
TXNs	Thioredoxins
CTCs	Circulating tumor cells
PMN	Pathologically activated Neutrophils (pmns)
MDSC	Myeloid-Derived Suppressor cells
PDO	Patient-derived organoids
TSS	Trans-sulfuration
CTH	Cystathionine gamma-lyase
GNMT	Glycine N-methyltransferase
SAH	S-adenosylhomocysteine
NSLC	Non-small cell lung cancer

CXCR4	C-X-C motif chemokine receptor 4
HBSS	Hanks' balanced salt solution
MFI	Mean fluorescence intensity
CXCL12	C-X-C chemokine ligand 12

**LIST OF FIGURES:**

- 2.1: TRPC6 is enriched in CSCs.
- 2.2: TRPC6 is enriched in TNBC CSCs and is sufficient to drive stemness
- 2.3: TRPC6 has a causal role in chemoresistance
- 2.4: TRPC6-mediated Ca<sup>2+</sup> entry represses the splicing protein ESRP1
- 2.5: Assessment of TRPC6, ESRP1 and  $\alpha 6$  integrin splice variant expression
- 2.6: ESRP1 suppression is key to maintaining self-renewal
- 2.7: TRPC6 maintains breast cancer stemness by enriching for  $\alpha 6B$  splice variant
- 2.8: TAZ/TEAD repress ESRP1 downstream of TRPC6
- 2.9: TRPC6-mediated Ca<sup>2+</sup> signaling activates RhoA and TAZ, which represses ESRP1
- 2.10: TRPC6-regulated  $\alpha 6$  integrin splicing sustains persister cells by repressing Myc
- 2.11: TRPC6 promotes quiescence
- 2.12: TRPC6-regulated  $\alpha 6$  integrin splicing contributes to Myc suppression
- 2.13: Summary schematic
- 3.1: TRPC6 inhibition sensitizes TNBC resistant populations to Ferroptosis
- 3.2: TRPC6 maintains a reduced environment that protects from Ferroptosis
- 3.3: Intracellular cysteine biosynthesis drives Ferroptosis resistance in persister cells
- 3.4: TRPC6 inhibition prevents metastatic colonization of breast cancer cells in the lungs

A.1: CXCR4 activates TRPC6-mediated calcium uptake

A.2: BCL11A regulates the expression of *TRPC6* in BCSCs

A.3: TRPC6 is enriched in a hybrid E/M population

A.4: TRPC6 expression in metastatic cell lines and clinical samples

## CHAPTER I: INTRODUCTION

### Overview

This thesis focuses on identifying novel drivers of therapy persistence in triple negative breast cancer (TNBC) and deciphering the mechanisms involved. I discovered that the calcium channel Transient Receptor Potential cation channel, subfamily C, member 6 (TRPC6) promotes stemness and treatment resistance in TNBC. TRPC6 regulates the self-renewal of Breast Cancer Stem Cells (BCSC) by suppressing Epithelial Splicing Regulatory Protein 1 (ESRP1) that sustains the integrin  $\alpha 6 \text{B}$  splice variant. I also investigated how TRPC6-mediated MYC suppression promotes a treatment persister cell state. Gene Set Enrichment Analysis (GSEA) of RNA-Seq data comparing cells in which TRPC6 had been inhibited to control cells revealed a transcriptomic signature for ferroptosis. This observation led me to investigate whether TRPC6 promotes resistance to ferroptosis in persister cells. Indeed, I provide strong evidence that inhibition of TRPC6 sensitizes treatment persister cells to ferroptosis. This finding has relevance to metastasis because metastatic cells need to acquire mechanisms to buffer the oxidative stress that could trigger ferroptosis. To this point, I demonstrated that inhibition of TRPC6 significantly reduced metastatic colonization in the lungs by a mechanism involving ferroptosis. Considering the limited therapeutic options for treating patients with TNBC, the data that I obtained in this thesis suggest that TRPC6 could be an effective therapeutic target for reducing metastatic burden in TNBC.

## Breast cancer subtypes

Breast cancer is a result of abnormal unregulated proliferation of the breast epithelial cells in the mammary gland. Statistically speaking breast cancer is the most common form of cancer amongst women worldwide accounting for about 2.3 million cases annually (1-3). The wide variety of cell types that constitute the mammary gland makes breast carcinomas complex specifically with respect to composition and tumor cell of origin. To get a better understanding of the disease, a lot of research has been directed towards classifying breast cancers. Initially there were two major schemes to classify breast carcinomas: histological and molecular (4, 5). Histological classification divides breast carcinomas into ductal and lobular carcinomas. Ductal carcinomas arise from the breast epithelial cells in the mammary duct. Lobular carcinomas are a result of oncogenic transformation of the epithelial cells in the terminal ductal lobular units (TLDU). Histological classifications provide information about the cellular state and type of carcinoma, but modern-day research has revealed a complexity far higher than that indicated by this classification. The molecular classification attempts to dig deeper than just cellular morphology and identity. As the name suggests, this classification is based on the genetic imprint of tumors that have been used to broadly classify breast carcinomas (6-8). The major molecular classification of breast carcinomas is based on the expression profile and status of the hormone receptors (Estrogen receptor, ER, and Progesterone receptor, PR) and the Epidermal growth factor receptor 2 (HER2) in the patient tumors (8). This information enables targeted therapies tailored for patients with specific receptor profile. The targeted therapy strategy involves anti-hormonal therapy (for ER/PR+ tumors) or anti-HER2 function blocking antibody. The subtype that does not express any of the hormone receptors i.e. Estrogen and Progesterone, or the HER2 receptor is classified as TNBC. This form of

classification has been informative in terms of biomarkers as well as identification of strategies for targeted therapies based on their respective gene expression profile (6, 7, 9, 10). However, despite these advancements in targeted therapy, breast cancers remain highly heterogeneous in terms of their clinical outcome as well as cellular identities.

Thus, beyond the receptor expression-based classification, a more comprehensive approach of classifying tumors based on their molecular signature was undertaken. The major aim was to be able to better predict prognosis of different subtypes as well as to identify groups that show poor clinical outcome. A pilot study using microarray analysis of gene expression patterns in 74 samples (including patient tumors and 8 normal breast tissue) laid the groundwork for classifying breast cancer based on their molecular signatures. Analysis from independent patient gene expression data sets revealed the following subtypes: Normal breast-like, Luminal A, Luminal B, HER2+, Claudin low, and Basal-like (6, 8). The most common form of breast tumors falls under Luminal A (ER high/HER2 low; ~40% of cases) and Luminal B (ER low/HER2 low; ~20% of cases). The HER2+ group encompasses those tumors that have an amplified HER2+ and the associated HER2 gene set that drives a highly proliferative phenotype. The claudin-low subtype accounts for a small fraction of tumors that have Epithelial to Mesenchymal-like gene expression patterns. The Basal-like tumors lack the expression of the hormone receptors as well as HER2. They are typically the most aggressive subtype with no targeted therapies available against them. The Basal-like tumors depict a basal/myoepithelial like gene signature. TNBCs fall under the Basal and Claudin-low subtypes. Most these studies employed immunohistochemistry (IHC) to classify TNBCs, which led to the identification of five distinct hierarchical clusters, where 91% (88 of 97) of the TNBCs were associated with the basal-like subtype (11-13). However, this study did not include molecular analysis of the tumors, and its conclusions were constrained to clinical outcomes derived from

pathological markers. Given TNBC's aggressive nature, there is a critical need for a deeper understanding of its molecular characteristics and the development of targeted treatments.

Addressing this gap, the groundbreaking work by Lehmann et. al. undertook the significant task of defining the molecular signatures of TNBC, classifying them into different clinically relevant subtypes (14). Their study analyzed gene expression profiles from 21 breast cancer datasets, identifying 587 TNBC cases and categorizing them into six distinct subtypes: two basal-like (BL1 and BL2), immunomodulatory (IM), mesenchymal (M), mesenchymal stem-like (MSL), and luminal androgen receptor (LAR).

**Basal-Like 1 (BL1) and Basal-Like 2 (BL2):** These subtypes are characterized by high expression of genes related to cell proliferation and DNA damage response. They show a higher pathological complete response (pCR) to taxane-based and radiation treatments, indicating their sensitivity to therapies targeting proliferative and DNA-damage response pathways.

**Immunomodulatory (IM):** The IM subtype is rich in immune cell signaling genes, including those associated with T-cell activation and antigen processing. This subtype's gene profile might include contributions from immune cell infiltrates, suggesting a significant role of the immune environment in this cancer type.

**Mesenchymal (M) and Mesenchymal Stem-like (MSL):** Both subtypes share pathways involved in epithelial-mesenchymal transition (EMT) and stem cell-like properties, showing higher expression of genes related to TGF- $\beta$ , mTOR, and Wnt/ $\beta$ -catenin signaling. The M subtype shows higher proliferation rates and a worse relapse-free survival (RFS), hinting at its aggressive nature.

**Luminal Androgen Receptor (LAR):** This subtype is defined by an androgen receptor (AR) gene signature and luminal cytokeratin expression. LAR tumors tend to have a higher RFS, potentially

due to less effective standard chemotherapy regimens. These tumors may arise from hormone-replacement therapy, and their molecular profile suggests sensitivity to AR-targeting therapies like bicalutamide and PI3K inhibitors.

The study's major conclusion is that the diversity in TNBC subtypes necessitates tailored therapeutic approaches based on distinct molecular characteristics. The identification of cell line models representing each TNBC subtype facilitates preclinical studies, provides a platform for testing pre-clinical therapies. The findings also emphasize the importance of further molecular characterization of TNBC to uncover new therapeutic targets and improve patient outcomes.

Despite advances in these molecular classifications, there is only a moderate improvement in the prognosis of TNBC (8, 15, 16). One of the primary causes is the lack of targeted therapies against TNBC and the lack of understanding of the intratumor cellular heterogeneity of TNBC that is a major driver of therapy resistance (17). Thus, it is imperative to uncover the mechanisms that directly contribute to cellular heterogeneity of TNBC to improve clinical efficacy.

To better understand such clonal diversity, we therefore need to discuss the cancer stem cell population and its role in tumor heterogeneity and therapy response.

### **Cancer stem cells**

It's important to note that breast cancer heterogeneity refers to both inter-patient and intra-tumor heterogeneity. Thus, several efforts have been made to understand the source of the heterogeneity and identify the cellular types and states within a tumor. The theory of CSC model was initially proposed to address and explain the presence of such hierarchical clonal populations of different cell states in breast tumors. Indeed, with modern sequencing techniques, specifically

the use of single cell RNA sequencing (sc-RNA-Seq) and pseudo time analyses, it is now established that breast tumors have a high degree of intratumor heterogeneity with clonal populations varying in their respective cell state, type, and function (18).

Like the name suggests, CSCs share similar characteristics to the normal stem cell, having the potential to differentiate into varied morphological and functional states. Besides that, CSCs can self-renew, which sustains tumor growth (19, 20). This highlights the underlying origin of the clonal populations with CSCs at the apex. Thus, one of the primary characteristics of the CSC population is the ability to initiate a tumor. Its role in tumor initiation is supported not only by biological xenograft experimental data but also by the computational data of patient tumors that indicate the presence of a naïve stem-like population. A pioneering study from Al-Hajj identified the CSC population in breast cancer, showing that the  $CD44^+/CD24^{-/low}$  has tumor initiating capacity and generates the heterogeneity of the primary tumor after transplantation into immunocompromised mice (21). This was followed by a huge breadth of work in breast cancer that identified several other cell surface markers to identify and isolate CSCs. However, there is some degree of discrepancy in the cell surface markers used to identify them, varying not only between the different molecular subtypes but also within each group (22). Therefore, the most widely accepted tests for CSCs rely on functional/phenotypic assays such as tumor initiation *in-vivo* and serial passage mammosphere assays *in-vitro* (23). Since this CSC population is responsible for replenishing and maintaining the stem cell pool, they have enhanced cell survival mechanisms specially under stressful conditions. These enhanced survival mechanisms improve their ability to resist therapeutic strategies such as Chemotherapy and Radiation and also promote metastasis (24, 25).

There has been a lot of effort in deciphering the origin of the cancer stem cell, specifically to understand what event leads to malignant transformation. There are two major hypotheses to explain the origin of the CSC. Recent sc-RNA-Seq and pseudo time experiments have been informative in that regard (18, 26). However, there is still not a clear consensus. Much of the evidence supports the hypothesis that oncogenic mutation in a mammary stem cell of origin confers tumorigenicity while retaining the ability to differentiate into luminal, alveolar, and basal progenitor cells (27, 28). In terms of cell surface markers, there is little similarity between mammary stem cells and the breast cancer stem cell population. On the other hand, the second hypothesis about CSC origin, suggests that CSCs can arise from fully differentiated or progenitor mammary cell populations. They propose that oncogenic transforming events including DNA-damaging agents such as chemo and radiation cause de-differentiation of these cells into more Stem-like state (29, 30). In fact, there is evidence that mutations and chemo can cause reprogramming of differentiated mammary cells into CSCs (31, 32). This theory explains a possible mechanism of CSC enrichment upon receiving chemotherapy. However, it is unclear whether that is due to the better survival mechanisms of CSCs than bulk tumor or due to the direct effect of the environmental stresses that can induce stem-like traits in a fully differentiated tumor cell.

The CSC population contributes directly to the prognosis and efficacy of the standard line of therapy. Hence it is essential to understand how it correlates with the different breast cancer subtypes. Clinically speaking, TNBC is quite aggressive, having a low level of differentiated cells and showing a far higher rate of therapy resistance than other subtypes. Thus, we need to understand the relationship between TNBC and the CSC population in that context.

## **Triple Negative Breast Cancer and Cancer Stem Cell**

I have discussed the contribution of the CSC population in determining hierarchical tumor lineage and state (differentiated vs undifferentiated) and specifically therapy response. It is important to incorporate that with the molecular breast tumor subtypes to specifically design effective therapy that has the potential for better clinical outcomes. In that regard, clinical studies of different cohorts of breast cancer patients from around the world have been instrumental. Besides xenograft and cell line experiments, this patient data from different breast cancer subtypes has established that breast cancer stem cell frequency varies amongst the different subtypes, and they are most frequently found in TNBC samples (33). This discovery was supported by data from several groups that associated the TNBC aggressive traits (such as chemoresistance and recurrence) to the CSC population that it harbors (16, 34).

Thus, beyond this correlative evidence we need to identify causal drivers of CSC to improve the prognosis of TNBC. This sheds light on the need to uncover and identify the signaling pathways that enrich and sustain the CSC population. Insight into these pathways will help us identify targets that can potentially be therapeutically exploited to improve progression-free survival and patient outcome. In that context I will discuss calcium signaling which not only plays a pivotal role in driving several cellular processes but most importantly also sustains CSC population as will be described in this thesis.

### **Overview: Calcium signalling**

At the core of almost every aspect of cellular life lies calcium ions. A fundamental aspect of higher organisms is the ability to sense changes in the environment and be able to adapt or respond to the

demands of the cellular processes by signalling. Signalling relies on messengers and calcium and phosphate ions have become the key messenger molecules of cellular life on earth (35). The crux of calcium ion mediated signalling is to alter local electrostatic charge on proteins by adding positive charge, which changes their conformation, and that has various functional consequences. Mammalian cells invest a considerable amount of cellular energy to maintain a gradient of calcium (~20,000 fold) across the plasma membrane. The chemistry of calcium ions does not allow them to be modified, so the cell keeps a tight regulation of intracellular calcium by chelating, compartmentalizing, or expelling it. These functions are carried out by proteins that bind to calcium with a wide range of affinity. These protein-calcium binding interactions are primarily exploited to buffer the concentration in the cell but are also used to signal cellular processes. The mobility and speed of calcium trafficking, along with the affinity of the binding proteins, allows for swift and reversible signalling pathways that lie at the heart of ideal cell functioning and developmental processes. Introduction to the essential role of calcium and calcium-mediated cellular signalling warrants a discussion about different classes of calcium-binding proteins, transporters, and channels.

**Calmodulin:** One of the most ancient proteins is calmodulin that binds to calcium with a high affinity. Upon binding to calcium, there is a conformational change in the calmodulin domains, resulting in the release of protein autoinhibition, dimerization or active site remodel (36). The cell has over hundreds of proteins with a domain for recruitment of calmodulin (36-38). By interacting and binding to downstream target proteins (such as Myosin light chain kinase, or MLCK), Calmodulin transduces the calcium-mediated signal. Calmodulin also binds to a family of protein kinases called Calmodulin kinases (CaMK), enabling calcium to activate phosphorylation

pathways. Besides calcium-binding proteins, another key component are proteins involved in calcium trafficking (such as pumps and channels) into and out of cell and organelles.

**Pumps:** This is an important class of proteins that move calcium against the gradient. These are typically ATPase pumps, also known as Sarcoendoplasmic reticulum calcium ATPase pump, (SERCA) that, as the name suggests, hydrolyze ATP to aid in the uphill calcium movement in exchange for two protons. Another class of similar pumps are the  $\text{Na}^+/\text{Ca}^{2+}$  exchangers (NCX, or SLC8A1-3), and the  $\text{Na}^+/\text{Ca}^{2+}-\text{K}^+$  exchangers (NCKX; SLC24A1-5) that have a slightly different mechanism. Again, to maintain a low cytoplasmic calcium concentration, they move calcium out of the cell in exchange for three  $\text{Na}^+$  ions or even transport calcium along with one  $\text{K}^+$  ion for the exchange of four  $\text{Na}^+$  ions. These pumps are majorly responsible for generation of neuronal action potentials (39).

**Channels:** There are two major classes of calcium channels: voltage-gated channels and Transient Receptor Potential (TRP) channels.

**Voltage gated channels** could move over a million  $\text{Ca}^{2+}$  ions across the channel down the gradient. This makes them likely the fastest in calcium conductance. The pore in the channel has a considerably high affinity for calcium, which makes them selective towards calcium (40). However, that selectivity is context dependent - in normal extracellular media or conditions, voltage-gated channels are only selective towards calcium, but upon removal of extracellular calcium they become non-selective, allowing the passage of  $\text{Na}^+$  and  $\text{K}^+$ .

**Transient Receptor Potential (TRP) channels** are only slightly sensitive to voltage and display non-selectivity for ions. The TRP channels are formed by tetramerization around the pore that then allows the passage of ions. The majority of them (~28 of the mammalian TRP family members)

are plasma membrane channels. Now, the central question has been how TRP channels get activated. The major mechanism involves phospholipase C (PLC) activation by G protein-coupled receptor (GPCR) or tyrosine-kinase receptors (TKR) (41). Given their rapid response to changes in the extracellular environment such as pH, temperature, stress and even volatile compounds, there is speculation that this might not be the complete picture and there might be additional mechanisms of activating TRP channels *in-vivo*. Certain studies have also alluded to a non-canonical role of TRP channels as being mediators of Store-operated calcium entry (SOCE). This function widens the role of TRP channels in cellular processes which were strictly considered in the context of neuronal cells.

**Store-Operated Calcium entry (SOCE):** The cell has a calcium reservoir in the endoplasmic reticulum (ER) which constantly seeps into the cytosol. However, low calcium conditions could cause the ER calcium reservoir to move more rapidly into the cytosol through SERCA and plasma membrane  $\text{Ca}^{2+}$  ATPase (PMCA) pumps (42, 43). This leakage would result in the depletion of calcium in the stores (ER), and the phenomenon of calcium entry activation to replenish these stores is referred to as SOCE (43). In certain cases, TRP channels have been shown to replenish the ER-calcium stores by binding to certain channels on the ER (Stim and Orai) (44). This binding allows them to directly move the calcium ions taken up by the channel to replenish the ER. Thus, these are the major backbone for calcium carrier in and out of the cell as well as between the intracellular stores. The downstream effects of these calcium movements generate temporal and spatial calcium oscillations that directly impact measurable and observable features such as contraction, motility, and secretion (45, 46). Beyond these cell biological changes, calcium dynamics directly impact gene expression changes through certain transcription factors such as, nuclear factor of activated T cells (NFAT), and cAMP Response Element-Binding Protein (CREB)

(47, 48). Calcineurin is a phosphatase which when activated dephosphorylates NFAT, revealing its nuclear localization signal. Once imported into the nucleus, NFAT activates its target genes such as chemokines in lymphocytes (49). These gene expression changes allow the calcium signals to create both short and long-term effects downstream. As discussed, calcium is tightly regulated within membrane bound organelles and can bind to over hundreds of proteins and alter their localization, function, and activation state. Thus, it is not hard to appreciate that calcium signalling impacts every cellular process. This field is ever evolving, consisting of unique mechanisms of calcium buffering and storage. It particularly interests me how calcium signalling pathways functionally affect tumor traits.

## Calcium signaling in cancer

Research over the past two decades has highlighted the importance of  $\text{Ca}^{2+}$  sensitive oncogenic pathways in tumour progression. Most of these studies focused on three main themes: 1. Altered expression of calcium channels in tumour tissues; 2. Differential regulation of calcium influx and efflux proteins (by means of activation and translocation) 3. Downstream effects of altered calcium signalling in terms of tumour phenotypes such as proliferation, migration, invasion, and metastasis.

Several groups have reported altered expression of calcium channels during early tumorigenesis such as SERCA3 downregulation during colon carcinogenesis (50) and elevated expression of TRPM8 in multiple cancers (prostate, breast, colon, pancreas, and lung) (51-53). There are also incidences where more than one channel is deregulated in tumors such as TRPM8 and TRPV6 in prostate cancer (54). These discoveries provided this correlative information which then brought up a central question as to what oncogenic pathways are being driven by these altered protein and expression changes of calcium channels. The other ways of impacting cellular processes besides altered expression are to alter activity or localization. In one such instance ORAI1 mediated translocation of TRPV6 plasma membrane localization has been shown to increase prostate cancer cell proliferation (55). Another study observed a different mechanism of TRPM7 activation, involving cleavage of TRPM7 which exposes the kinase domain that can cause gene expression changes through remodeling of the chromatin (56). The above studies expanded on novel alternate ways of deregulating calcium signalling in cancer cells besides altered expression levels of the proteins. Hence it became crucial to understand the downstream effects of altered calcium protein activation/expression. Though not all deregulated pathways have causal roles, initial pharmacological and siRNA mediated inhibitions hint that calcium channels are

promoting different tumor phenotypes such as proliferation, adhesion, survival, migration and, in some cases, survival under stressful conditions (57-69). In oesophageal squamous cell carcinoma, ORAI1 elevation promotes proliferation and supports tumor growth (70) and Secretory Pathway  $\text{Ca}^{2+}$  ATPase (SPCA2) overexpression has been shown to attribute transforming capacities (growth in soft agar) to non-malignant MCF10A (71). We appreciate that calcium is a key messenger molecule that impacts almost all cellular processes. Indeed, there is considerable evidence of how calcium signalling can sense and help cancer cells respond to changes in the microenvironment and in turn play a causal role in effecting phenotypes such as angiogenesis, Epithelial to mesenchymal transition (EMT), and survival in stressful conditions (such as Hypoxia). It is well established how certain factors such as EGF, Transforming growth factor-beta ( $\text{TGF}\beta$ ), and Hypoxia drive EMT in tumors (72-75). Now, there are studies that have shown that calcium signalling has a central role in the induction of EMT and is differentially regulated in epithelial vs mesenchymal cells (46, 76-79). In MDA-MB-468 cells, TRPC1 and ORAI1 differentially contribute to EMT. These studies expand our understanding of the scope of calcium signalling in cancer (78).

These studies have cemented the concept that spatial and temporal regulation of calcium is exploited to induce specific oncogenic pathways. However, the potential of targeting calcium-sensitive pathways remains largely unexplored due to limited mechanistic understanding.

## Overview: Ferroptosis

Cell death is an inevitable and necessary process for the development of multicellular organisms. Deregulation of this process is seen in a large number of diseases (80). The prevailing belief until the late 1950s was that cell death occurred in an unregulated fashion. However, the concept of programmed cell death, introduced by Kerr et al., catalyzed a paradigm shift and charted a new course for scientific inquiry. The seminal work of Kerr and colleagues not only identified apoptosis but also delineated its cell biological characteristics, thereby paving the way for subsequent research (81). Research in this area progressed as Hengartner et. al., identified important molecules involved in apoptosis using the model organisms *Caenorhabditis elegans* and *Drosophila melanogaster* (82). Their work explained the unique molecular processes that control cell death. Ferroptosis was only recently discovered about 12 years ago (80). It is a form of cell death that is caused primarily due to the accumulation of an overwhelming amount of membrane phospholipid peroxidation and the biochemical reaction (Fenton reaction) requires iron. A small molecule screen gave insight into the primary mechanism of Ferroptosis. They discovered that inhibition of an antioxidant enzyme Glutathione peroxidase 4 (GPX4) causes a lethal level of accumulation of lipid peroxides (83). GPX4 is the central hub of neutralization of the peroxy radicals. After the initial discovery of Ferroptosis, there was a huge interest in understanding the regulatory mechanisms of ferroptosis. In simplistic view there are three arms of ferroptosis regulation, 1) Iron availability: Since the Fenton reaction requires iron hence cellular processes that affect iron chelation, import, storage, and efflux influence ferroptosis (84). 2) Lipid and specifically lipid species in the membrane: The substrate for peroxidation is Poly-unsaturated fatty acids (PUFAs) and hence mechanisms that enrich for Mono-unsaturated fatty acids (MUFAs) can prevent ferroptosis and vice-versa (85, 86); 3) Amino-acid metabolism: Cysteine metabolism in the cell generates the

primary cellular antioxidant glutathione (GSH) which is also the substrate for GPX4 to remove peroxyl ions from the membrane phospholipids (87). Extensive research over the past 12 years have identified several key proteins that in turn impact either one or more of the above three factors and promote either sensitivity or resistance to ferroptosis. For e.g., Brown. *et. al* showed that Prominin2 (Prom-2) mediated iron transport out of the cell is hijacked to maintain ferroptosis resistance in normal and certain cancer cells. Another pioneering discovery was that of Ferroptosis suppressor protein 1 (FSP1) (88) which is another antioxidant enzyme that reduces Coenzyme Q10 (CoQ) to neutralize membrane lipid peroxidation. Xuejun Jiang's group pointed out that the enzyme ASCL4 can introduce poly-unsaturated fatty acids into the membrane making cells more sensitive to ferroptosis (85, 89).

Thus, overall, this metabolic form of cell death has opened a very critical question as to whether it is relevant in diseases and if so, how can we better understand the mechanistic regulation to target it.

### **Ferroptosis in cancer**

As mentioned above ferroptosis is a tightly regulated metabolic cell death and several studies have established the role of redox homeostasis, iron handling, mitochondrial activity and metabolism of amino acids, lipids which also play a central role in disease biology. As we uncover more and more mechanistic details of ferroptosis and gain insight into the regulators, it has become increasingly relevant to look at its role in the pathological disease setting. There has been mounting evidence that ferroptosis is indeed tumor suppressive. In fact, there are now studies from different groups that have shown the metabolic basis of p53's tumor suppression function is ferroptosis mediated

(90). One such mechanism was demonstrated using the p53 acetylation defective mutant. This has a loss of function phenotype losing the ability to cause cell cycle arrest, senescence, and apoptosis but retains the ability of tumor suppression *in-vivo*. They showed that the ability of tumor suppression was due to ferroptosis, which was metabolically regulated by p53-mediated suppression of the cysteine glutamate transporter, SLC7A11 (xCT) (91). However further loss of the acetylation site of p53 led to a complete loss of tumor suppression as well as ferroptosis regulation (92).

Cancer cells proliferate quickly, but this rapid growth comes with the downside of increased reactive oxygen species (ROS) production (93-97). These ROS are mainly responsible for damaging cell membranes through lipid peroxidation (98-100). In contrast, normal cells regulate their growth and maintain a balance, preventing excessive ROS buildup and making them less susceptible to ferroptosis. Therefore, there's a significant interest in targeting this vulnerability to selectively induce death in cancer cells.

Further investigation into the susceptibility of cancer cells to ferroptosis reveals some cancer cells have evolved a variety of strategies to mitigate the effects of ferroptosis. These strategies involve alterations in lipid composition, such as increases in monounsaturated fatty acids (MUFAs), as well as the enhancement of antioxidant defenses through pathways involving proteins like ferroptosis suppressor protein (FSP1), nuclear factor erythroid 2-related factor 2 (NRF2), and xCT (88, 101-108). These adaptive mechanisms indicate the complexity of targeting ferroptosis in cancer therapy and underscore the need for a nuanced approach when considering this strategy for clinical applications.

## **Rationale for thesis work**

There is ample evidence from experimental as well as computational patient data that breast tumor heterogeneity is a hurdle towards therapeutic efficacy and overall progression free survival. Indeed, TNBC affects ~42,000 women per year, is associated with 37% of patients dying within 5 years, and results in a median survival of 9 months after recurrence (1). Thus, there is an urgent need to understand the nature of TNBC heterogeneity in more detail, especially its resistance to most current therapies and to develop novel strategies for diminishing the morbid statistics associated with it. The overarching goal of my thesis has been to identify novel proteins that have causal roles in regulating tumor heterogeneity and sustaining CSC population. People have adopted different strategies to obtain insight into the cellular identity of such populations. These studies have contributed to the discovery of novel biomarkers for CSCs in the respective tumor subtypes. On the other hand, research is also directed at identifying signaling pathways that are sustaining this population. In that context, particular studies of interest that have identified roles for calcium signaling in promoting tumorigenic traits (proliferation, adhesion, migration, and invasion) are particularly relevant for the findings in this thesis (109, 110). There is a lot of correlative evidence indicating the central role of calcium signaling in promoting tumorigenesis, but we do not have much mechanistic insight into the functional roles in tumorigenicity.

In this thesis, an unbiased approach of RNA-sequencing using a BCSC enriched model revealed that a calcium channel TRPC6 is significantly upregulated in the CSCs. Given the role of calcium signaling in promoting specific oncogenic functions, my overall goal was to first identify the causal role of TRPC6 in cancer and in the context of CSC function. Since CSCs are implicated in chemotherapy resistance, I investigated the role of TRPC6's role in therapy response. But most importantly, in this thesis my major goal was to also understand how TRPC6 promotes aggressive

traits in breast cancer. Here, I detail the mechanisms by which TRPC6-mediated calcium signaling sustains therapy persister cells. The mechanisms that promote quiescent treatment persister cells, also inform us about their unique metabolic nature. These data give us further insight into novel ways of designing effective therapies against such aggressive populations.

## CHAPTER II: The Calcium Channel TRPC6 Promotes Chemotherapy-Induced Persistence by Regulating Integrin $\alpha 6$ mRNA Splicing

This work was originally published in *Cell Reports*.

**Authors:** Dimpi Mukhopadhyay<sup>1</sup>, Hira Lal Goel<sup>1</sup>, Choua Xiong<sup>1</sup>, Shivam Goel<sup>1</sup>, Ayush Kumar<sup>1</sup>, Rui Li<sup>1</sup>, Lihua Julie Zhu<sup>1</sup>, Jennifer L. Clark<sup>2</sup>, Michael A. Brehm<sup>3</sup>, Arthur M. Mercurio<sup>1\*</sup>

### **Affiliations**

<sup>1</sup>Department of Molecular, Cell and Cancer Biology, <sup>2</sup>Department of Pathology, and <sup>3</sup>Molecular Medicine, University of Massachusetts Chan Medical School, Worcester, Massachusetts, USA 01605

\*Corresponding author

### **CONTRIBUTIONS:**

Dimpi Mukhopadhyay conceptualized the study, performed experiments, and wrote the manuscript. Hira Goel, Shivam Goel also performed experiments. Choua Xiong performed certain gene expression experiments and also made the figures. Ayush Kumar generated the ITGA6 knock-out cell line. Jennifer Clark provided the breast cancer subtype patient slides for staining. Rui Li and Lihua Julie Zhu performed bioinformatics analyses. Michael Brehm maintained the PDX models in humanized mouse models. Hira Lal Goel provided feedback on data. Arthur M. Mercurio oversaw and conceptualized the study, provided feedback on experiments and the manuscript.

## Introduction

Understanding the mechanisms that contribute to intratumor heterogeneity is a challenging biological problem and a key factor in therapy resistance. In this context, cancer stem cells (CSCs) have an essential role because of their ability to differentiate into various morphological and functional cancer cell states and, importantly, their resistance to therapy (111). However, the plasticity of CSCs is a complicated process that involves regulation by the tumor microenvironment and intrinsic metabolic alterations (112, 113). To understand intratumor heterogeneity better and develop strategies to overcome treatment resistance, it is necessary to investigate the mechanisms that sustain CSCs further and exploit them to improve therapy.

The importance of investigating the contribution of CSCs to intratumor heterogeneity and therapy resistance is exemplified by triple-negative breast cancer (TNBC) because it is characterized by extensive intratumor heterogeneity (17), a high frequency of CSCs compared to other breast cancer subtypes (33) and resistance to standard chemotherapy. Thus, there is an urgent need to understand the nature of TNBC heterogeneity in more detail, especially its resistance to most current therapies and to develop novel strategies for diminishing the morbid statistics associated with it. One approach to this problem involves investigating mechanisms that distinguish the function of CSCs from other populations, especially in the context of therapy resistance. Our unbiased approach to this problem revealed the potential contribution of calcium channels to the biology of CSCs. This observation piqued our interest because their contribution to TNBC and other cancers merits further investigation for several reasons. Calcium signaling is fundamental to cell proliferation, migration, invasion, and survival (35), processes that underlie tumor progression. Numerous studies have highlighted the importance of calcium signaling in the

behavior of tumor cells and their response to chemotherapy. More specifically, calcium signaling has been shown to maintain a partial/hybrid epithelial-to-mesenchymal transition (EMT) state (114), which is associated with stemness in many cancer models. Another significant finding is that chemotherapy can induce an increase in intracellular  $\text{Ca}^{2+}$  that causes enrichment of breast CSCs (66). Although these and many other studies have highlighted the importance of calcium channels and calcium signaling in cancer, much less is known regarding the contribution of specific calcium channels to sustaining CSC sub-populations present in heterogeneous tumors and about how such channels impact CSC functions, especially the response to therapy (64, 115-118).

In this study, we report that transient receptor potential channel 6 (TRPC6) expression, a non-selective cation channel that mediates calcium entry in TNBC (119), marks CSCs in TNBC and that its calcium signaling function has a causal role in maintaining stemness and chemoresistance. We also demonstrate that TRPC6 contributes to these functions by regulating mRNA splicing, especially the splicing of the  $\alpha 6$  integrin mRNA that contributes to CSC function. Tumor cells that persist after chemotherapy are dependent on TRPC6 and a splice variant of the  $\alpha 6$  integrin. Therapeutic targeting of TRPC6 blocks this splicing mechanism and sensitizes TNBC to chemotherapy.

## Results

**TRPC6 is associated with CSCs in TNBC and has a causal role in stemness:** Initially, we analyzed our previously published RNA-seq data that compared the transcriptomes of immortalized mammary epithelial cells (S1 cells) to their transformed counterparts, which are enriched in CSCs (120). Analysis of these data revealed that the expression of *TRPC6* (transient receptor potential cation channel, subfamily C, member 6), is significantly increased in the

transformed compared to the immortalized population (**Fig. 2.1A**). The RNA-seq data were verified by qPCR to quantify the expression of several calcium channels known to promote tumorigenic pathways including *ORAI-1* (121), *ORAI-3* (121), *TRPC6* (122), *TRPV6* (65), and *TRPM8* (123, 124) (**Fig. 2.1B**). To assess whether the expression of *TRPC6* is associated with TNBC compared to other subtypes of breast cancer, we performed qPCR on patient-derived organoids (PDO) and observed that its expression is higher in TNBC relative to ER<sup>+</sup> organoids (**Fig. 2.2A**). We also found that *TRPC6* is expressed substantially more in TNBC than in non-TNBC (ER<sup>+</sup>) tumor specimens (**Fig. 2.2B**)

We extended our initial findings on *TRPC6* to other CSC models. TE3 cells are a variant of MDA-MB-231 cells that were selected for their tumor initiation capacity (125), and we observed that *TRPC6* expression is significantly higher in TE3 cells than in MDA-MB-231 cells (**Fig. 2.1C**). We also investigated *TRPC6* expression in Ras-transformed, human mammary luminal cells (HMLER)(126), which contain a CD104<sup>low</sup>/CD24<sup>low</sup> sub-population (HMLER<sup>-/-</sup>) that is enriched in stem cell properties (120) and observed that the expression of *TRPC6* in the CSC (HMLER<sup>-/-</sup>) fraction is significantly higher than in the non-CSC subpopulation (CD104<sup>high</sup>/CD24<sup>high</sup> or HMLER<sup>+/+</sup>) (**Fig. 2.1D**). We also isolated a CSC population (CD44<sup>high</sup>/CD24<sup>low</sup>) from a TNBC patient-derived xenograft (PDX) and found that *TRPC6* expression is associated with the CSC population compared to the non-CSC population (CD44<sup>low</sup>/CD24<sup>high</sup>) (**Fig. 2.1E**). Thus, *TRPC6* expression is a marker of CSCS in multiple models.

Given that *TRPC6* is a cell surface protein, we postulated that it could be used as a marker to enrich CSCs from heterogeneous tumor cell populations. To test this possibility, we used HCC1806 cells, a heterogeneous TNBC cell line that contains CSC and non-CSC populations based on our previous studies (127). Two distinct populations of *TRPC6*<sup>high</sup> and *TRPC6*<sup>low</sup> cells

(**Fig. 2.2D**) were identified by fluorescence-activated cell sorting (FACS), and we found that the TRPC6<sup>high</sup> population harbors a significantly higher frequency of CSCs than the TRPC6<sup>low</sup> population (**Fig. 2.2E**).

To investigate a causal role for TRPC6 in stemness, we used shRNAs to knockdown its expression in TE3 and CAL-51 cells (**Fig. 2.2A**) and observed a significant decrease in self-renewal as assayed by serial mammosphere formation (**Fig. 2.1F, G**). To substantiate these results, we re-expressed either wild-type TRPC6 or a pore mutant TRPC6<sup>G757D</sup> (mut TRPC6) (**Fig. 2.2B**) that is defective in calcium uptake (128). Consistent with our hypothesis that TRPC6-mediated calcium signaling sustains a CSC state, wild-type TRPC6, but not the pore mutant, rescued serial mammosphere formation (**Fig. 2.1F, G**). We substantiated these findings using the TRPC6-specific inhibitor BI-749327 (129) and observed that the inhibitor treated cells formed significantly fewer mammospheres compared to control cells (**Fig. 2.2H, I**). We also treated the TRPC6<sup>high</sup> CSC population sorted from HCC1806 cells with either DMSO or BI-749327 and observed a significant decrease in mammosphere formation ability upon channel inhibition (**Fig. 2.1F**). Importantly, expression of WT TRPC6 but not the pore mutant (**Fig. 2.2G**) increased mammosphere formation in the TRPC6<sup>low</sup> population of HCC1806 cells providing evidence that TRPC6 is sufficient to drive stemness (**Fig. 2.2F**). Subsequently, an *in vivo* assay was done to assess the contribution of TRPC6 to tumor initiation using extreme limiting dilution analysis (ELDA) (130). The data obtained revealed that loss of TRPC6 caused a significant reduction in the frequency of CSCs (**Fig. 2.1H**). We investigated the role of TRPC6 in facilitating tumor onset *in vivo* by xenograft implantation of TRPC6 shRNA knockdown CAL-51 cells that had been rescued with either WT or pore mutant TRPC6. A significant delay in tumor onset was observed in the TRPC6 knockdown cells compared

to control cells, which was rescued by the WT TRPC6 but not the pore mutant TRPC6<sup>G757D</sup> (**Fig. 2.11**). Together, these data implicate a causal role for TRPC6 in stemness.

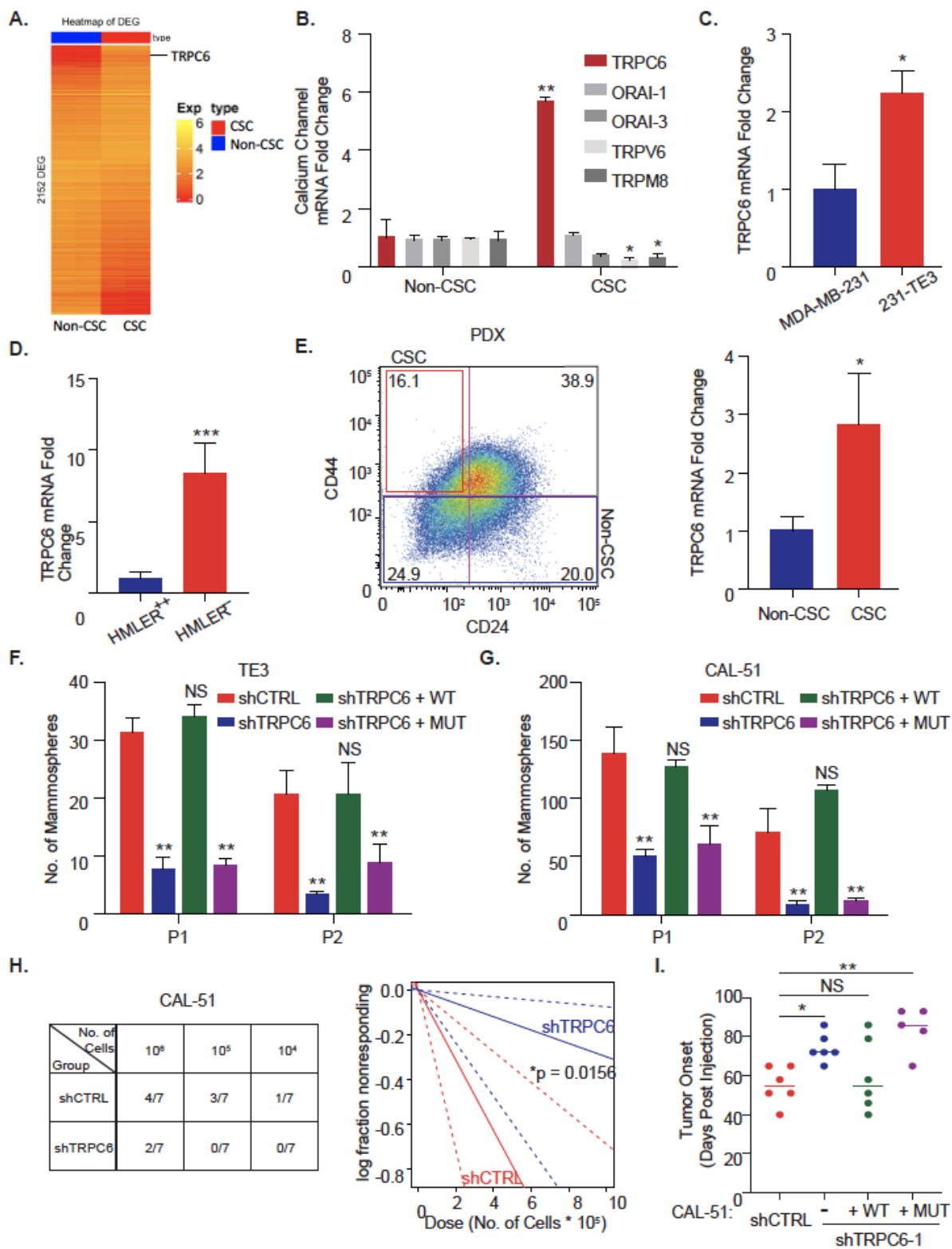


**Fig. 2.1. TRPC6 is enriched in CSCs.** **A.** Heatmap of differentially expressed genes in the CSC and non-CSC populations from a published model system (14). TRPC6 is highlighted in the heatmap. FDR < 0.05 and  $|\log_2\text{FC}| > 1$ . **B.** Expression of TRPC6 and other calcium channels was compared in the same CSC vs non-CSC populations by qPCR. **C.** *TRPC6* expression was compared in MDA-MB-231 cells and their TE3 variant. **D.** HMLER cells were sorted into CD104<sup>-</sup>/CD24<sup>-</sup> (CSC; HMLER<sup>-/-</sup>) and CD104<sup>+</sup>/CD24<sup>+</sup> (Non-CSC; HMLER<sup>+/+</sup>) populations and *TRPC6* expression was quantified by qPCR. **E.** The CSC (CD44<sup>high</sup>/CD24<sup>low</sup>) and non-CSC (CD44<sup>low</sup>/CD24<sup>high</sup>) populations was sorted from a TNBC PDX (left panel) and *TRPC6* expression levels measured was quantified by qPCR. **F, G.** TRPC6 expression was knocked down in either TE3 (**F**) or CAL-51 (**G**) cells using shRNA and expression was rescued with either a wild-type TRPC6 construct (WT) or a pore mutant (G757D) that is deficient in calcium uptake (MUT). These populations were assessed for self-renewal by serial passage of mammospheres (P1- passage 1; P2- passage 2). **H.** CAL-51 control shRNA (shCtrl) or TRPC6 knockdown (shTRPC6) cells were injected into the mammary fat pads of NSG mice in limiting dilution (10<sup>6</sup>, 10<sup>5</sup>, and 10<sup>4</sup> cells) and the frequency of tumor incidence was determined (right panel). Tumor incidence was plotted utilizing ELDA in a log-plot to estimate the frequency of tumor initiating cells in each group. **I.** CAL-51 cells (shCtrl, shTRPC6-1, sh+ WT TRPC6, and sh+ mut TRPC6) were injected into the mammary fat pads of NSG mice and tumor onset in terms of days post injection was compared amongst the groups. The TRPC6 expression data shown in (C) and (D) represent the mean  $\pm$  SD of a representative experiment performed three times independently. The mammosphere data shown represent the mean  $\pm$  SD of three times independently. For (H) data are presented as a log-log plot, and the frequency of tumor initiating cells is calculated by extreme limiting-dilution analysis. The tumor onset data represents the median days post-injection between the groups. \*P < 0.05, \*\*P < 0.01, \*\*\*P < 0.001, and \*\*\*\*P < 0.0001.

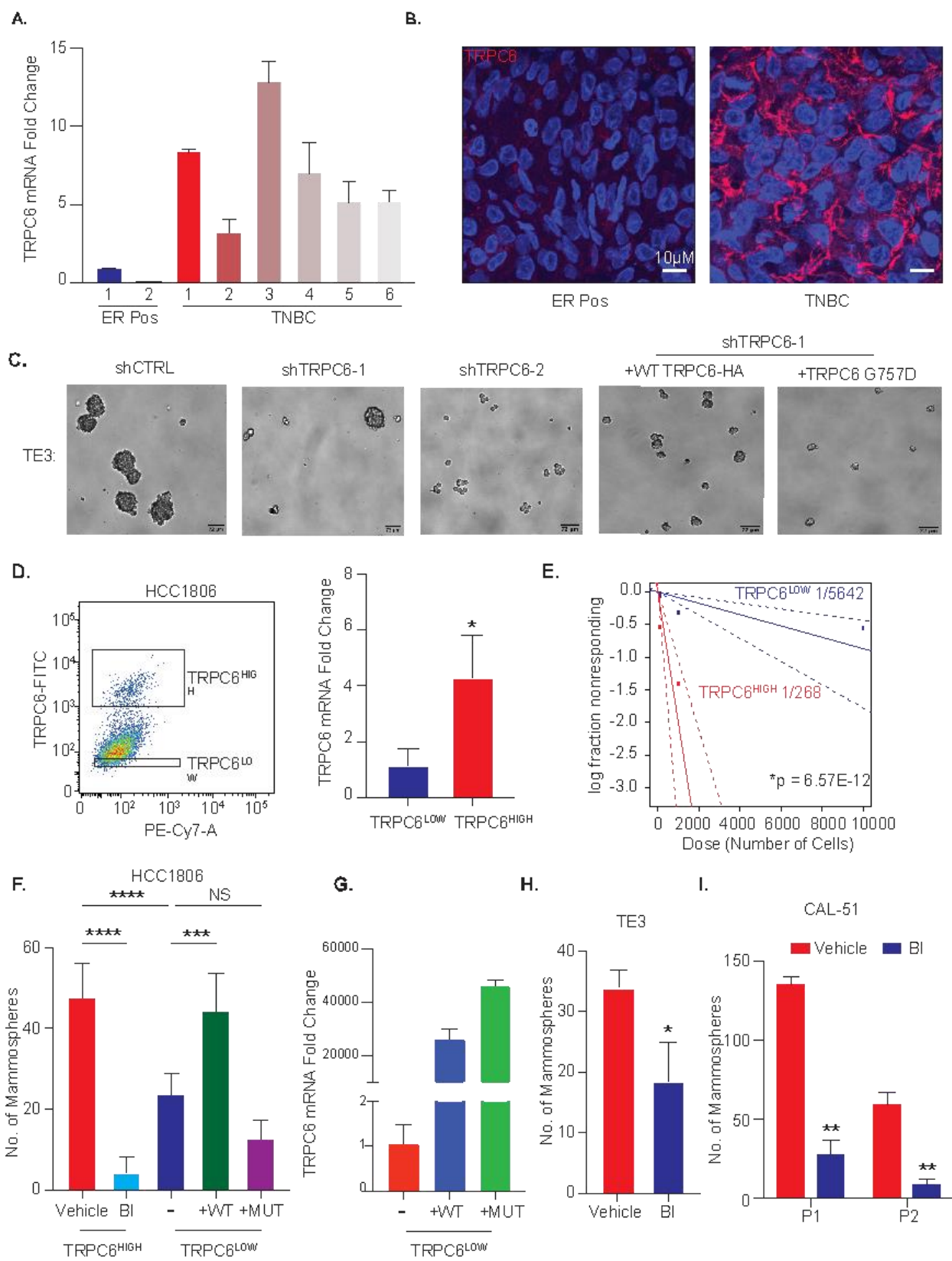


**Fig. 2.2: TRPC6 is enriched in TNBC CSCs and is sufficient to drive stemness.** **A.** *TRPC6* expression was quantified in estrogen receptor (ER<sup>+</sup>) (Pos) and TNBC organoids derived from breast cancer patients. **B.** Immunofluorescent images of specimens of ER positive and TNBC tumors stained with a TRPC6 Ab. Scale bar, 10uM. Red channel: TRPC6. Blue: DAPI. **C.** Representative brightfield images of mammosphere (passage P1) from TE3 cells (shCtrl, shTRPC6-1, shTRPC6-2, sh TRPC6-1+WT TRPC6, and shTRPC6-1+ mut TRPC6) were taken at 10X magnification. **D.** The TNBC cell line HCC1806 was sorted into a TRPC6<sup>high</sup> and a TRPC6<sup>low</sup> population (left panel). qPCR data quantifying TRPC6 expression in HCC-1806 TRPC6<sup>low</sup> and TRPC6<sup>high</sup> populations (right panel). **E.** TRPC6<sup>high</sup> and TRPC6<sup>low</sup> sorted populations were used in a limiting dilution mammosphere assay, and the frequency of tumor-initiating cells was determined using ELDA. **F.** The TRPC6<sup>high</sup> population of HCC1806 cells was treated with either DMSO or BI-749327 (BI) and assayed for mammosphere formation. The TRPC6<sup>low</sup> population from the same cell line was transfected with either empty vector, WT TRPC6 (WT) or the pore mutant TRPC6<sup>G757D</sup> (mut TRPC6) and assayed for mammosphere formation. **G.** TRPC6 mRNA expression in HCC-1806 TRPC6<sup>low</sup> cell transfected with either empty vector, WT-TRPC6 or mut TRPC6. **H, I.** Either TE3 (**H**) or CAL-51 (**I**) were treated with 10 uM BI-749327 (BI) and assayed for mammosphere formation. The immunofluorescent images shown in (B) are a representative image from ten images of each sample. The mammosphere images in (C) are representative images from each group from 20 images per sample. For (E) data are presented as a log-log plot, and the frequency of stem cells is calculated by extreme limiting-dilution analysis. The mammosphere data in (H) and (I) represent the mean  $\pm$  SD of a representative experiment performed three times independently. \*P < 0.05, \*\*P < 0.01, \*\*\*P < 0.001, and \*\*\*\*P < 0.0001.

**TRPC6 has a causal role in chemoresistance:** Based on the hypothesis that chemotherapy selects for the survival of cells with CSC properties, we sought to assess the functional role of TRPC6 in chemoresistance. For this purpose, we generated TNBC cells (CAL-51) that were resistant to paclitaxel, a drug that is standard of care for TNBC (131, 132) (**Fig. 2.3A**). Following paclitaxel treatment, we quantified *TRPC6* mRNA expression and observed that it was ~13 fold higher in the resistant (CAL-51-R) compared to the sensitive population (CAL-51-S) (**Fig. 2.3B**), an increase that was also observed in TRPC6 protein (**Fig. 2.4E**). Using a limiting dilution spheroid assay to determine the frequency of CSCs, we observed that the resistant population (CAL-51-R) contained a significantly higher frequency of CSCs than the sensitive population (CAL-51-S) (**Fig. 2.3C**). Moreover, inhibition of TRPC6 activity using BI-749327 caused a significant decrease in the frequency of CSCs in the CAL-51-R population (**Fig. 2.3D**). These results suggested that TRPC6

has a causal role in chemoresistance based on the reports that CSCs are chemoresistant (133). In support of this possibility, we observed that treatment of the CAL-51-R cells with the TRPC6 inhibitor BI-749327 increased their sensitivity to paclitaxel significantly compared to vehicle control-treated cells (**Fig. 2.3E**). We verified these findings using a paclitaxel-resistant organoid from a TNBC patient tumor (9883T). Paclitaxel resistance was associated with a significant increase in *TRPC6* expression (**Fig. 2.3F**). Of note, treatment of this resistant organoid with BI-749327 increased its sensitivity to paclitaxel (**Fig. 2.3G**) indicating that cells that persist paclitaxel treatment are dependent on TRPC6.

A critical issue that arose from our data on chemoresistance is whether TRPC6 inhibition could be an effective therapeutic approach *in vivo* for TNBC. To assess this possibility, we made use of an aggressive PDX model of TNBC that was reported recently (HCI028) (134). Treatment of these tumors with either paclitaxel or BI-749327 alone did not have a significant impact on tumor growth. Combined treatment, in contrast, resulted in tumor regression (**Fig. 2.3H**).

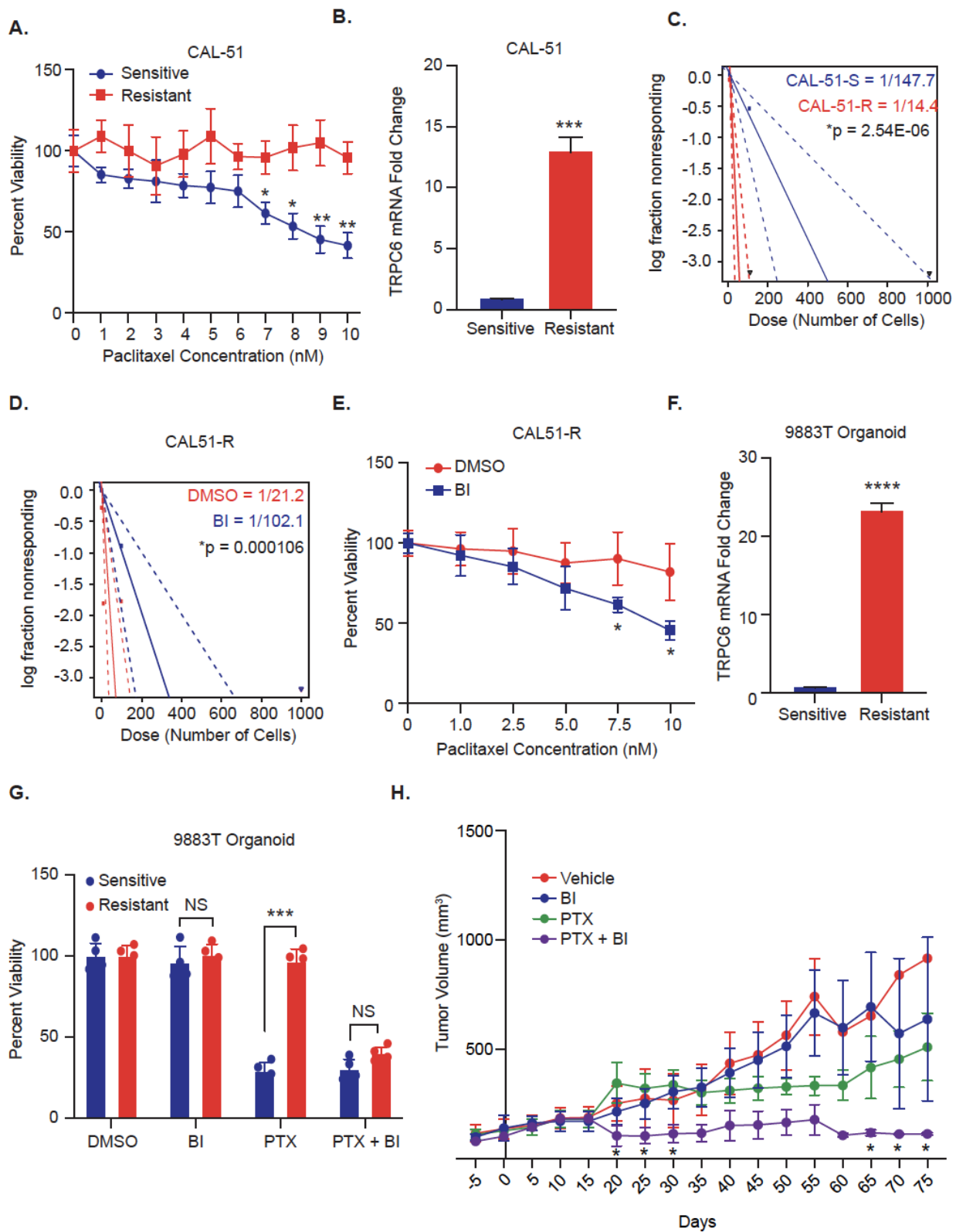


**Fig. 2.3: TRPC6 has a causal role in chemoresistance.** **A.** Characterization of CAL-51 chemotherapy resistant cells. CAL-51 cells were made resistant to paclitaxel as described in Methods and then compared to parental cells (termed Sensitive) for viability in response to increasing concentrations of paclitaxel. **B.** TRPC6 mRNA expression was quantified in CAL-51-Sensitive and Resistant cells. **C.** CAL-51-Sensitive and Resistant cells were assayed for the frequency of CSCs using a limiting dilution mammosphere assay and the data were analyzed by ELDA. **D.** CAL-51 resistant cells were treated with vehicle control or BI-749327 (10  $\mu$ M) for 24 hrs. and the frequency of CSCs was determined using a limiting dilution mammosphere assay and ELDA. **E.** CAL-51 resistant cells (CAL-51-R) were treated with increasing concentration of paclitaxel in combination with either DMSO or BI-749327 (10  $\mu$ M) for 24 hours and cell viability was assessed. **F.** TRPC6 mRNA expression was quantified in chemo sensitive, and resistant models of a patient-derived organoid (9883T) as described in Methods. **G.** The organoid models described in F were treated with either DMSO, paclitaxel (PTX; 20 nM), BI-749437 (10 $\mu$ M) or Paclitaxel+BI (PTX+BI) for 96 hrs. and cell viability was measured. **H.** Tumors volumes (in mm<sup>3</sup>) in mice that had been implanted orthotopically with a human TNBC PDX (PDX HCI028). The mice were divided into 4 groups of 5 mice each. When tumors reached an  $\sim$  volume of 100mm<sup>3</sup>, the mice were treated with either vehicle, paclitaxel (15mgs/kg), BI-749327 (15mgs/kg) or a combination of paclitaxel and BI-749327. Paclitaxel was injected I.P twice a week and BI-749327 was administered by oral gavage four days a week. Day 0 on the x-axis indicates the start of the treatments. Tumor volume was measured every 5 days.

For (C) and (D) data are presented as a log-log plot, and the frequency of stem cells is calculated by extreme limiting-dilution analysis. The viability data shown (E) and (G) represent the mean  $\pm$  SD of a representative experiment performed three times independently.

The tumor volume data shown in (H) are represented as mean  $\pm$  SEM of the number of mice in the respective groups. \*P < 0.05, \*\*P < 0.01, \*\*\*P < 0.001, and \*\*\*\*P < 0.0001.

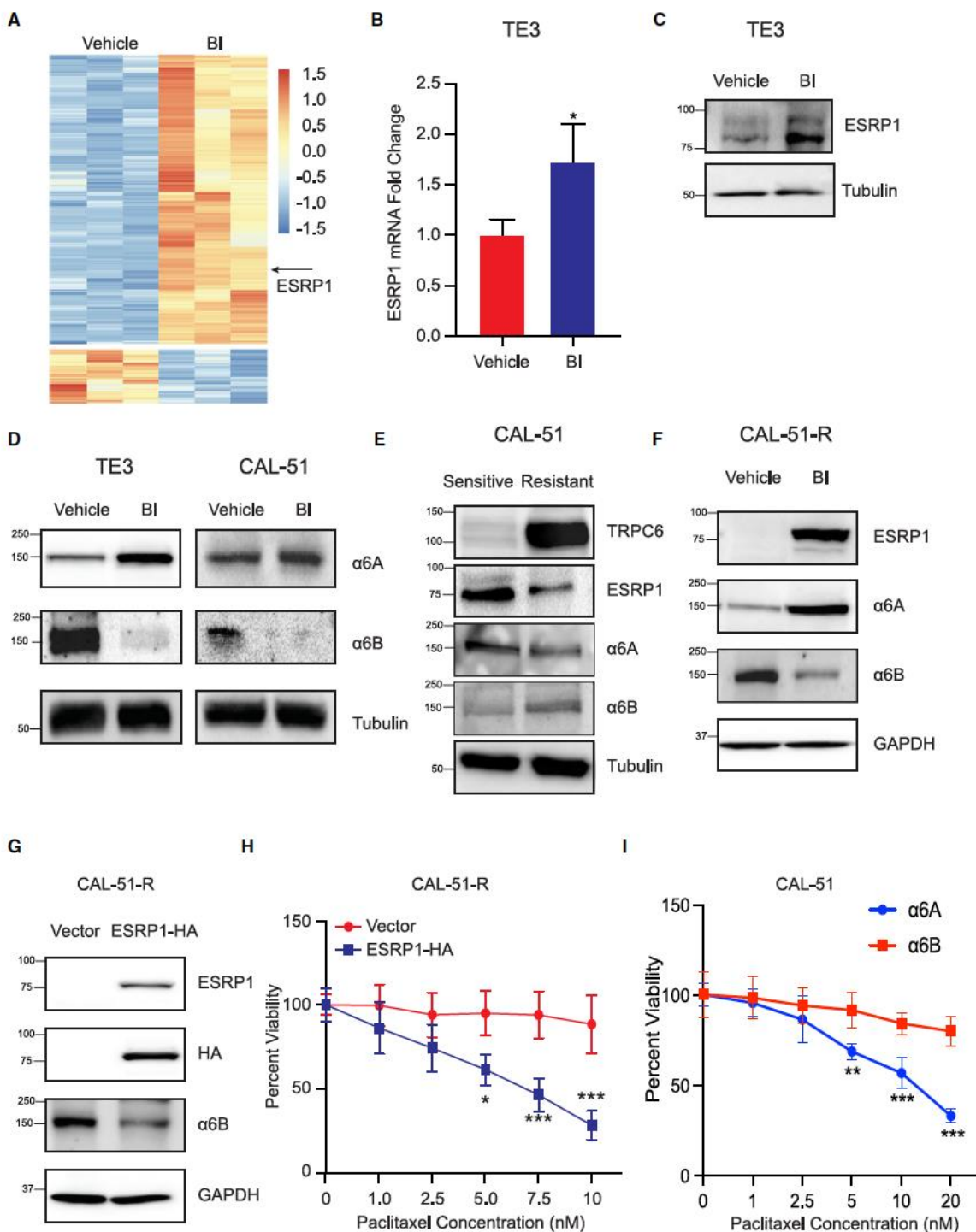
**TRPC6 suppresses ESRP1, which enriches for the  $\alpha$ 6B integrin splice variant:** To investigate the mechanism by which TRPC6 sustains CSCs and promotes chemoresistance, we used an unbiased approach and performed RNA sequencing on TE3 cells that had been treated with either DMSO or BI-749327 for either 6 or 12 hrs. Analysis of the data revealed that Epithelial Splicing Regulatory Protein 1 (*ESRP1*) was one of the top mRNAs upregulated in the inhibitor treated cells (**Fig. 2.4A**). *ESRP1* regulates the splicing of mRNAs associated with an epithelial phenotype and its loss has been associated with EMT (135) and stemness (136) programs in breast cancer. Our own studies have shown that the expression of *ESRP1* is significantly lower in TNBC patients than in patients with other subtypes of breast cancer and that it has a causal role in controlling stemness

(136, 137). Moreover, similar pattern of ESRP1 expression was observed in organoids derived from TNBC and non-TNBC patients (**Fig. 2.5A**). We validated the RNA-Seq data by qPCR using TNBC cells treated with BI-749327 and confirmed that TRPC6 inhibition increases ESRP1 expression (**Fig. 2.4B, 2.5B**). We also observed a significant increase in ESRP1 protein levels compared to control conditions in TE3 cells upon TRPC6 inhibition (**Fig. 2.4C**).

The ability of TRPC6 to suppress *ESRP1* captured our attention because we had previously reported that it regulates splicing of the  $\alpha 6$  integrin (137). There are two splice variants of the  $\alpha 6$  integrin cytoplasmic domain:  $\alpha 6A$  and  $\alpha 6B$ . We have previously shown that the  $\alpha 6B$  variant promotes stemness (137). In contrast, the  $\alpha 6A$  variant lacks this ability and is associated with non-CSC populations (137). ESRP1-mediated mRNA splicing generates the  $\alpha 6A$  variant and, consequently, loss of ESRP1 results in a predominance of the  $\alpha 6B$  variant (137). Consistent with these findings, we observed that inhibition of TRPC6 caused a decrease in  $\alpha 6B$  and a concomitant increase in  $\alpha 6A$  protein levels (**Fig. 2.4D**). To obtain evidence for the role of calcium in TRPC6-mediated repression of ESRP1 and the consequent splicing of  $\alpha 6$  integrin, we treated CAL-51 cells with the calcium chelator BAPTA, and we observed an increase in ESRP1 and  $\alpha 6A$  and a concomitant decrease in  $\alpha 6B$  expression (**Fig. S2E**). Therefore, we hypothesized that TRPC6 suppresses *ESRP1* and, consequently, sustains the  $\alpha 6B$  splice variant that promotes stemness and chemoresistance. To test this hypothesis, we first depleted *ESRP1* expression in TRPC6 knockdown cells (TE3 and CAL-51) (**Fig. 2.5C**) and observed that loss of ESRP1 was sufficient to rescue self-renewal compared to control cells (**Fig. 2.6C, D**). Moreover, expression of the  $\alpha 6B$  variant in the TRPC6 knockdown cells (**Fig. 2.7C**) was sufficient to rescue self-renewal (**Fig. 2.7A,**

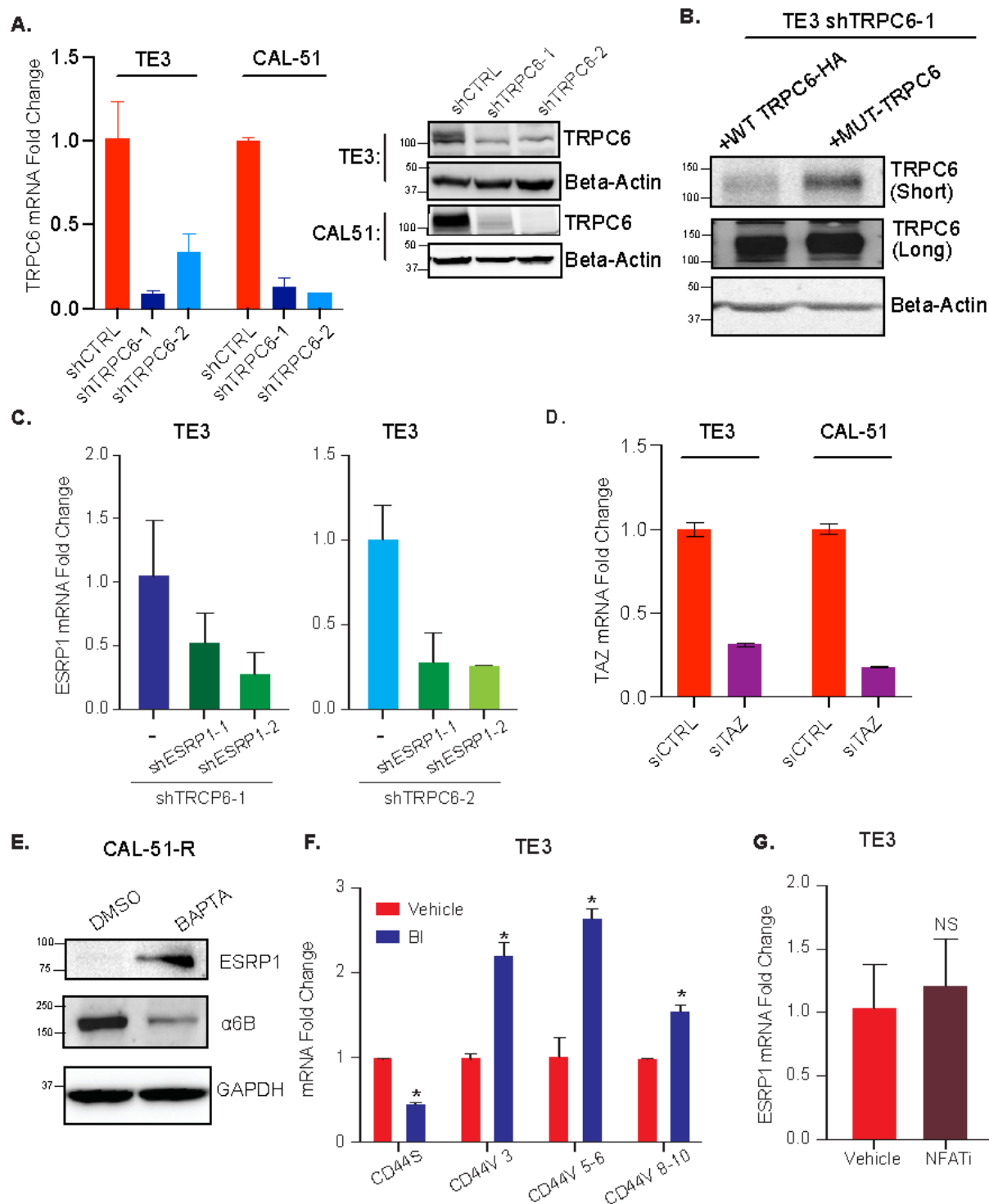
**B).** Importantly, the exogenously expressed  $\alpha 6B$  is functional because these transfected cells were able to bind to the  $\alpha 6B$  ligand laminin 511 (138) (**Fig. 2.7D**).

We extended our analysis to the CAL-51-S and CAL-51-R populations described in **Fig. 2.3** based on the assumption that cells that persist after chemotherapy have increased TRPC6 and  $\alpha 6B$  expression but diminished ESRP1 expression. Using immunoblotting to assess protein expression, we verified that the CAL-51-R cells had increased TRPC6 expression compared to the CAL-51-S cells (**Fig. 2.4E**). We also observed that the CAL-51-R cells had higher expression of  $\alpha 6B$  and lower levels of ESRP1 and  $\alpha 6A$  than the CAL-51-S cells (**Fig. 2.4E**). Inhibition of TRPC6 activity in CAL-51-R cells caused an increase in ESRP1 and the  $\alpha 6A$  splice variant and a concomitant decrease in  $\alpha 6B$  (**Fig. 2.4F**). These data indicated that the TRPC6/ESRP1 axis, which regulates  $\alpha 6$  integrin splicing, contributes to the survival of persister cells, and that it can be a therapeutic target to enhance chemosensitivity. In support of this possibility, exogenous expression ESRP1 in the CAL-51-R cells increased  $\alpha 6A$  and decreased  $\alpha 6B$  expression (**Fig. 2.4G**) and, importantly, increased their sensitivity to paclitaxel (**Fig. 2.4H**). Conversely, expression of the  $\alpha 6B$  variant but not  $\alpha 6A$ , in CAL-51-S cells that has been depleted of integrin  $\alpha 6$  using CRISPR (**Fig. 2.7E**) increased resistance to paclitaxel (**Fig. 2.4I**).



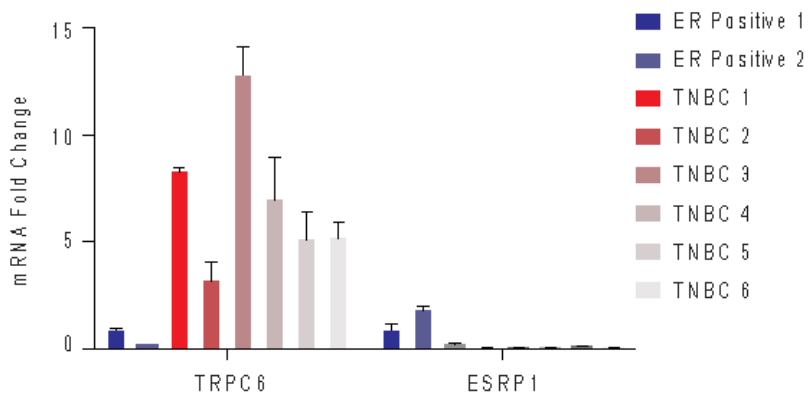
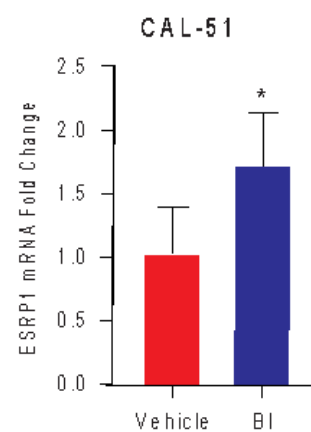
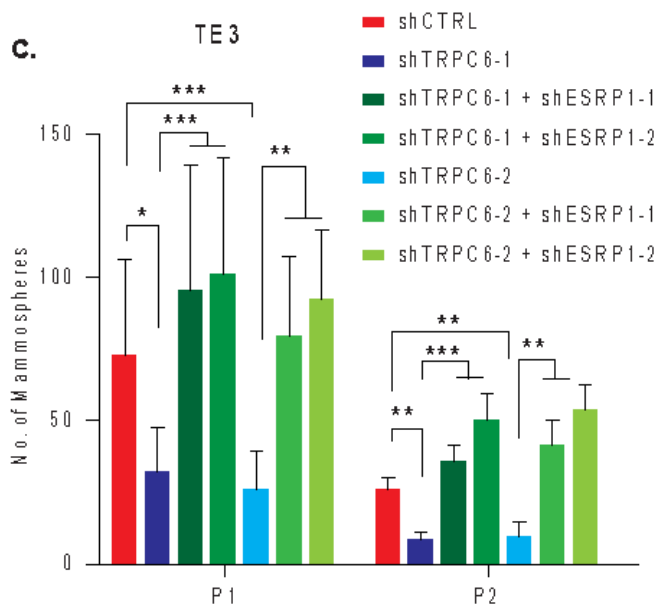
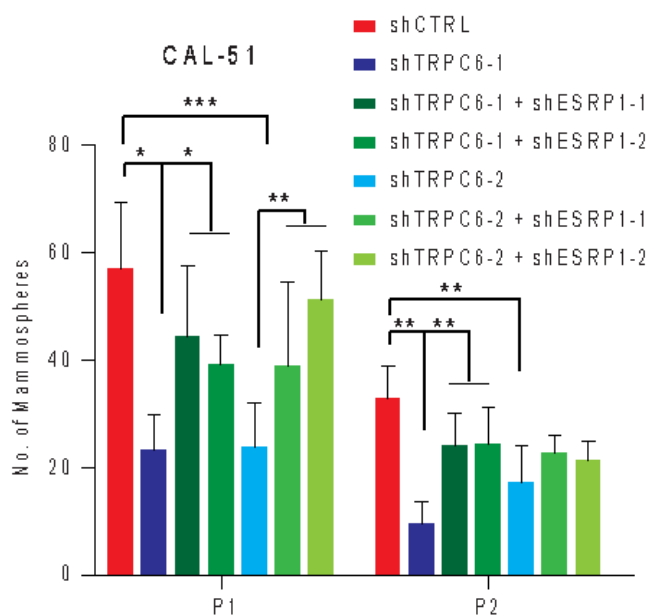
**Fig. 2.4: TRPC6-mediated  $\text{Ca}^{2+}$  entry represses the splicing protein ESRP1.** **A.** Heatmap showing genes that are differentially expressed in vehicle and BI-749327 (10uM) treated TE3 cells (12 hours).  $\text{FDR} < 0.05$  and  $|\log_2\text{FC}| > 1$ . **B., C.** ESRP1 mRNA (**B**) and protein (**C**) expression was assessed in TE3 cells treated with either vehicle control or BI-749327 (10 uM) for 24 hrs. **D.**

TE3 and CAL-51 cells were treated with either vehicle control or BI-749327 (10  $\mu$ M) for 24 hrs. and the expression of the  $\alpha$ 6A and  $\alpha$ 6B integrin splice variants was assessed by immunoblotting. **E.** The expression of TRPC6, ESRP1,  $\alpha$ 6A and  $\alpha$ 6B was assessed in the CAL-51 sensitive and resistant cells by immunoblotting. **F.** The expression of ESRP1,  $\alpha$ 6A and  $\alpha$ 6B in CAL-51-R cells that had been treated with either DMSO or BI-749327 (10  $\mu$ M) for 24 hrs. was assessed by immunoblotting. **G.** CAL-51-R cells were stably transfected with either a control plasmid (Vector) or an ESRP1 expression plasmid (ESRP1-HA) and the expression of ESRP1, HA and  $\alpha$ 6B was assessed by immunoblotting. **H.** The same cells as in **G** were assayed for their sensitivity to increasing concentrations of Paclitaxel. **I.** Parental CAL-51 cells that had been depleted of  $\alpha$ 6 integrin using CRISPR were stably transfected with either  $\alpha$ 6A or  $\alpha$ 6B plasmids. Cell viability in response to increasing concentrations of paclitaxel was measured. The TRPC6 expression data shown in (B) represent the mean  $\pm$  SD of three independent experiments. \*P < 0.05, \*\*P < 0.01, \*\*\*P < 0.001, and \*\*\*\*P < 0.0001.



**Fig. 2.5: Assessment of TRPC6, ESRP1 and  $\alpha 6$  integrin splice variant expression.** **A. (Left)** *TRPC6* mRNA expression was quantified by qPCR in TE3 and Cal51 cells that has been transfected with either shCtrl or two shRNAs specific for TRPC6 (shTRPC6-1, shTRPC6-2). **(Right)** Immunoblot showing TRPC6 protein expression in TE3 and CAL-51 cells that has been transfected with either shCtrl or two shRNAs specific for TRPC6. **B.** TRPC6 protein expression

in TE3 cells that has been stably transfected with an shRNA against TRPC6 and rescued with either a wild-type TRPC6 construct (WT) or a pore mutant (G757D) that is deficient in calcium uptake (MUT). **C.** ESRP1 mRNA expression was quantified in stable TE3 TRPC6 knockdown cells that were then re-transfected with either of two ESRP1 shRNAs (shESRP1-1 and shESRP1-2). **D.** TAZ mRNA expression was quantified in cells (TE3, CAL-51) transfected with either control siRNA (siCtrl), or siRNA targeting TAZ (siTAZ). **E.** ESRP1 and  $\alpha$ 6B protein expression was assessed by immunoblotting in CAL-51 cells that had been treated with either DMSO or BAPTA (20  $\mu$ M) for 12 hours. **F.** Expression of the CD44 splice variants shown on the x-axis was quantified in TE3 cells that had been treated with either DMSO or 10  $\mu$ M BI-749327 for 24 hrs. **G.** ESRP1 mRNA expression was quantified in TE3 cells that had been treated with either DMSO or an NFAT inhibitor (100  $\mu$ M) for 24 hrs. The ESRP1 expression levels shown in (D) represent the mean  $\pm$  SD of a representative experiment performed three times independently.

**A.****B.****C.****D.**

**Fig. 2.6: ESRP1 suppression is key to maintaining self-renewal.** **A.** The expression of *TRPC6* and *ESRP1* mRNAs was quantified in ER positive and TNBC organoids derived from breast cancer patients (*TRPC6* data is from **Fig. 1**). **B.** *ESRP1* mRNA expression was quantified in CAL-51 cells that had been treated with either DMSO or BI (10 $\mu$ m) for 24 hrs. **C, D.** TE3 (**C**) and CAL-51 (**D**) cells were stably transfected with either control shRNA (shCtrl) or a *TRPC6* shRNAs (sh*TRPC6*-1 and sh*TRPC6*-2). These stable *TRPC6* knockdown cells were then re-transfected with either of two *ESRP1* shRNAs (sh*ESRP1*-1 and sh*ESRP1*-2) and these populations were assessed for self-renewal by serial passage of mammospheres (P1- passage 1; P2- passage 2). The mammosphere data shown in (C) and (D) represent the mean  $\pm$  SD of three independent experiments. \*P < 0.05, \*\*P < 0.01, \*\*\*P < 0.001, and \*\*\*\*P < 0.0001.

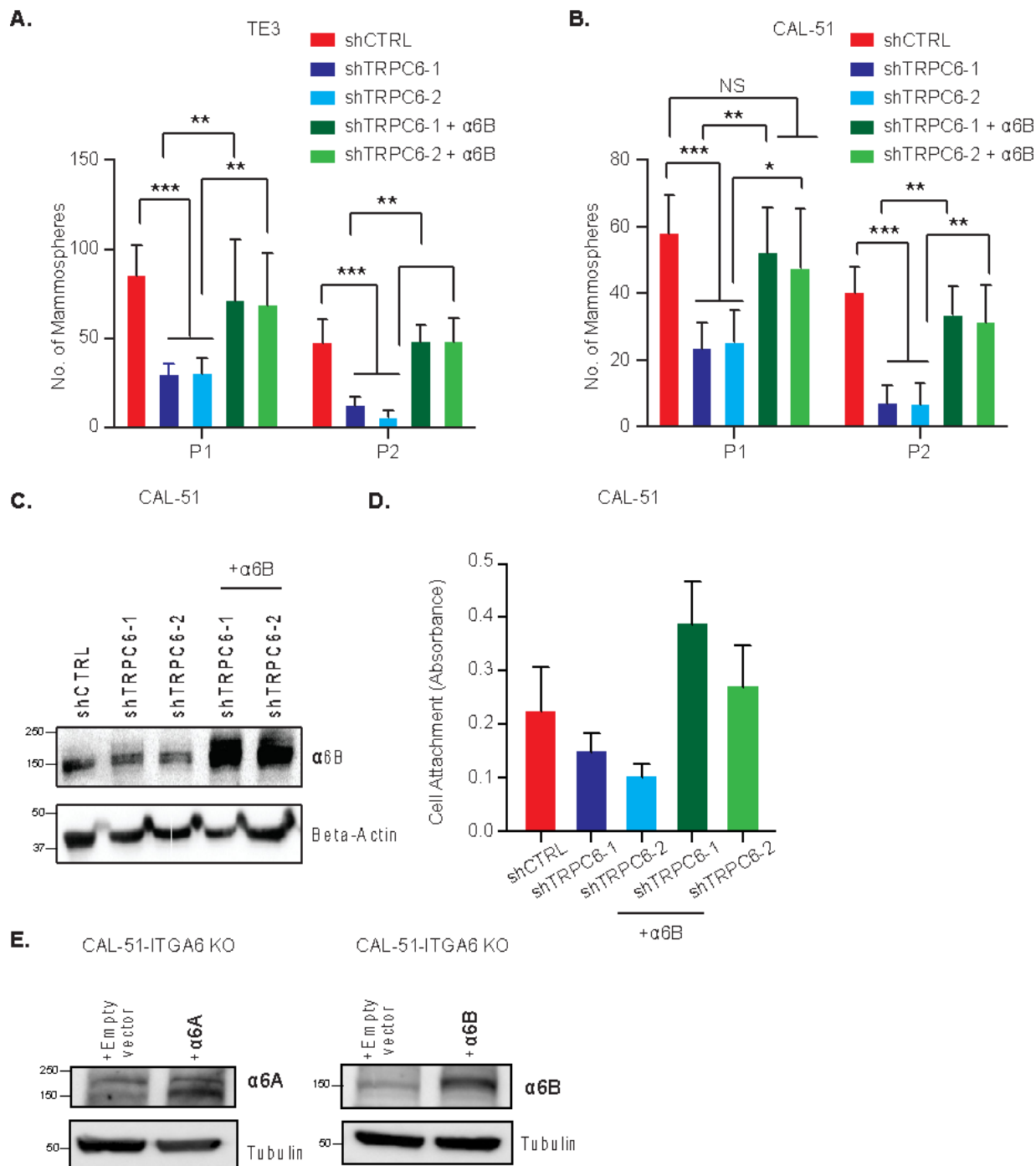


**Fig. 2.7: TRPC6 maintains breast cancer stemness by enriching for  $\alpha 6B$  splice variant.** **A, B.** Either TE3 (**A**) or CAL-51 (**B**) cells that had been stably transfected with either a control (shCtrl) or TRPC6 shRNAs (shTRPC6-1, shTRPC6-2) were re-transfected with an  $\alpha 6B$  expression plasmid ( $\alpha 6B$ -GFP) followed by knockdown of the endogenous  $\alpha 6$  integrin (shITGA6). These populations were assayed for self-renewal by serial passage of mammospheres (P1-passage 1, P2-passage 2). **C.** Immunoblot comparing  $\alpha 6B$  integrin expression in the following populations of CAL-51 cells:

Ctrl (shCTRL), TRPC6 knockdown (shTRPC6-1, shTRPC6-2) and TRPC6 knockdown cells (shTRPC6+ $\alpha$ 6B) transfected with an  $\alpha$ 6B plasmid. **D.** The CAL-51 populations described in **C** were assayed for their adhesion to laminin 511. Adhesion was quantified by crystal violet staining followed by absorbance at 600nm. **E.** Immunoblots showing expression of  $\alpha$ 6A (left) and  $\alpha$ 6B (right) protein in CAL-51 cells that had been depleted of endogenous integrin  $\alpha$ 6 using CRISPR and stably transfected with either  $\alpha$ 6A or  $\alpha$ 6B plasmids. The mammosphere data shown in (A) and (B) represent the mean  $\pm$  SD of three independent experiments. \*P < 0.05, \*\*P < 0.01, \*\*\*P < 0.001, and \*\*\*\*P < 0.0001.

To gain insight into how TRPC6 represses ESRP1 expression, we used a dataset that highlights transcription factor and gene interactions based on compiled ENCODE Chromatin immunoprecipitation (ChIP) data (139). This analysis identified TEAD4 as one such factor. Given that the TEAD family of transcription factors primarily associate with the Hippo effectors YAP and TAZ (140), this observation indicated that TRPC6 may contribute to TAZ activation and the regulation of ESRP1. Indeed, knockdown of TRPC6 or pharmacological inhibition of its activity using BI-749327 caused a significant decrease in TAZ nuclear localization (**Fig. 2.8A, B**) and in the expression of the TAZ target genes *CTGF* and *ANKRD1* (**Fig. 2.8C, D**). Subsequently, we used siRNAs to diminish *TAZ* (**Fig. 2.5D**) and observed a concomitant increase in *ESRP1* expression (**Fig. 2.8E**). We also knocked-down the expression of *TEADs* 1-3-4 using shRNA (**Fig. 2.8G**) and observed a similar increase in ESRP1 protein levels (**Fig. 2.8F**). To investigate the TRPC6-mediated repression of *ESRP1* by TAZ more rigorously, we expressed constitutively active TAZ (4SA-TAZ) in TRPC6 knockdown cells and observed that active TAZ was sufficient to repress *ESRP1* in these cells (**Fig. 2.8H**).

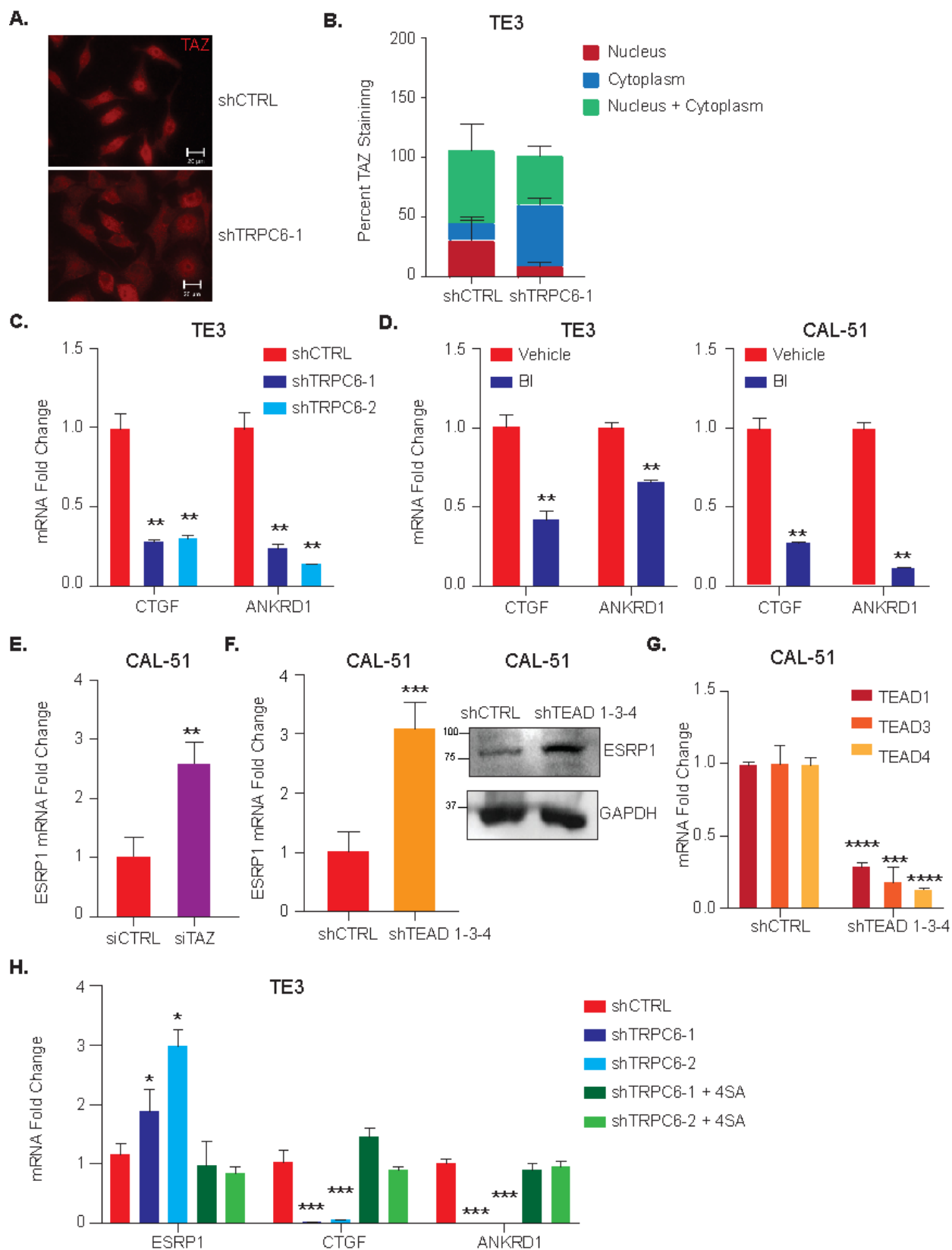


**Fig. 2.8: TAZ/TEAD repress ESRP1 downstream of TRPC6.** **A, B.** The subcellular localization of TAZ was assessed by immunofluorescence microscopy in TE3 cells transfected with either control (shCTRL) or TRPC6 shRNAs (**A**) and the relative localization of TAZ in the nucleus and cytoplasm was quantified in 20 cells (**B**). **C.** Expression of TAZ target gene (CTGF and ANKRD1) mRNAs were quantified by qPCR in shCTRL and shTRPC6 (shTRPC6-1, shTRPC6-2) TE3 cells. **D.** Expression of TAZ target gene (CTGF and ANKRD1) mRNAs were quantified by qPCR in either TE3 or CAL-51 cells that had been treated with either DMSO or BI-749327 (10  $\mu$ M) for 24 hrs. **E.** ESRP1 mRNA expression was quantified in CAL-51 cells that had been transfected with control siRNA (siCtrl), or siRNA targeting TAZ (siTAZ). **F.** ESRP1 mRNA (left graph) and protein (right immunoblot) expression was assessed in CAL-51 cells transfected with either control shRNA (shCTRL) or shRNAs targeting TEAD1, TEAD3, and shTEAD4 (shTEAD1-3-4). **G.** TEAD1, 3, and 4 mRNA expression was quantified in cells transfected with either control shRNA (shCTRL) or shRNAs targeting TEAD1, TEAD3, and shTEAD4 (shTEAD1-3-4). **H.** TE3 cells that had been transfected with either control shRNA (shCTRL) or TRPC6 shRNAs (shTRPC6-1, shTRPC6-2) were re-transfected with a constitutively active TAZ-4SA plasmid (4SA) and ESRP1 mRNA expression was quantified in these populations. The immunofluorescent image shown in (**A**) represents a representative image per condition from 10 different images. The quantification of TAZ localization shown in (**B**) represents the mean number for 20 cells (average per field) in each group. The CTGF, ANKRD1 expression data shown in (**C**) and (**D**) represent the mean  $\pm$  SD of a representative experiment performed three times independently. The ESRP1 expression data shown in (**E**) shown represent the mean  $\pm$  SD of three independent experiments. \* $P < 0.05$ , \*\* $P < 0.01$ , \*\*\* $P < 0.001$ , and \*\*\*\* $P < 0.0001$ .

Given that cell contractility can activate TAZ by a mechanism that involves Rho GTPases (141) and previous work demonstrating that TRPC6 can activate RhoA in a calcium dependent manner (142), we evaluated the contribution of RhoA to the repression of *ESRP1* expression. Initially, we assessed RhoA activation in TNBC cells in which *TRPC6* expression had been knocked down and then rescued with either wild-type TRPC6 or the pore mutant TRPC6<sup>G757D</sup>. The data obtained substantiate the finding the TRPC6 activates RhoA in a calcium-dependent manner (**Fig. 2.9A**). Subsequently, we assessed a causal role for RhoA-mediated contractility in TAZ activation and ESRP1 repression using the ROCK inhibitor (Y26739). This inhibitor caused a significant decrease in TAZ activation as assessed by expression of TAZ target genes (**Fig. 2.9B**), as well as an increase in *ESRP1* expression (**Fig. 2.9C, D**). To validate that RhoA activation downstream of TRPC6 causes repression of *ESRP1*, we transfected a constitutively active RhoA (RhoV14-GST)

in TRPC6 knockdown cells and observed that the expression of active RhoA was sufficient to reduce ESRP1 levels (**Fig. 2.9E**). Together, these data support the hypothesis that TRPC6-mediated RhoA activation contributes to TAZ activation and the consequent repression of ESRP1.

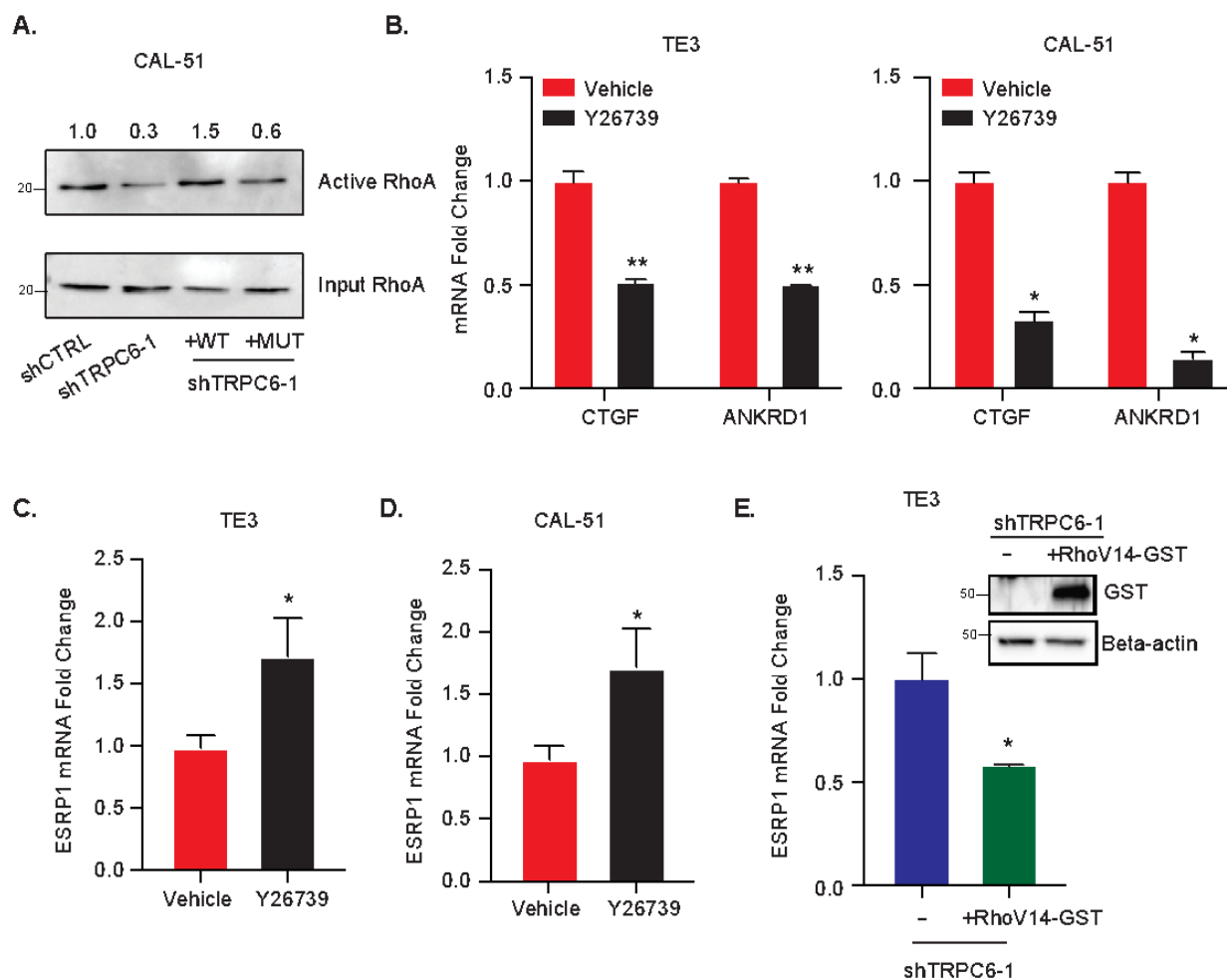


**Fig. 2.9: TRPC6-mediated Ca<sup>2+</sup> signaling activates RhoA and TAZ, which represses ESRP1.**

**A.** CAL-51 cells that had been stably transfected with either Control or TRPC6 shRNAs were re-transfected with either WT TRPC6 (sh+WT TRPC6) or a pore mutant TRPC6 (sh+ mut TRPC6). RhoA activity was assessed using the Rhotekin assay and the level of active RhoA was normalized to total RhoA by densitometry in the immunoblot shown (densitometric values are on top). **B.** Expression of TAZ target gene (CTGF and ANKRD1) mRNAs were quantified in TE3 and CAL-51 cells after treatment with either vehicle (H<sub>2</sub>O) or Y26732, a Rho kinase inhibitor (ROCKi) (20 uM for 12 hrs). **C, D.** Expression of ESRP1 was quantified in TE3 (**C**) and CAL-51 (**D**) cells after treatment with either vehicle (H<sub>2</sub>O) or Y26732 (20 uM for 12 hrs.). **E. (Left)** TE3 TRPC6 stable knockdown cells (shTRPC6-1) were transfected with an empty vector or a constitutively active RhoA (RhoV14-GST) plasmid, and ESRP1 mRNA expression was quantified. **(Right)**

Immunoblot showing the expression of GST in the TE3 shTRPC6-1 cells that has been transfected with either empty vector or constitutively active RhoV14-GST plasmid. The CTGF, ANKRD1 expression data shown in (B) represent the mean  $\pm$  SD of an experiment performed three times independently. The ESRP1 expression data shown in (E) shown represent the mean  $\pm$  SD of a representative experiment performed three times independently. \*P < 0.05, \*\*P < 0.01, \*\*\*P < 0.001, and \*\*\*\*P < 0.0001.

**TRPC6-regulated  $\alpha 6$  integrin splicing sustains persister cells by repressing Myc:** In pursuit of the mechanism by which TRPC6-regulated  $\alpha 6$  integrin splicing promotes chemoresistance, we were informed by the report of Dhimolea *et. al* that repression of Myc has a causal role in sustaining persister cells in breast cancer (143). In support of a role for Myc repression in our mechanism, we observed that Myc expression is significantly lower in the CAL-51R cells compared to the CAL-51S cells (**Fig. 2.10A**). We also observed that TRPC6 was significantly enriched in the chemoresistant organoid models used by Dhimolea *et. al* (**Fig. 2.10B**). Moreover, TRPC6 knock-down in TE3 and CAL-51 cells (**Fig. 2.10C, D**) or inhibition of its function using BI-749327 increased Myc mRNA (**Fig. 2.10E**) and protein expression (**Fig. 2.10F**). A critical finding in this regard is that the PDX tumors that were treated with BI-749327 had higher levels of Myc than control tumors as assessed by immunoblotting of tumor extracts (**Fig. 2.10F**). To verify a causal role for Myc repression in chemoresistance, we expressed exogenous Myc in CAL-51-R cells (**Fig. 2.10G, right panel**) and observed a significant increase in their sensitivity to paclitaxel (**Fig. 2.10G**). Conversely, pretreatment of the cells with the Myc inhibitor 10074-G5 increased resistance to paclitaxel (**Fig. 2.10H**). Inhibition of Myc activity by 10074-G5 is evidenced by the downregulation of its target gene *CDC25A* (**Fig. 2.10I**).

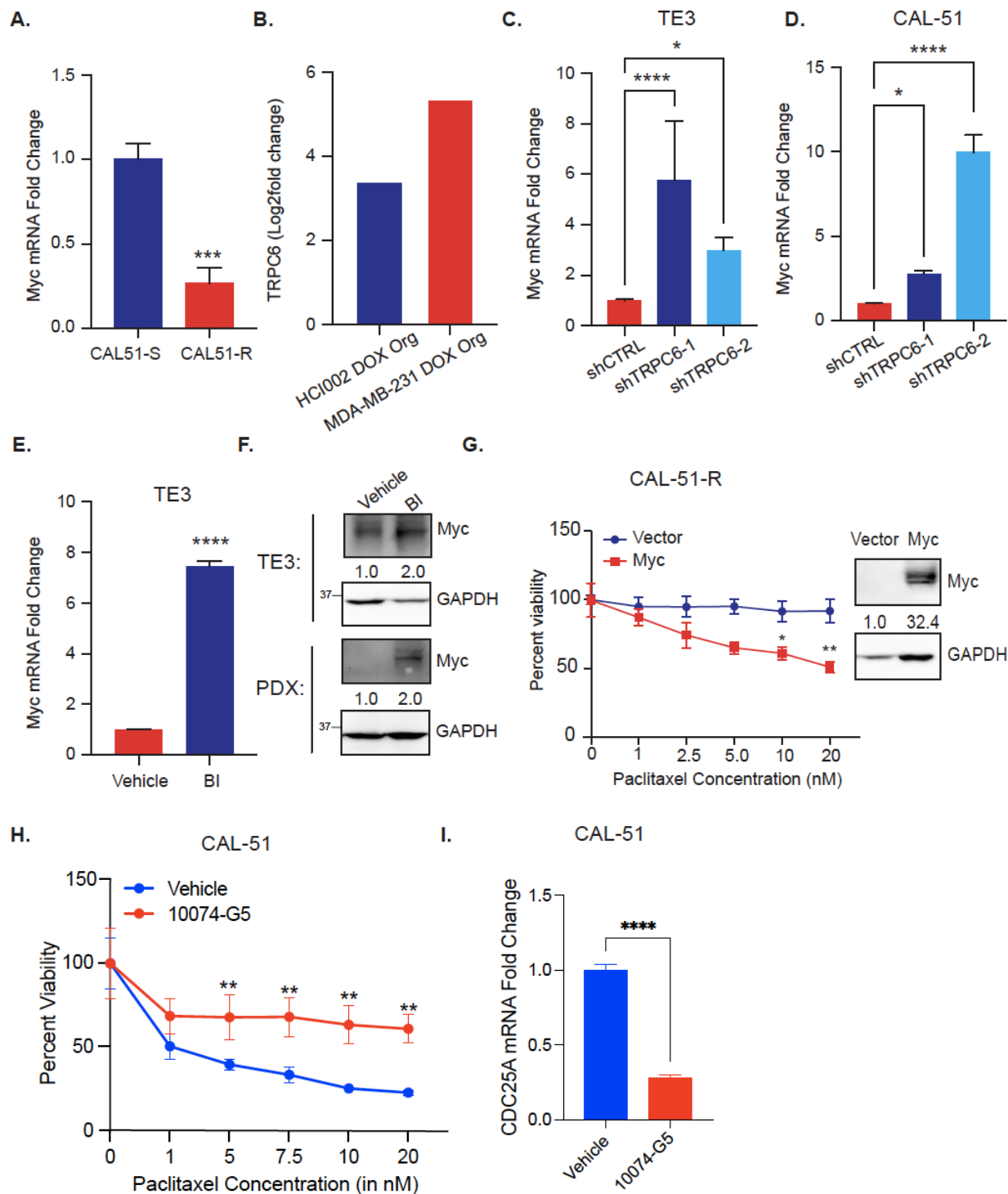


**Fig. 2.10: TRPC6-regulated  $\alpha 6$  integrin splicing sustains persister cells by repressing Myc.** **A.** Myc mRNA expression was quantified by qPCR in CAL-51-S and CAL-51-R cells. **B.** *TRPC6* expression (Log2fold) was analyzed from a published dataset of chemoresistant (doxorubicin) organoid models that were derived from patient tumors or cell lines (see ref. 37). **C. D.** Myc mRNA expression was quantified in TE3 (**C**) or CAL-51 (**D**) cells that had been stably transfected with either a control (shCtrl) or TRPC6 shRNAs (shTRPC6-1, shTRPC6-2). **E.** TE3 cells were treated with either DMSO or BI-749327 (BI) (10  $\mu$ M) for 24 hrs. Myc mRNA expression was quantified by qPCR in TE3 cells. **F.** Myc protein expression by immunoblotting was detected: in TE3 cells treated with either vehicle or 10  $\mu$ M BI-749327 (BI) for 24 hours. Freshly harvested PDX tumors that had been treated with either vehicle or BI-749327 (BI) (**see Fig. 2H**) were used to extract protein and RNA. Protein lysates were immunoblotted with a Myc antibody. Densitometric values are shown below the immunoblot. **G.** CAL-51-R cells were transfected with either vector alone or a Myc expression vector and their sensitivity to increasing concentrations of paclitaxel was assessed by quantifying cell viability (left). Immunoblot showing Myc protein levels in CAL-51-R cells transfected with either an Empty Vector or Myc overexpression plasmid (right). **H.** CAL-51 parental cells that has been pre-treated with either DMSO or 10074-G5 (50  $\mu$ M) for 24 hours were assessed for their sensitivity to increasing concentrations of paclitaxel, either alone or in combination with 1007-G5 (50  $\mu$ M) for an additional 24 hours. **I.** Expression of the Myc target gene *CDC25A* was quantified by qPCR in CAL-51 cells treated with either DMSO or 10074-G5 (50  $\mu$ M). The Myc expression levels in (A), (C), (D), and (E) represent the mean  $\pm$  SD of three independent experiments. \* $P < 0.05$ , \*\* $P < 0.01$ , \*\*\* $P < 0.001$ , and \*\*\*\* $P < 0.0001$ .

**TRPC6 promotes quiescence:** Based on the finding that Myc sustains persister cells by inducing quiescence, we sought to determine whether TRPC6 promotes quiescence. For this purpose, we used SETD4 as a functional readout of quiescence because it has been shown to mark quiescent populations in sub-populations of breast cancers (144, 145). We found that TRPC6 knockdown in TE3 cells resulted in a significant decrease in SETD4 expression (**Fig. 2.11A**). Further in the PDX tumors that were treated with BI-749327 had significantly less SETD4 mRNA expression than control tumors (**Fig. 2.11B**). To obtain additional evidence that TRPC6-mediated signalling has a causal role in quiescence we used a reporter consisting of an inactive CDK-binding domain of p27 fused to an mVenus tag (146). This reporter has been used to identify p27<sup>+</sup> quiescent cells in breast cancer (147). Using this reporter, we observed that CAL-51 and HCC-1806 cells treated with the TRPC6 inhibitor exhibited a significant decrease in the p27<sup>+</sup> population (**Fig. 2.11C, 5F**),

indicating a shift towards a more proliferative phenotype. We also sorted the p27<sup>high</sup> and p27<sup>low</sup> populations from both CAL-51 and HCC-1806 cells that had been transfected with the p27-mVenus reporter and observed a significant enrichment of TRPC6 and SETD4 expression in the p27<sup>high</sup> population compared to the p27<sup>low</sup> population (**Fig. 2.11D, 5G**). In contrast, the p27<sup>low</sup> population had higher expression of ESRP1 (**Fig. 2.11D, 5G**), a result that is consistent with our previous data (see **Fig. 2.4**). We also observed a significant decrease in mammosphere formation in the p27<sup>high</sup> population upon TRPC6 inhibition (**Fig. 2.11E, 5H**). Based on these data, we hypothesized that the p27<sup>high</sup> cells are more resistant to paclitaxel than the p27<sup>low</sup> cells. To test this hypothesis, we sorted the p27<sup>high</sup> and p27<sup>low</sup> populations from CAL-51 cells and observed that the p27<sup>high</sup> cells are significantly more resistant to paclitaxel than p27<sup>low</sup> cells (**Fig. 2.11I**).

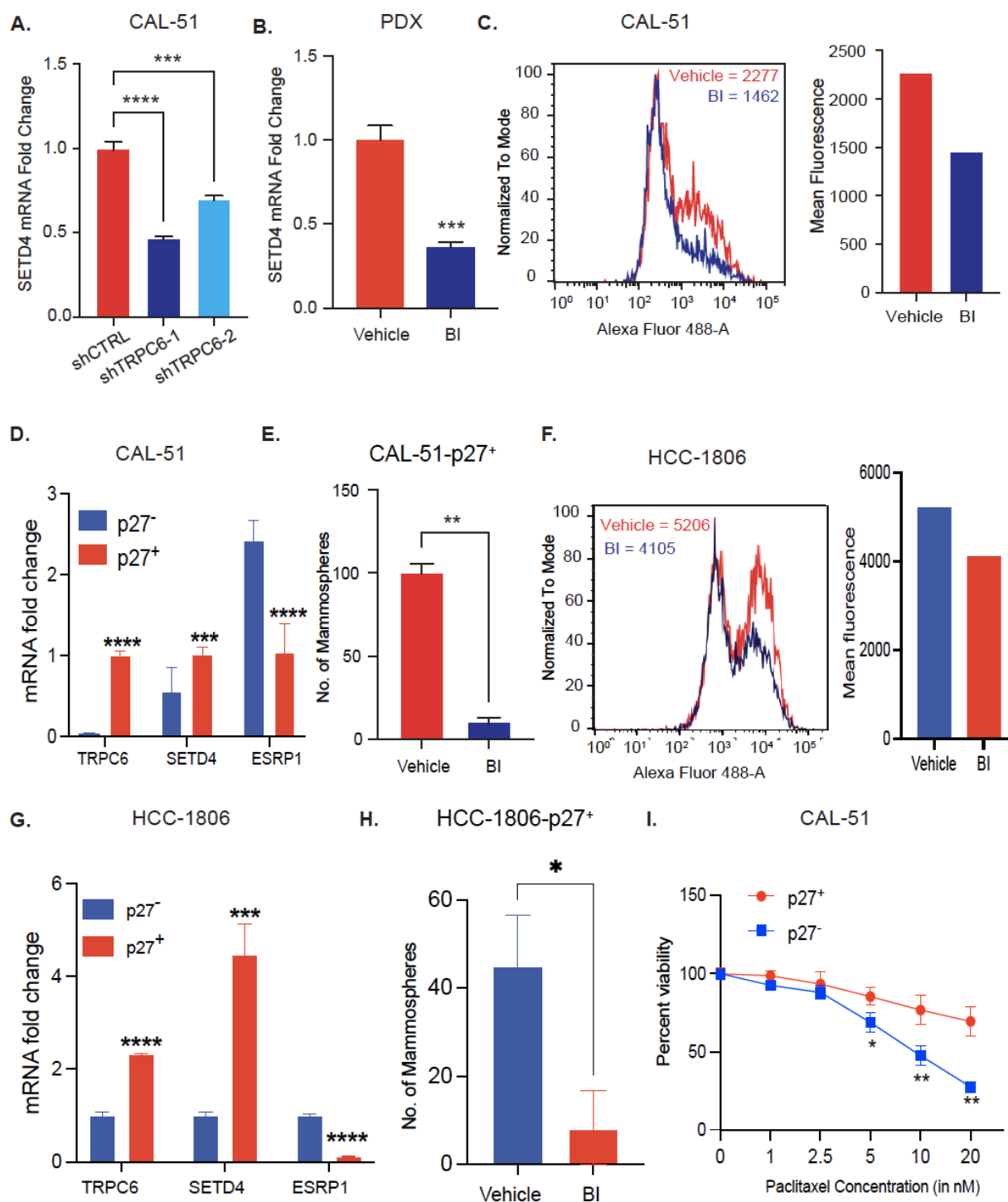


**Fig. 2.11: TRPC6 promotes quiescence.** **A.** SETD4 mRNA expression was quantified in TE3 cells that had been stably transfected with either a control (shCTRL) or TRPC6 shRNAs (shTRPC6-1, shTRPC6-2). **B.** SETD4 mRNA expression was quantified in a TNBC PDX that had been treated with either vehicle or BI-749327. **C.** CAL-51 cells expressing a p27-mVenus reporter

were treated with either vehicle or BI-749327 for 24 hours. Cells were detached and processed for flow cytometry (mean fluorescence indicated by the number on top left). Bar graph plotted using mean fluorescence intensity is shown on the right. **D.** Comparison of TRPC6, SETD4, and ESRP1 mRNA expression between the CAL-51 p27<sup>high</sup> and p27<sup>low</sup> populations. **E.** The p27<sup>high</sup> population of CAL-51 cells was treated with either vehicle or BI-749327 for 24 hours and their ability to form mammospheres was assessed. **F.** HCC-1806 cells expressing the p27-mVenus reporter were treated with either vehicle or BI-749327 for 24 hours and processed for flow cytometry. Bar graph of mean fluorescence intensity is shown on the right. **G.** HCC-1806 cells were transfected with a p27-mVenus reporter and sorted into p27<sup>high</sup> and p27<sup>low</sup> populations. The expression of TRPC6, SETD4, and ESRP1 mRNAs was compared between these populations. **H.** Mammosphere formation was assayed in the p27<sup>high</sup> population of HCC-1806 cells that had been treated with either DMSO or BI-749327 (10 uM). **I.** The sensitivity of the p27<sup>high</sup> and p27<sup>low</sup> populations of CAL-51 to increasing concentrations of paclitaxel was assessed. The SETD4 expression data shown represent the mean  $\pm$  SD of three independent experiments. \*P < 0.05, \*\*P < 0.01, \*\*\*P < 0.001, and \*\*\*\*P < 0.0001.

**TRPC6-regulated  $\alpha 6$  integrin splicing represses Myc:** Given our data that TRPC6-mediated splicing of the  $\alpha 6$  integrin has a casual role in chemoresistance (see **Fig. 2.4**), we investigated whether the  $\alpha 6B$  splice variant has a causal role in repressing Myc. Indeed, exogenous expression of the  $\alpha 6B$  splice variant in TRPC6 knockdown cells (**Fig. 2.7C**) was sufficient to rescue Myc suppression in both TE3 and CAL-51 cells (**Fig. 2.12A, B**). To investigate the mechanism by which  $\alpha 6B$  represses Myc, we pursued our previous finding that  $\alpha 6B$  signaling activates TAZ in breast CSCs (138) based on our observation that constitutively active TAZ represses Myc (**Fig. 2.12C**). This possible mechanism was strengthened by our observation that exogenous expression of  $\alpha 6B$  in the TRPC6 knockdown cells rescued TAZ activation and consequent ESRP1 suppression (**Fig. 2.12D**). To implicate TAZ directly in Myc repression, we found that knockdown of TAZ (**Fig. 2.5D**) caused a significant increase in Myc expression (**Fig. 2.12E, F**). Most importantly, to strengthen this connection we expressed a constitutively active TAZ (4SA) in our TRPC6 KD cells. Indeed, expression of a constitutively active TAZ construct was sufficient to rescue Myc expression in the knockdown cells to control levels.

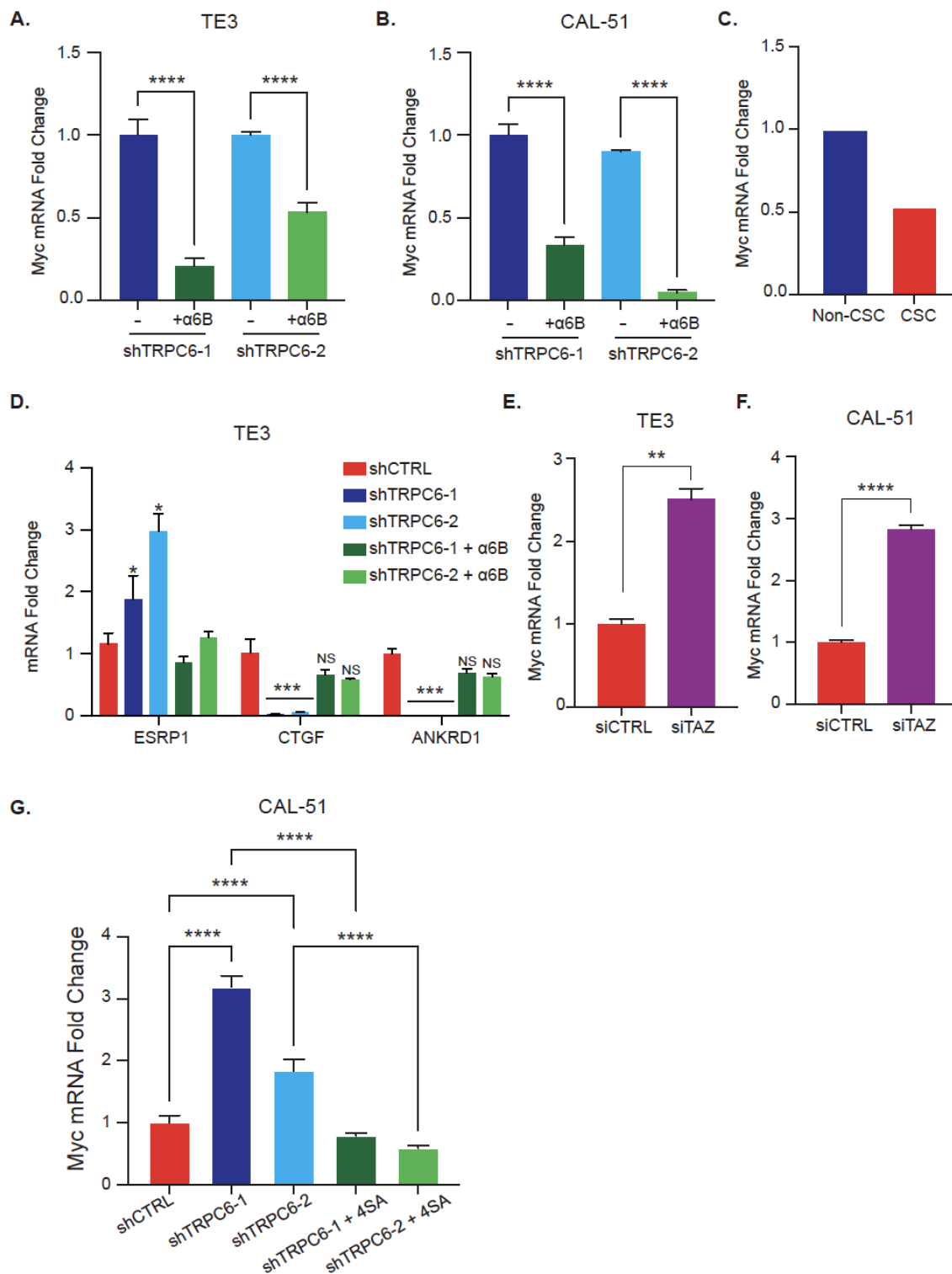


**Fig. 2.12: TRPC6-regulated  $\alpha 6$  integrin splicing contributes to Myc suppression.** **A, B.** Either TE3 (**A**) or CAL-51 (**B**) TRPC6 knockdown cells (shTRPC6-1, shTRPC6-2) were re-transfected with an  $\alpha 6B$  expression plasmid ( $\alpha 6B$ -GFP) followed by knockdown of the endogenous  $\alpha 6$  integrin (shITGA6). Myc mRNA expression was quantified by qPCR. **C.** Myc expression in the

non-CSC and CSC populations described in Fig. 1A. **D.** TE3 cells had been stably transfected with either a control (shCTRL) or TRPC6 shRNAs (shTRPC6-1, shTRPC6-2) were re-transfected with an  $\alpha 6B$  expression plasmid ( $\alpha 6B$ -GFP) followed by knockdown of the endogenous  $\alpha 6$  integrin (shITGA6). Expression of ESRP1, CTGF, and ANKRD1 mRNAs was quantified by qPCR. **E, F.** Myc mRNA expression was quantified in TE3 (**E**) and CAL-51 (**F**) cells that had been transfected with control siRNA (siCtrl), or siRNA targeting TAZ (siTAZ). **G.** Myc mRNA expression was quantified in CAL-51 cells transfected with either control shRNA (shCTRL) or TRPC6 shRNAs (shTRPC6-1, shTRPC6-2) were re-transfected with a constitutively active TAZ-4SA plasmid (4SA). The Myc expression shown in (A), (B), (E) and (F) represent the mean  $\pm$  SD of two independent experiments. \* $P < 0.05$ , \*\* $P < 0.01$ , \*\*\* $P < 0.001$ , and \*\*\*\* $P < 0.0001$ .

Taken together, our data indicate that TRPC6 and the  $\alpha 6B$  integrin synergize to activate TAZ and, consequently, repress Myc.

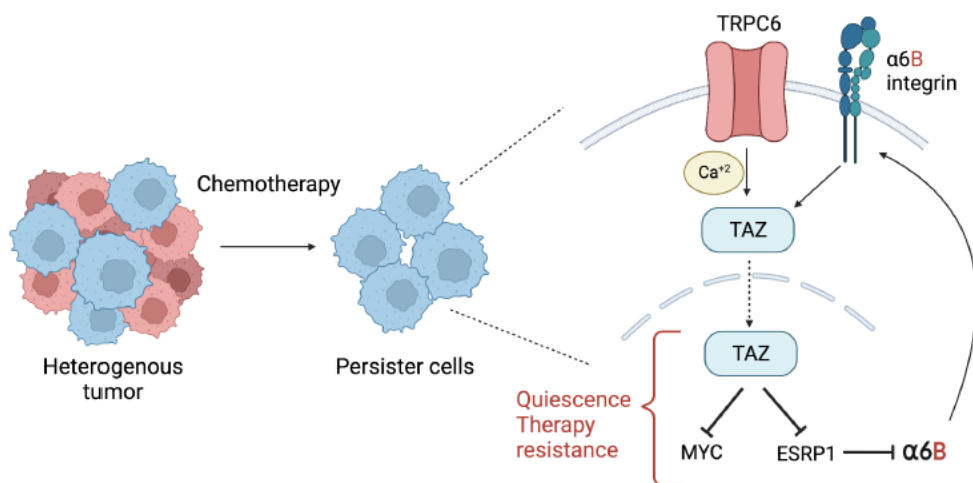


**Fig. 2.13: Summary schematic.** This schematic depicts the key findings in this study. Treatment of a heterogeneous tumor with chemotherapy results in the survival of persister cells that are resistant to chemotherapy. These cells have high TRPC6 expression levels and stem cell properties. TRPC6 sustains the expression of  $\alpha 6B$  in this population through suppression of the splicing factor ESRP1. Enrichment of  $\alpha 6B$  in this population drives chemoresistance through a TAZ-mediated MYC suppression. This suppression of Myc maintains these cells in a quiescent state to survive chemotherapeutic stress.

## Discussion

In this study, which is summarized in the schematic shown in **Fig. 2.13**, we demonstrate that a specific cation channel, TRPC6, which is known to regulate calcium entry in TNBC (44), is intimately associated with a CSC population and has a causal role in stemness and chemoresistance. The most novel aspect of the study is the mechanism by which TRPC6-mediated calcium entry promotes these functions. Our data revealed that TRPC6 is at the nexus of a signaling network that regulates mRNA splicing. More specifically, we discovered that TRPC6-mediated calcium entry sustains a splice variant of the  $\alpha 6$  integrin,  $\alpha 6B$ . TRPC6 and integrin  $\alpha 6B$  signaling function in tandem to repress Myc and, consequently, sustain a quiescent state that is resistant to chemotherapy. In other terms, tumor cells that resisted chemotherapy in our study were dependent on the TRPC6/ $\alpha 6B$  signaling axis for their survival. Importantly, we demonstrate that it is possible to sensitize TNBC organoids and PDX tumors to chemotherapy using a specific inhibitor of TRPC6, which disrupts this signaling axis.

A major finding in this study is that TRPC6-mediated calcium signaling regulates alternative mRNA splicing. Alternative splicing is a key mechanism for ensuring proper developmental programs that demand vast genetic diversity. Tumors hijack alternative splicing programs that contribute to the intratumor transcriptomic heterogeneity, EMT and therapy resistance (148, 149). Although previous studies have implicated  $Ca^{2+}$  signaling in the regulation of splicing (150), the mechanisms reported are distinct from ours (151-153). These studies focused largely on how calcium-mediated signaling impacts splicing by directly binding RNA elements of specific genes. For example, the  $Ca^{2+}$ -calmodulin dependent kinase IV (CaMKIV) regulates splicing of the STREX exon of the calcium-activated potassium channel in neurons by directly

binding to the CaMKIV-responsive RNA element (152, 153). In contrast, we demonstrate that TRPC6 regulates the expression of a specific splicing protein, ESRP1. ESRP1 is of interest because it is known to differentially enrich for splice variants that play a crucial role in cell fate decisions specifically associated with epithelial cell fate (135, 136, 154). The focus of our study was the  $\alpha 6$  integrin, which exists as two splice variants:  $\alpha 6A$  and  $\alpha 6B$  (155, 156) that are regulated by ESRP1. Specifically, the UGC-rich recognition motif on the  $\alpha 6$  mRNA binds ESRP1 and, consequently through exon exclusion, generates  $\alpha 6A$  (154). Previous studies by our group established that the  $\alpha 6B$  variant promotes stemness, a property that is not shared by the  $\alpha 6A$  variant, and that the relative expression of ESRP1 determines expression of these variants and, consequently, regulates stem cell properties (137). The novelty of the current study is that we link this integrin splicing mechanism to a specific calcium channel and a calcium-mediated signaling pathway. Although we focused on the splicing of the  $\alpha 6$  integrin in this study, ESRP1 is known to regulate the splicing of other mRNAs that contribute to stemness. Of note, ESRP1 enriches for the CD44V splice variant relative to the CD44S variant that has a causal role in stemness (136). Consistent with this observation, we observed that TRPC6-mediated suppression of ESRP1 maintains high levels of CD44S compared to CD44V (**Fig S2F**). This ability of TRPC6 to orchestrate a differential splicing pattern reveals a novel,  $Ca^{2+}$ -dependent mechanism to generate transcriptomic diversity that drives stemness in cancer. It is worth noting that these findings may also have relevance for non-cancer diseases that involve TRPC6. Specifically, defects in the *TRPC6* gene are associated with stage 5 chronic kidney disease that are often mediated by deregulated expression or activity of adhesion proteins such as  $\alpha 3\beta 1$  integrins. These changes alter laminin binding and downstream actin cytoskeletal arrangement that ultimately leads to detachment of podocytes from basement membrane (157, 158).

Arguably, the most consequential aspect of our data is the involvement of the TRPC6-mediated splicing mechanism in chemoresistance. Our findings revealed that TNBC cells and organoids that persist after paclitaxel treatment are characterized by high expression of *TRPC6* and  $\alpha 6B$  and low expression of ESRP1. Importantly, we also demonstrated that each of these molecules has a causal role in sustaining the survival of these persister cells. These data are substantiated by our analysis of a publicly available dataset (143) that revealed a correlation between *TRPC6* expression and chemoresistance (**Fig. 2.3B, F**). In pursuit of the mechanism involved, we were informed by a seminal study that treatment-persistent tumor cells adopt a state that resembles embryonic diapause characterized by suppressed Myc activity (143). Of particular interest to us was their finding that Myc upregulation sensitizes persister cells to chemotherapy. The data in our study provide a novel mechanism for how Myc can be repressed that involves the ability of the TRPC6/ $\alpha 6B$  signaling axis to repress Myc by activating TAZ. These data also provide a mechanism for how TRPC6/ $\alpha 6B$  enable cells to persist after paclitaxel treatment. Most likely, the repression of Myc by TRPC6 maintains cells in a more quiescent state that is less amenable to paclitaxel-mediated killing.

Our study adds significantly to the existing literature on the mechanism by which calcium signaling regulates the function of CSCs. Much of the literature on calcium signaling in cancer has focused on the regulation of transcription mediated by calcium-dependent transcription factors, most notably, NFAT (159). Interestingly, however, our data do not support a role for NFAT in TRPC6-mediated regulation of CSC function (**Fig. 2.5G**). This observation is consistent with the report that calcineurin/NFAT are dispensable for promoting a partial EMT by  $Ca^{2+}$  influx (114). Rather, our data reveal a more biophysical mechanism that involves the ability of TRPC6-mediated RhoA activation and consequent increase in contractility to activate TAZ and repression of ESRP1.

Although previous studies have demonstrated the ability of TRPC6 to activate RhoA (142) and the ability of RhoA-mediated contractility to activate TAZ (141), the regulation of TAZ activation and its impact on mRNA splicing by Ca<sup>2+</sup> signaling is novel and significant.

In summary, the data we report reveal a novel mechanism that contributes to stemness and chemoresistance in TNBC that involves the regulation of integrin  $\alpha$ 6 mRNA splicing by TRPC6-mediated Ca<sup>2+</sup> signaling. The TRPC6/ $\alpha$ 6B signaling axis enables TNBC cells to persist after paclitaxel treatment by a mechanism that involves the repression of Myc. Our ability to sensitize TNBC organoids *in vitro* and PDX tumors *in vivo* to chemotherapy using a specific inhibitor of TRPC6 suggests that this approach could be effective to mitigate the aggressiveness of TNBC, especially for tumors that have become resistant to standard of care chemotherapy.

## Materials and Methods

**Cells and reagents:** HMLER cells were provided by R. Weinberg (Massachusetts Institute of Technology). MDA-MB-231 and HCC1806 cells were purchased from the American Type Culture Collection, and the TE3 variant of MDA-MB-231 cells was provided by S. Tavazoie (Rockefeller University). CAL-51 cells were obtained from the Leibniz Institute DSMZ, Germany. The TRPC6 inhibitor BI-749327 was purchased from MedChem Express (Catalogue no. HY-111925). The paclitaxel was purchased from Selleckchem (Catalogue no. S1150). The NFAT inhibitor was purchased from Cayman Chemicals (Catalogue no. 13855). The following Abs that were used for flow cytometry were purchased from BioLegend: CD24–allophycocyanin (APC; ML5, BioLegend), CD44-FITC (IM7, BioLegend) and anti-rabbit FITC (MRM-47, BioLegend), anti-

Rabbit-555 (Invitrogen-A32732), TRPC6 (18236-1-AP, Proteintech). For immunoblotting, the following Abs were used: Tubulin [Cell Signaling Technology (3873)], Beta-Actin (3700S, Cell Signaling Technology)TRPC6 (ACC-017, Alomone Labs), GAPDH (14C10) [Cell Signaling Technology 2118S],  $\alpha$ 6A (1A10) (MAB1356, Millipore), and  $\alpha$ 6B (6B4) (MAB1358, Millipore), Myc (Y69) (32072, Abcam), ESRP1 (PA5-25833, ThermoFisher), HA (3724, Cell Signaling Technology), and GST-HRP (5475, Cell Signaling Technology). For immunofluorescence the following antibodies were used: TRPC6 (18236-1-AP, Proteintech), TAZ (clone M2-616, 560235, BD-Pharmingen).

**shRNAs and expression constructs:** The following lentiviral shRNAs were obtained from our core facility: TRPC6 (TRCN0000431016, TRCN0000044106). Lentiviral shRNAs specific for ESRP1 (pLV[shRNA] NeoU6>hESRP1[shRNA]) were designed and purchased from Vector Builder (Vector ID: VB220524-1274mnz, and VB220524-1275vdm). TEAD 1/3/4 shRNA were provided by J. Mao (University of Massachusetts Chan Medical School). A TRPC6-HA lentiviral plasmid (pLV[Exp]-Bsd CMV>hTRPC6[NM\_004621.6]/HA) was also designed and purchased from Vector-Builder (Vector ID: VB191024-1847whk). A site-directed mutagenesis kit (Q5<sup>®</sup> Site-Directed Mutagenesis Kit, E0554S) (New England BioLabs) was used to make the desired TRPC6 G757D pore-mutant lentiviral vector based on the backbone (cDNA TRPC6-HA vector). HA-ESRP1 constructs were provided by Dr. Chonghui Cheng (Baylor College of Medicine). pRC- $\alpha$ 6A or  $\alpha$ 6B plasmids were prepared as described (Shaw et al., 1993) and subcloned into the lentiviral vector pCDH. We used the Myc expression plasmid as described in Goel *et. al*, 2016. The quiescent reporter plasmid pCDH-EF1-mVenus-p27K was bought from Addgene (plasmid #176651). Lipofectamine 3000 (Thermo Fisher Scientific) was used for plasmid

transfections. SMARTpool siRNAs against TAZ were purchased from Horizon Discovery and used to transfect the cells as per manufacturer's instructions at a total concentration of 25 nM.

**ITGA6 CRISPR knockout system:** To generate ITGA6 knockout cells, we used Alt-R CRISPR-Cas9 System (IDT). The following gRNAs were used: (Human sgITGA6-1: CCTTCGGGAGGACAACGTGATC, sgITGA6-2: TTTCCAGTTAATAAGTACCCG). The following reagents were purchased from IDT: Alt-R CRISPR crRNA (2 nmol), CRISPR-Cas9 tracrRNA (Cat. 1072532), and Cas9 Nuclease (Alt-RTM S.p. Cas9 Nuclease 3NLS, Cat. 1074181) and were used to assemble Cas9:crRNA:tracrRNA RNP complex. The RNP complexes were transfected in  $1 \times 10^6$  Cal51 cells using Nucleofector Device (Amaxa) with program X-001. After five days in culture, pooled ITGA6 negative cells were sorted using flow cytometry with the ITGA6-APC antibody (Biolegend, Cat. 324208).

**Cell-based assays:** For mammosphere assays, single cell suspensions of TE3 and HCC1806 cells ( $10^3$  cells) or CAL-51 cells ( $5 \times 10^2$ ) were plated on ultra-low attachment plates (24 well; Corning Costar; catalogue no. CLS3473) in serum-free, mammary epithelial cell growth medium (MEGM) supplemented with EGF (2ng/mL), bFGF 2ng/mL, heparin (4ng/mL), methylcellulose (1%), and B27 supplement diluted 1:50 (136). The mammospheres were counted after 5 days using Celigo Imaging Cytometer (Nexcelom) and processed for secondary passage as we described previously (127). For mammosphere assays using PDXs, tumors were chopped into fragments with scalpel blades and digested with 2 mg/mL of collagenase (Sigma, C0130) and 100 mg of 1 mg/mL hyaluronidase (Sigma, H3506) for 4–6 h at 37°C with shaking. Tissue fragments were vortexed gently every 15–30 min. The single-cell suspension was then passed through a 40- $\mu$ m cell strainer, centrifuged at 2000 rpm for 5 min and washed three times with PBS. The washed cells were plated as mentioned above for the respective serial passage or limiting dilution mammosphere assays.

For flow cytometry, cells were incubated with primary antibodies and the appropriate secondary antibodies following the manufacturer's instructions. To assay cell viability, cells were seeded at a density of  $5 \times 10^3$  cells per well. After 24 hours, cells were treated with either BI-749327 or paclitaxel as described in the figure legends and viability was assessed using crystal violet staining. The absorbance measured at 600 nm was normalized to the saline solution control. For immunofluorescence microscopy, cells were cultured on glass-bottom dishes (Ibidi #81218-200), fixed with paraformaldehyde (2%) for 20 minutes and permeabilized with Triton X-100 (0.5%) for 5 min and then blocked in buffer (PBS, 5% normal goat serum, 0.1% Triton X-100, and 2 mM sodium azide) for 30 min. The cells were then incubated with primary antibodies in blocking buffer for 1 h at room temperature, washed with Triton X-100 (0.1%) in PBS and then stained with secondary antibodies for 1 hour at room temperature. After washing, the cells were mounted in Vectashield with DAPI (Vector Laboratories, UX-93952-24). Images were captured at x20, x40 and x60 magnification using a confocal microscope (Zeiss).

**Biochemical assays:** For immunoblotting, adherent cells were washed with PBS and scraped on ice in radioimmunoprecipitation assay (RIPA) buffer, which was supplemented with protease and phosphatase inhibitors (Roche). Laemmli 6X SDS sample buffer (BP-111R, Boston BioProducts) was added to each sample, which were boiled for 10 min prior to SDS-polyacrylamide gel electrophoresis. Immunoblotting primary antibodies were used in the following dilutions: TRPC6 ACC-017 (Alomone Labs) 1:1000, Tubulin and GAPDH 1:2000, ESRP1 (Thermofisher) 1:2000,  $\alpha$ 6A 1:1000,  $\alpha$ 6B 1:1000, HA 1:2000. RhoA activity was assessed using a GST fusion protein containing the Rho-binding domain of ROCK (RBD) as previously described (160, 161)

**Real time qPCR:** mRNA quantification was accomplished using an RNA isolation kit (BS88133, Bio Basic Inc.), and complementary DNAs (cDNAs) were produced using an Azura cDNA synthesis kit (AZ-1996, Azura Genomics). Azura View GreenFast qPCR Blue Mix LR was used as the qPCR Master Mix (AZ-1996, Azura Genomics).

**RNA sequencing:** RNA was extracted from the indicated cells using a Qiagen RNeasy Micro Kit (74004) and sent to Quick Biology for quantification, sequencing, and analysis.

Quick Biology Sequencing method: Library for RNA-Seq was prepared according to KAPA Stranded mRNA Hyper prep polyA selected kit with 201-300 bp insert size (KAPA Biosystems, Wilmington, MA) using 250 ng total RNAs as input.

Final library quality and quantity was analyzed by Agilent Technologies 4200 station and Qubit 3.0 (Thermo Fisher Scientific Inc, Waltham, MA) Fluorometer. 150 bp paired-end reads were sequenced on Illumina HiSeqX (Illumina Inc., San Diego, CA).

Each sample had a sequencing depth of 20-30 million. RNASeq analysis was performed with OneStopRNAseq workflow (162). Paired-end reads were aligned to human primary genome hg38, with star\_2.5.3a (163), annotated with GENCODE GRCh38.p12 annotation release 34 (164). Aligned exon fragments with mapping quality higher than 20 were counted toward gene expression with featureCounts\_1.5.2 (165). Differential expression (DE) analysis was performed with DESeq2\_1.20.0 (166). Within DE analysis, 'ashr' was used to create log<sub>2</sub> Fold Change (LFC) shrinkage for each comparison (167). Significant DE genes (DEGs) were filtered with the criteria

FDR < 0.05. Heatmaps were created with Prism. Gene set enrichment analysis were performed with GSEA (168).

**Patient derived organoids and chemoresistance models:** Freshly resected biopsies from de-identified TNBC patients were received from UMass Cancer Center Tumor Bank. The tumor tissue was digested utilizing the tissue dissociation kit (Miltenyi Biotech) and gentleMACS Dissociator. The dissociated tumor was washed 3X with PBS and embedded into reduced growth factor basement membrane extract (Cultrex). These TNBC tumor derived organoids were cultured in organoid media as described previously (169). The paclitaxel resistant CAL-51 cells and TNBC organoids were generated by culturing them in increasing concentrations of paclitaxel (1-20nM) for 6 weeks.

**Animal studies:** For the limiting dilution experiment, CAL-51 cells were suspended in 35 ul of PBS and injected into the mammary fat pad of 6–8-week-old NOD.Cg-Prkdc<sup>scid</sup> IL2rg<sup>tm1Wjl</sup> (abbreviated as NSG) mice. Tumor occurrence in each group was noted and the results were analyzed using ELDA (130). Mice were monitored for 12-15 weeks, and tumor volume was measured using calipers. Once the tumors reached 1 cm<sup>3</sup>, the mice were euthanized, and the tumors collected for histological analysis. For therapeutic studies, a PDX (HCI028) obtained from the Huntsman Cancer Institute was implanted orthotopically into the mammary fat pad of 6–8-week-old NSG mice. The mice were divided into 4 groups of 5 mice each. When the tumor volume reached 100mm<sup>3</sup>, mice were treated as described in the legend to Fig. 2. All mouse procedures were done under the guidance of the University of Massachusetts Medical School Institutional Animal Care and Use Committee in accordance with the institutional and regulatory guidelines.

**Quantification and statistical analysis:**

Student's t test was used for comparison between two groups. Multiple group comparisons were performed using one-way analysis of variance (ANOVA). Statistical tests were carried out using GraphPad Prism version 9.0, and a P value of less than 0.05 was considered significant. The bars in graphs represent mean  $\pm$  SD. \*P < 0.05, \*\*P < 0.01, \*\*\*P < 0.001, and \*\*\*\*P < 0.0001.

Table 2:

REAGENT or RESOURCE	SOURCE	IDENTIFIER
<b>Antibodies</b>		
APC anti-human CD24	BioLegend	Cat# 311118; RRID: AB_2072735
FITC anti-mouse/human CD44	BioLegend	Cat# 103006, RRID: AB_312957
Goat anti-Rabbit IgG (H+L) Highly Cross-Adsorbed Secondary Antibody, Alexa Fluor Plus 488	Invitrogen	Cat# A32731; RRID: AB_2633280
Goat anti-Rabbit IgG (H+L) Highly Cross-Adsorbed Secondary Antibody, Alexa Fluor Plus 555	Invitrogen	Cat# A32732; RRID: AB_2633281
Rabbit polyclonal Anti-TRPC6 Antibody	Alomone Labs	Cat# ACC-017, RRID: AB_2040243
Rabbit polyclonal anti-TRPC6	Proteintech	Cat# 18236-1-AP, RRID: AB_10859822
Mouse monoclonal anti- $\beta$ -Actin (8H10D10)	Cell Signaling Technology	Cat# 3700, RRID: AB_2242334
Rabbit Monoclonal Anti-GAPDH Antibody, Unconjugated, Clone 14C10	Cell Signaling Technology	Cat# 2118, RRID: AB_561053
Mouse Monoclonal Anti-alpha-Tubulin Antibody, Unconjugated, Clone DM1A	Cell Signaling Technology	Cat# 3873, RRID: AB_1904178
Rabbit polyclonal anti-ESRP1 Antibody	Thermo Fisher Scientific	Cat# PA5-25833, RRID: AB_2543333
Mouse monoclonal Anti-Integrin alpha6A, cytoplasmic domain, clone 1A10	Millipore	Cat# MAB1356, RRID: AB_94179
Mouse monoclonal Anti-Integrin alpha6B, cytoplasmic domain, clone 6B4	Millipore	Cat# MAB1358, RRID: AB_94180

Rabbit monoclonal anti-c-Myc antibody [Y69]	Abcam	Cat# ab32072, RRID: AB_731658
Rabbit monoclonal anti-RhoA (67B9) mAb	Cell Signaling Technology	Cat# 2117, RRID: AB_10693922
Rabbit monoclonal anti-HA-Tag (C29F4) mAb	Cell Signaling Technology	Cat# 3724, RRID: AB_1549585
Rabbit monoclonal anti-GST (91G1) mAb (HRP Conjugate)	Cell Signaling Technology	Cat# 5475, RRID: AB_10707323
Mouse monoclonal anti-TAZ	BD-Pharmingen	Cat# 560235, RRID: AB_1645338
Mouse monoclonal APC anti-human CD326 (Ep-CAM)	BioLegend	Cat# 324208, RRID: AB_756082
<b>Bacterial and virus strains</b>		
NEB 5-alpha Competent <i>E.coli</i>	New England Biolabs	Cat# C2987
<b>Biological samples</b>		
Breast cancer derived Organoids	As described in Walker <i>et. al.</i> , 2022 (24)	N/A
PDX (HCI028)	Huntsman Cancer Institute	N/A
<b>Chemicals, peptides, and recombinant proteins</b>		
Animal-Free Recombinant Human EGF	Peprtech	Cat# AF-100-15-1mg
MEGM bullet kit	lonza	Cat# cc-3150
Recombinant Human FGF-basic	Peprtech	Cat# 100-18B
B-27 supplement (50X)	Gibco	Cat# 17504-001
Insulin	Millipore Sigma	Cat# I1882-100MG

BI-749327	MedChem Express	Cat# HY-111925
Y27632 2HCL	Selleckchem	Cat# S1049
10074-G5	Selleckchem	Cat# S8426
NFAT Inhibitor	Cayman Chemical	Cat# 13855
<b>Critical commercial assays</b>		
AzuraQuant cDNA synthesis kit	Azura genomics	Cat# AZ-1995
AzuraView greenfast qPCR blue mix	Azura genomics	Cat# AZ-2401
Tumor Dissociation Kit, human	Miltenyi BioTec	Cat# 130-095-929
Q5® Site-Directed Mutagenesis Kit	New England Biolabs	Cat# E0554S
Qiagen RNeasy Micro Kit	Qiagen	Cat# 74104
<b>Deposited data</b>		
Public data: RNAseq from Dhimolea, <i>et. al.</i> 2021	GEO	GEO: GSE162285
RNA-Seq: TE3 cells Vehicle, BI treatment	GEO	GEO: GSE242592
<b>Experimental models: Cell lines</b>		
MDA-MB-231-TE3	Kindly provided by Dr. S. Tavazoie, Rockefeller University).	N/A
MDA-MB-231	American Type Culture Collection	Cat# HTB-26

CAL-51	Leibniz Institute DSMZ, Germany	ACC-302
HCC-1806	American Type Culture Collection	Cat# CRL-2335
HMLER	Kindly provided by Dr. R. Weinberg, Massachusett s Institute of Technology	N/A
<b>Experimental models: Organisms</b>		
NOD.Cg-Prkdscid IL2rgtm1Wjl (NSG)	Jackson Laboratory	N/A
<b>Experimental model: Strain of bacteria</b>		
DH5 $\alpha$	NEB	Cat# C2987H
<b>Oligonucleotides</b>		
<i>h18S</i> fwd 5'-GTCGCTCGCTCCTCTCCTACT-3'; rev 5' TCTGATAAATGCACGCATCCC-3'	IDT	N/A
<i>hTRPM8</i> fwd, 5'-GTGAAAGCGACTTGGTGAATTTT-3; rev 5'-GTGGCCTTGGAAATCTTTGGTAA-3'	IDT	N/A
<i>hTRPV6</i> fwd 5'-ACTGACCTCGACTCTCTATGAC-3'; rev 5'-GTGGTGATGATAAGTTCCAGCAG-3'	IDT	N/A
<i>hORAI1</i> fwd 5'- GACTGGATCGGCCAGAGTTAC-3'; rev 5'-GTCCGGCTGGAGGCTTTAAG-3'	IDT	N/A

<p><i>hORAI3</i></p> <p>fwd 5'-TGGGTCAAGTTTGTGCCCAT-3'; rev 5'-AGCTGGACTAAGGGAGGTAGC-3'</p>	IDT	N/A
<p><i>hTRPC6</i></p> <p>fwd 5'-TTGAGGATGACGCTGATGTG-3'; rev 5'-CCAGATTGAAGGGTACAGGAAG-3'</p>	IDT	N/A
<p><i>hTRPC6 (G757D) primer for sequencing</i></p> <p>fwd 5'-AAAGAACTTGACATTTTAGGAAGTCATG-3'; rev 5'-TCTTCATTTATCTTGTTTCATCTC-3'</p>	Genewiz	N/A
<p><i>hESRP1</i></p> <p>fwd: 5'-CAGAGGCACAAACATCACAT-3'; rev: 5'-AGAACTGGGCTACCTCATTGG-</p>	IDT	N/A
<p><i>hCTGF</i></p> <p>fwd 5'-CAGCATGGACGTTTCGTCTG-3'; rev 5'-AACCACGGTTTGGTCCTTGG 3</p>	IDT	N/A
<p><i>hANKRD1</i></p> <p>fwd 5'-AGTAGAGGAACTGGTCACGG-3' rev 5'-TGTTTCTCGCTTTTCCACTGTT-3'</p>	IDT	N/A
<p><i>hSETD4</i></p> <p>fwd 5'-GGAGAACAAGCCGGATCAGAA-3'; rev 5'-AGCAGGCGCTAAGTTTGAATC-3'</p>	IDT	N/A
<p><i>hMYC</i></p> <p>fwd: 5'- CTC AAA GCT GGC CAG TAG AA-3' rev 5'- CGT CAC ACG AAC CGA CAA TA-3'</p>	IDT	N/A
<p><i>hCDC25A</i></p> <p>fwd: 5'- TCTGGACAGCTCCTCTCGTCAT-3'; rev: 5'- ACTTCCAGGTGGAGACTCCTCT-3'</p>	IDT	N/A
<p>sgITGA6-1: CCTTCGGGAGGACAACGTGATC, sgITGA6-2: TTTCCAGTTAATAAGTACCCG</p>	IDT	N/A

Alt-R CRISPR crRNA (2 nmol)	IDT	
Alt-RTM S.p. Cas9 Nuclease 3NLS	IDT	Cat. 1074181
<b>Recombinant DNA</b>		
pLV[Exp]-Bsd CMV>hTRPC6[NM_004621.6]/HA	Vector Builder	VB191024-1847whk
pLV[shRNA] NeoU6>hESRP1[shRNA]	Vector Builder	VB220524-1274mnz, and VB220524-1275vdm
HA-ESRP1	Kindly provided by Dr. Chonghui Cheng (Baylor College of Medicine)	N/A
pRC-alpha6A and pRC-alpha6B	As described Shaw et al., 1993 (69)	N/A
GST-RBD plsamid	As described in Ren et al EMBO J. 1999 (59)	Addgene , Cat #15247
plasmid pCDH-EF1-mVenus-p27K	As described in Correia et al Nature. 2021 (70)	Addgene , Cat #176651
pCDH-puro-cMyc	As described in Cheng et al Clin Cancer Res. 2013 (71)	Addgene, Cat# 46970
<b>Software and algorithms</b>		
GraphPad Prism v 9.3.1	GraphPad Software	N/A

FlowJo Software (for MAC) [software application] Version 10.7.1.	Becton, Dickinson, and Company	<a href="https://docs.flowjo.com/flowjo/installation/">https://docs.flowjo.com/flowjo/installation/</a>
Fiji by ImageJ	Open Source	<a href="https://imagej.net/software/fiji/">https://imagej.net/software/fiji/</a>
ELDA: Extreme Limiting Dilution Analysis	Walter Eliza Hall institute of medical research	<a href="https://bioinf.wehi.edu.au/software/elda/">https://bioinf.wehi.edu.au/software/elda/</a>
Adobe Illustrator	Adobe Creative Cloud	N/A
Affinity DESIGNER 2	Serif	N/A
Biorender		N/A

## Chapter III: Inducing ferroptosis to impede metastasis

**Authors: Dimpi Mukhopadhyay, Hira Lal Goel, Emmet Karner, Mengdie Wang, Choua Xiong, Arthur Mercurio**

**Authors:** Dimpi Mukhopadhyay<sup>1</sup>, Hira Lal Goel<sup>1</sup>, Emmet Karner<sup>1</sup>, Arthur M. Mercurio<sup>1\*</sup>

### **Affiliations**

<sup>1</sup>Department of Molecular, Cell and Cancer Biology, University of Massachusetts Chan Medical School, Worcester, Massachusetts, USA 01605

\*Corresponding author

### **CONTRIBUTIONS:**

Dimpi Mukhopadhyay conceptualized the study, performed experiments, made figures, and wrote the manuscript. Hira Goel also performed experiments and provided feedback. Emmet Karner performed bioinformatics Gene set enrichment analysis. Arthur M. Mercurio oversaw and conceptualized the study, provided feedback on experiments and the manuscript.

## **Introduction**

Reducing the morbidity and mortality associated with the relapse and metastasis of breast cancer continues to be a major challenge. Considerable evidence indicates that relapse and metastasis are driven by stem-like treatment persister cells. In Chapter II, I reported that TRPC6 contributes to the survival of quiescent cancer stem cells that persist after chemotherapy in TNBC. TRPC6-mediated calcium signaling is implicated in the maintenance of persister cells. The suppression of MYC expression by TRPC6 is central to the preservation of the quiescent, slow-cycling population

that endures chemotherapy. Together, my work contributed to our understanding of mechanisms that sustain the persister cell state. However, we still don't fully understand how persister cells respond to stress and survive treatments like chemotherapy. Some studies in ovarian cancer have indicated that in Taxol resistant populations, GPX4 inhibition synergizes with Taxol to induce ferroptosis (170). This is a very interesting finding that highlights a key issue in cancer biology: our lack of understanding of the nature of persister cells and the metabolic adaptations that allow them to survive stressful conditions.

To characterize the persister population in more detail, I analyzed my RNA-Seq data comparing the transcriptomes of control and TRPC6-inhibited TNBC cells. GSEA of these data identified a transcriptional signature indicative of ferroptosis induction, in the inhibitor-treated group (171). As I described in the Introduction chapter, ferroptosis is a form of cell death resulting from the peroxidation of membrane phospholipids (80). This observation led me to investigate whether TRPC6 has a causal role in promoting ferroptosis resistance and, if so, to understand the mechanism involved. In this chapter, I report the results of this investigation.

## Results

**TRPC6 inhibition sensitizes TNBC resistant populations to ferroptosis:** GSEA was performed on the RNA-Seq data previously published for TE3 cells treated with the TRPC6 inhibitor BI-749327 (172). This analysis identified several pathways that were positively enriched upon TRPC6 inhibition (**Fig. 3.1A**). Notably, ferroptosis was among the top three enriched pathways affected by BI-749327 treatment. This transcriptional signature of ferroptosis had been described by Stockwell's group (171). This observation prompted me to explore whether TRPC6 plays a role in modulating the cell's response to ferroptosis. To investigate a role for TRPC6 in ferroptosis, I treated a TNBC organoid (9881T) with erastin and BI-749327, either alone or in combination. Erastin induces ferroptosis by inhibiting xCT. To discern whether loss of viability was due to ferroptosis or apoptosis, I included treatment groups with either the ferroptosis inhibitors deferoxamine or ferrostatin-1 or an apoptosis inhibitor ZVAD (173, 174). Deferoxamine binds to excess iron, and ferrostatin-1 prevents lipid peroxidation. Thus, they prevent the Fenton reaction between the phospholipid peroxy radical and iron from proceeding. The organoid was treated for 24 hours and then viability was measured using 3D Cell Titer Glow (CTG). Analysis of the viability assay clearly showed that the TNBC is quite resistant to erastin or BI-749327 when treated individually, but can be sensitized significantly when treated in combination, compromising cell viability. The loss of cell viability seen with the combination of erastin and BI-749327 was reversed by either deferoxamine or ferrostatin-1 (Fer-1), but not by ZVAD, suggesting a potential role of TRPC6 in ferroptosis resistance. To further substantiate this data, I treated CAL-51 cells with imidazole ketone erastin (IKE) and BI-749327 and the stable TRPC6 KD cells with increasing concentrations of IKE. In both cases, I saw a significant reduction of cell viability in the

combination treatment group (IKE and BI-749327) (**Fig. 3.1C**) and in TRPC6 KD compared to control cells (**Fig. 3.1D**). I also observed a rescue of cell viability with ferrostatin-1.

Previously, I had observed that the TNBC cell line HCC1806 has heterogeneous expression of TRPC6. In HCC1806 cells, treatment with FIN56 and BI-749327 caused significant cell death compared to control and FIN56 (ferroptosis inducer; by inhibiting both Xct and GPX4) treatment alone (**Fig. 3.1E**). This result makes a strong case for TRPC6 inhibition in combination with Ferroptosis inducers to target resistant cells. However, it is imperative to understand whether TRPC6 is sufficient to induce resistance. To investigate this possibility, I used the MDA-MB-231 cells, a TNBC cell line that is ferroptosis sensitive and expresses low levels of TRPC6. I stably transfected these cells with either an empty vector or WT TRPC6 tagged with HA. These cells were treated with increasing concentrations of IKE. Analysis of viability revealed that TRPC6 overexpression was sufficient to promote resistance compared to the control cells (**Fig. 3.1G**).

As previously discussed, ferroptosis results from excessive membrane phospholipid peroxidation, leading to cell death. To confirm that TNBC cells undergo ferroptosis when treated with IKE and BI, I assessed lipid peroxidation using the C11-Bodipy assay (175). Peroxidation of the lipid moiety in the dye causes the fluorophore to shift its emission from red to green channel. This allows a semi quantitative measurement of the extent of lipid peroxidation in the different cell types and treatments using flow cytometry. I observed a significant increase in the median fluorescence intensity of the GFP channel in the CAL51 TRPC6 KD cells treated with IKE compared to the control cells that was rescued by ferrostatin-1. This result substantiates my initial observation that TNBC cells that are resistant to ferroptosis can be sensitized when treated in combination with TRCPC6 channel inhibitors.

These significant findings, particularly in **Fig. 3.1B-F**, raise the question of whether TNBC cells exhibit a varied response to ferroptosis inducers? In Chapter II, I demonstrated that treatment persister cells, that are quiescent and slow cycling, are enriched in TRPC6. Utilizing the p27mVenus system, which facilitates the sorting of quiescent (p27<sup>high</sup>) from proliferative (p27<sup>low</sup>) populations, I successfully isolated a persister cell subset of CAL51 cells. As expected, the quiescent persister cells (p27<sup>high</sup>) have significantly high levels of TRPC6 (**Fig. 3.1H**). This model allows me to assess the heterogeneous response of TNBC cells to ferroptosis. To investigate this, I treated p27<sup>high</sup> and p27<sup>low</sup> cells with increasing doses of IKE alone, either alone or in combination with ferrostatin-1. My results demonstrate that p27<sup>high</sup> cells exhibit significant resistance to IKE compared to the p27<sup>low</sup> subset (**Fig. 3.1I**). To explore whether TRPC6 plays a causal role in driving resistance in this aggressive population, p27<sup>high</sup> cells were pretreated with BI-749327 for 48 hours, followed by exposure to IKE, IKE+BI, either alone or in combination with ferrostatin-1. Viability data clearly indicate that TRPC6 inhibition sensitizes the resistant aggressive population to IKE (**Fig. 3.1J**).

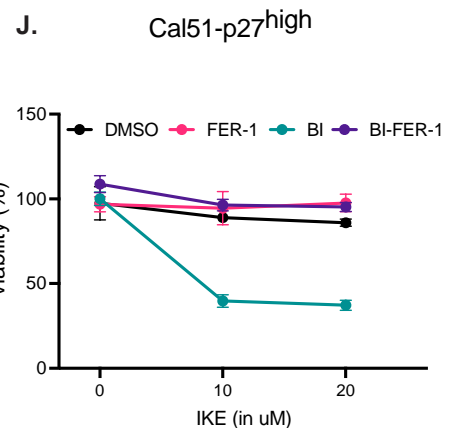
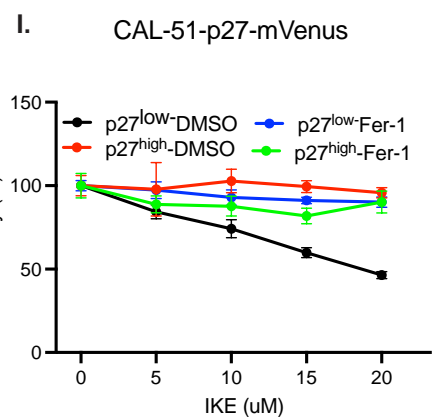
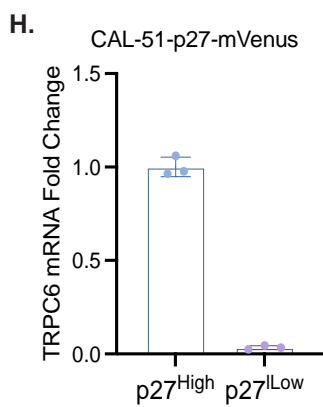
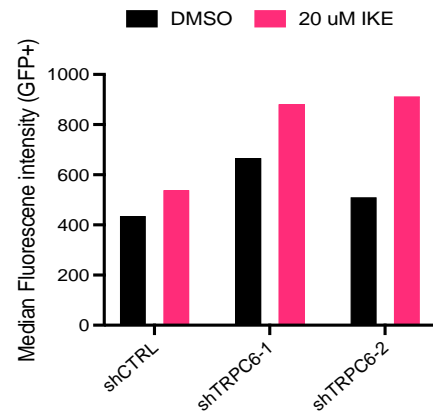
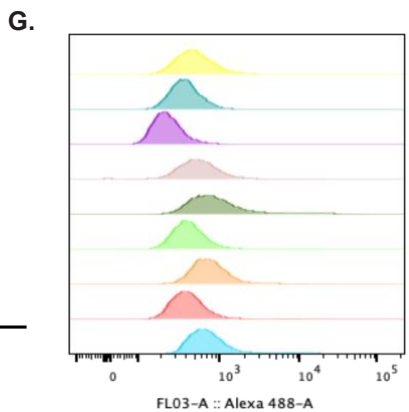
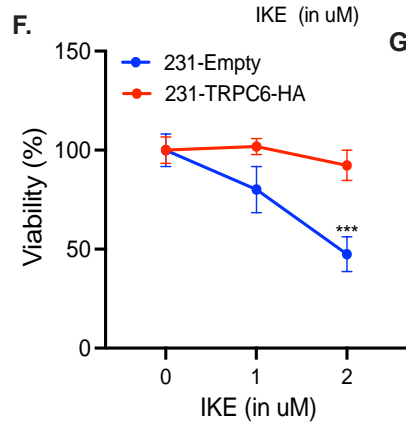
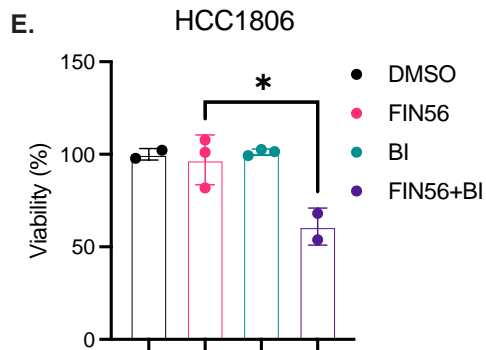
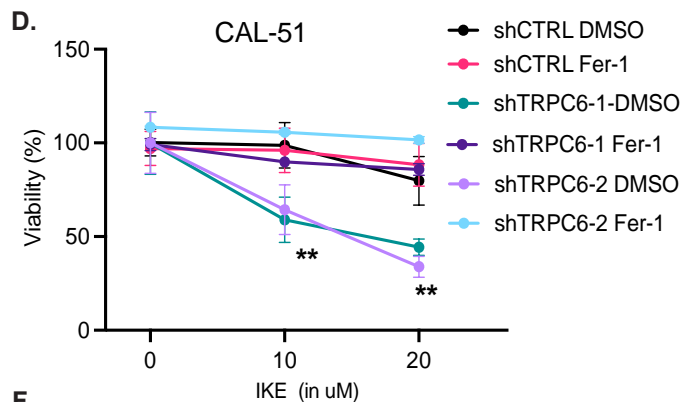
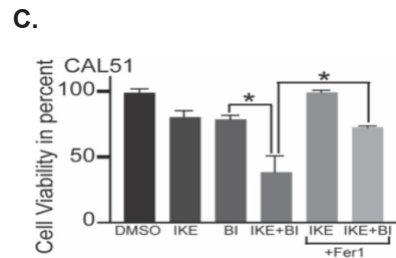
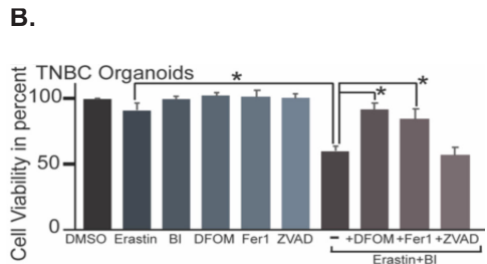
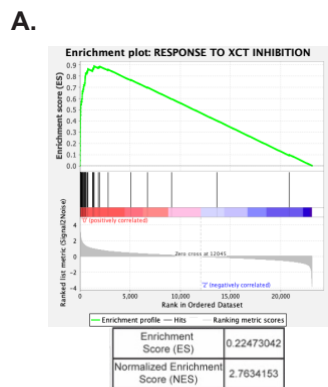


**Fig. 3.1. TRPC6 inhibition sensitizes TNBC resistant populations to Ferroptosis.** **A.** GSEA analysis of the RNA-Seq performed on TE3 cells treated with Vehicle and BI for 12 hours. This shows the enrichment score for the different pathways and highlighted is the transcriptional signature of Ferroptosis (as described by Dickson, et. al.). **B.** TNBC organoid (9811T) treated with: DMSO (control), Erastin (5 uM), BI (10uM), DFOM (Deferoxamine, 100 uM), Fer1 (Ferrostatin-1, 2 uM), ZVAD (20 uM), and Erastin and BI in combination with either of the following: DFOM, Fer1, or ZVAD. The viability was measured using 3d CTG. **C.** Viability measured after treatment of Cal51 cells with DMSO, IKE (5 uM), BI (10uM), IKE and Fer-1, BI and Fer-1, IKE with BI in combination with Fer-1. **D.** CAL-51 control shRNA (shCtrl) or TRPC6 knockdown (shTRPC6) cells were treated with increasing concentrations of IKE in combination with DMSO or Fer-1 for 24 hours and viability plotted. **E.** TNBC cell line HCC-1806 viability measured upon treatment with FIN56 in combination with DMSO or BI for 24 hours. **F.** TNBC cell line MDA-MB-231 was stably transfected with empty vector or WT TRPC6 construct. These cell types were treated with increasing concentration of IKE and the viability measured using CTG. **G.** CAL-51 control shRNA (shCtrl) or TRPC6 knockdown (shTRPC6) cells were treated with IKE (10 uM) alone or in combination with Fer-1. After 24 hours, C11-Bodipy assay was used to label peroxidized lipid (GFP+). (Left) Shows the histogram for GFP+ peak from each cell type and their respective treatments. (Right) Quantification of the median fluorescence intensity of the GFP channel between the control and TRPC6 KD cells for the treatments: Vehicle, IKE, and IKE with Fer-1. **H.** Expression levels of TRPC6 gene between the Cal51-p27<sup>high</sup> and CAL-51-p27<sup>low</sup> sorted cells from the CAL-51-p27mVenus transfected parental cells. **I.** The sorted Cal51-p27<sup>high</sup> and p27<sup>low</sup> populations treated with increasing concentrations of IKE with DMSO or Fer-1 for 24 hours and the viability percentage measured using CTG. **J.** CAL-51 p27<sup>high</sup> sorted cells were treated for 24 hours with increasing concentrations of IKE along with: DMSO, Fer-1, BI, and combination of BI and Fer-1. Viability was measured in each group and plotted.

**TRPC6 maintains a reduced environment that protects from ferroptosis:** My findings so far have shown that TRPC6 promotes resistance to ferroptosis in TNBC cell populations exhibiting aggressive characteristics. Another notable observation is that TNBCs exhibit a heterogeneous response to ferroptosis, with the aggressive persister cells being protected against such oxidative stress attack. Data from 3.1J hints at the central role of TRPC6 in promoting resistance in the persister population. To gain insight into the mechanism, it is essential to interpret this data from the perspective of ferroptosis regulatory mechanisms and the impact of TRPC6 on those pathways. Early studies, including those utilizing small molecule screens, revealed that inhibition of the enzyme GPX4 induces ferroptosis by preventing the neutralization of membrane phospholipid peroxidation (80). GPX4 catalyzes the conversion of reduced GSH to oxidized Glutathione (GSSG) while neutralizing lipid peroxide species (176, 177). The levels of reduced GSH, the substrate of GPX4, are indicative of the cell's ability to mitigate oxidative stress. My findings indicate a significant decrease in GSH levels upon TRPC6 loss following IKE treatment (**Fig. 3.2A**). This suggests that TRPC6 protects cells from oxidative stress by maintaining a reducing environment, as evidenced by GSH levels. Given the high levels of TRPC6 in persister cell populations, I sought to determine whether they also exhibit elevated GSH levels. To this end, I compared GSH levels between parental CAL51 and p27<sup>high</sup> cells treated with either DMSO or erastin for 24 hours. There was a significant decrease in the GSH pools in the CAL51 parental cells upon erastin treatment but an insignificant loss in the p27<sup>high</sup> cells (**Fig. 3.2B**). To understand whether TRPC6 is causal in maintaining high levels of GSH in the persister cells, I treated the p27<sup>high</sup> cells with either DMSO or BI-749327 for 48 hours, followed by treatment with either DMSO or IKE for 24 hours. The pools of reduced GSH were significantly lower in the p27<sup>high</sup> cells pretreated with BI-749327 compared to the control cells at the basal level (i.e. DMSO

treatment) and they were reduced further upon IKE treatment (**Fig. 3.2C**). This result underscores a mechanism by which TRPC6 protects the cells under oxidative stress by preserving the GSH pool. It remains to be understood how the persister cells are better at regulating GSH pools to neutralize oxidative stress. Several research groups have delineated that the cell generates GSH primarily through cysteine metabolism, largely facilitated by the uptake of Cystine by xCT (178). This is also one of the primary reasons why acute inhibition of xCT by erastin or IKE induces Ferroptosis. Considering the role of cysteine metabolism in GSH maintenance (179-181), I compared the viability of CAL-51-p27<sup>high</sup> cells pre-treated with DMSO and BI-749327 grown overnight in either of the following media conditions: complete medium, 1:1 mix of complete medium and cystine-free medium, and only cystine-free medium. Surprisingly, I observed that removing cystine from the medium did not cause significant cell death in the p27<sup>high</sup> cells pretreated with DMSO but only in those that were pretreated with BI-749327 (**Fig. 3.2D**). Taking this observation into account, I measured the GSH pools in these two treatment groups when grown in cystine free medium. GSH data mirrored what I observed in the viability assay, showing a significant downregulation of GSH pools in the p27<sup>high</sup> cells when grown in cystine free medium only when pretreated with BI-749327 (**Fig. 3.2E**). Thus, my results describe an unconventional mechanism of GSH maintenance in persister cells, which operates independently of cystine uptake through xCT.

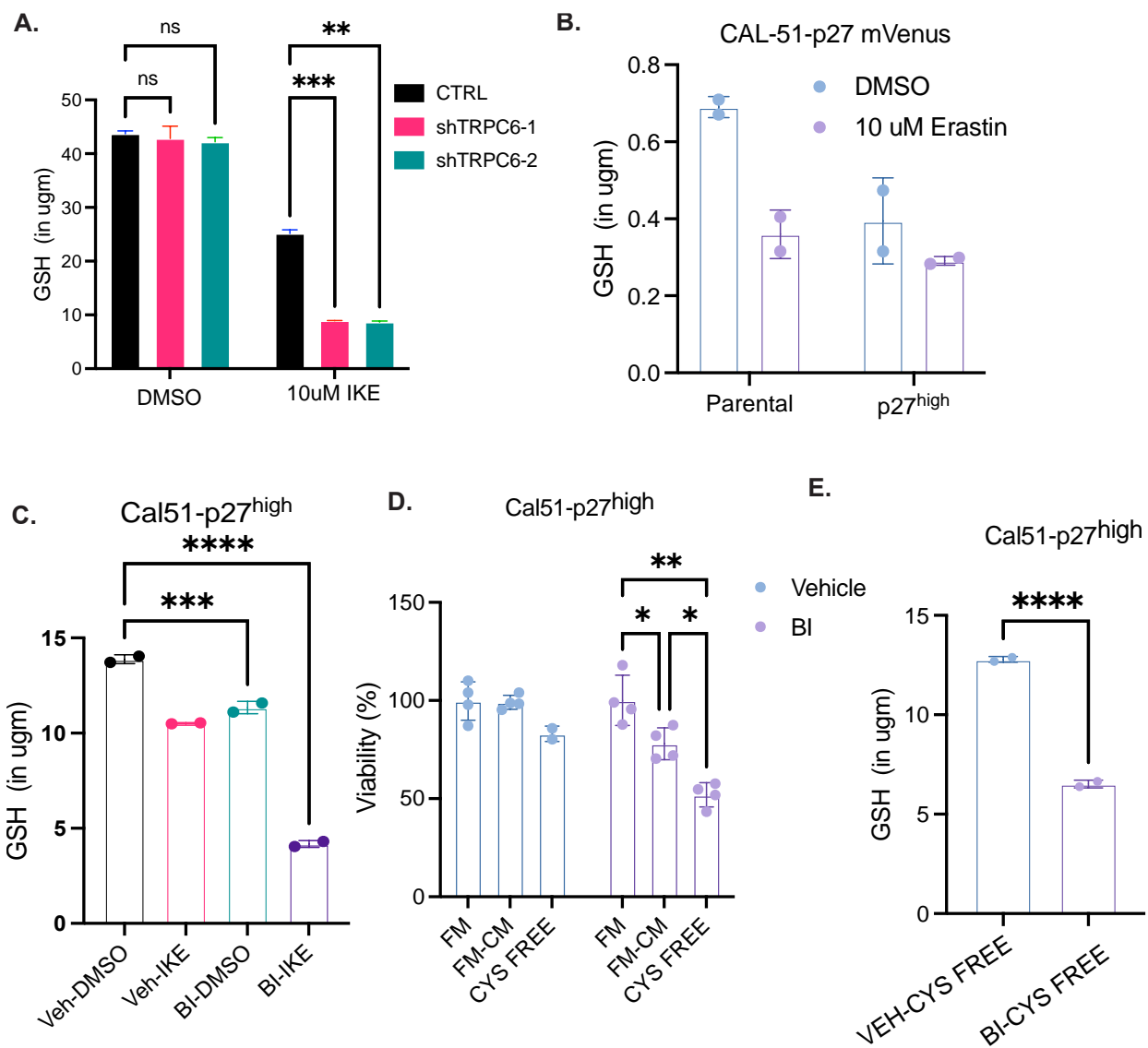
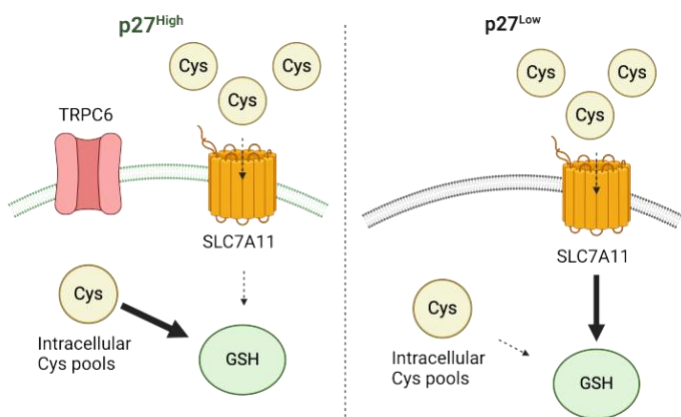


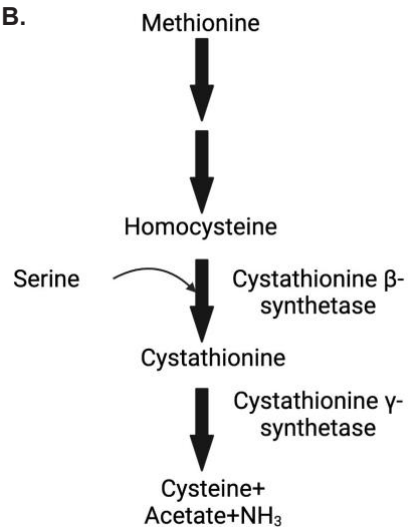
**Fig. 3.2. TRPC6 maintains a reduced environment that protects from Ferroptosis.** A. Graph showing the measurement of cellular reduced GSH in micrograms (ugms) using the Abcam kit (as described in the methods section) between the CAL-51 control shRNA (shCtrl) or TRPC6 KD (shTRPC6) cells upon treatment with DMSO or IKE (10 uM) for 24 hours. B. Reduced GSH pools using the Cayman kit (as described in the methods section) measured between CAL-51 parental cells and the p27<sup>high</sup> sorted cells from the Cal51-p27mVenus transfected cells upon IKE treatment for 24 hours. D. Cal51 p27<sup>high</sup> sorted population pre-treated with DMSO and BI for 48 hours were treated with DMSO or IKE for 24 hours. Reduced GSH pools were measured (in ugms) using the Cayman kit between the treatments and plotted. D. Cal51-p27<sup>high</sup> cells pretreated with vehicle and BI treatment were grown 24 hours either in: Full media (FM) or 1:1 mix of Full and Cysteine free media (FM:CFM) or Cysteine free media (CYS-FREE) and the viability measured using 2D CTG. E. CAL-51-p27<sup>high</sup> cells pretreated with vehicle and BI treatment were grown in Cystine free media overnight and the reduced GSH measured (in ugms) using the Cayman kit.

**Intracellular cysteine biosynthesis drives ferroptosis resistance in persister cells:** My hypothesis is that persister cells do not rely on extracellular cysteine uptake but instead generate sufficient cysteine from intracellular sources to maintain cellular reducing equivalents. This hypothesis is based on the observation that this population is slow cycling, suggesting lower biosynthetic requirements for building essential cellular components (specifically cysteine for protein synthesis) compared to actively dividing tumor cells (**Fig. 3.3A**). To test this hypothesis, I downregulated the rate-limiting enzyme of Trans-sulfuration pathway (TSS) Cystathione betasynthetase (CBS) using two different shRNAs (**Fig. 3.3C**). The TSS pathway is summarized in the schematic (**Fig. 3.3B**) This approach allowed me to test whether CBS KD sensitizes this resistant population to ferroptosis. Treatment of control (shCtrl) and CBS KD persister cells with RSL3 made them sensitive to ferroptosis (**Fig. 3.3D**). The crucial step was to measure the reduced GSH pools in the cell types (p27<sup>high</sup> control vs CBS KD), because it could explain how the loss of CBS leads to the viability defect. Measurement of reduced GSH pools substantiated my hypothesis that persister cells utilize intracellular cysteine pools to generate GSH, which subsequently mitigates oxidative stress and counteracts membrane phospholipid peroxidation (**Fig. 3.3E**). Collectively, my findings have provided insights into the metabolic adaptations in persister cells. I have demonstrated that there is a differential method of GSH generation that varies between the bulk tumor and the stem-like persister population.

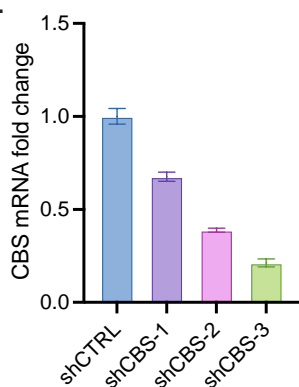
A.



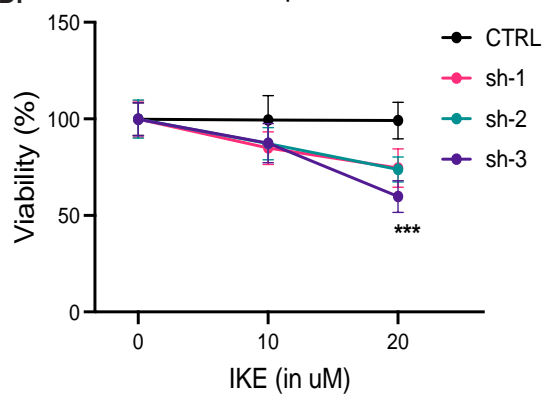
B.



C. Cal51-p27<sup>high</sup>



D. Cal51-p27<sup>high</sup>



E. Cal51-p27<sup>high</sup>

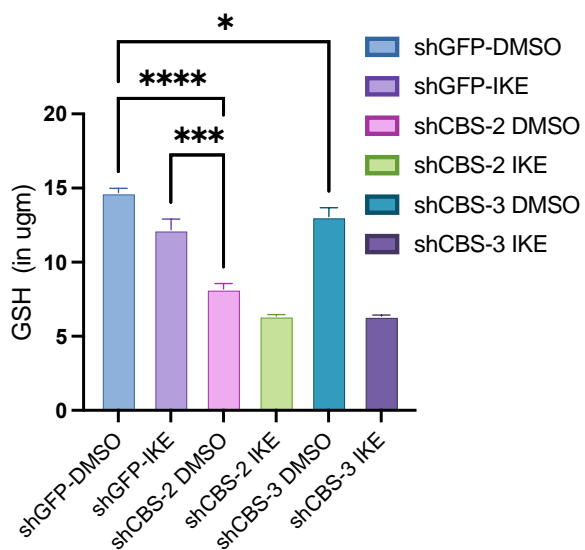


**Fig. 3.3. Intracellular cysteine biosynthesis drives Ferroptosis resistance in persister cells.** A. Schematic explaining the differential cysteine dependencies of persister cells and the bulk tumor. B. Schematic showing the trans-sulfuration pathway including the rate-limiting step catalyzed by Cystathionine beta-synthetase. C. qPCR data showing the expression levels of the gene Cysteine bio synthetase (CBS) between CAL-51 p27<sup>high</sup> shCtrl or CBS KD (shCBS-1, 2, 3). D. CAL-51 p27<sup>high</sup> control (shCtrl) and CBS KD cells treated with increasing concentrations of IKE and viability measured. E. Reduced GSH pools measured in the p27<sup>high</sup> control and CBS KD cells upon DMSO and IKE treatment for 24 hours.

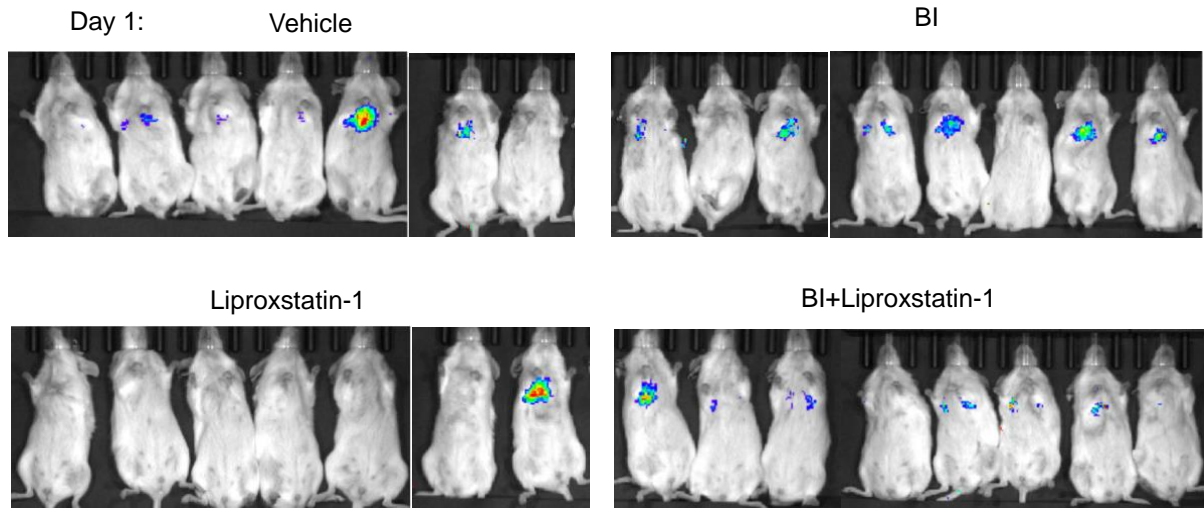
**TRPC6 inhibition prevents metastatic colonization of breast cancer cells in the lungs:** ROS serves a dual role within the complex landscape of cancer biology, exhibiting both pro-tumorigenic and anti-tumorigenic capabilities. This duality becomes particularly pronounced during the metastatic process, wherein cancer cells must navigate through varied environments to successfully colonize distant sites. Central to this investigation is the role of persister cells, which exhibit resilience against oxidative stress, a characteristic attributed to the protective function of TRPC6. This study aimed to explore whether TRPC6 similarly safeguards metastatic cells during their dissemination. To this end, the 231-LM2 cell line was selected as a model system because of its capacity for lung metastasis (182) and notably high expression of TRPC6 compared to other MDA-MB-231 cell variants as shown in the Appendix.

Given the limiting nature of ROS in metastasis and the propensity of TRPC6 to foster a reducing environment, my strategy entailed inhibiting TRPC6 in metastasizing cells to induce oxidative stress and evaluate its impact on their ability to colonize distant tissues. Preliminary results have confirmed that TRPC6 mitigates oxidative stress by sustaining GSH levels, thereby averting ferroptosis. To further elucidate whether TRPC6 inhibition precipitates ferroptosis in metastasizing cells, I incorporated treatment groups for Liproxstatin-1 and a combination of BI with Liproxstatin-1, assessing whether such interventions could restore metastatic competency.

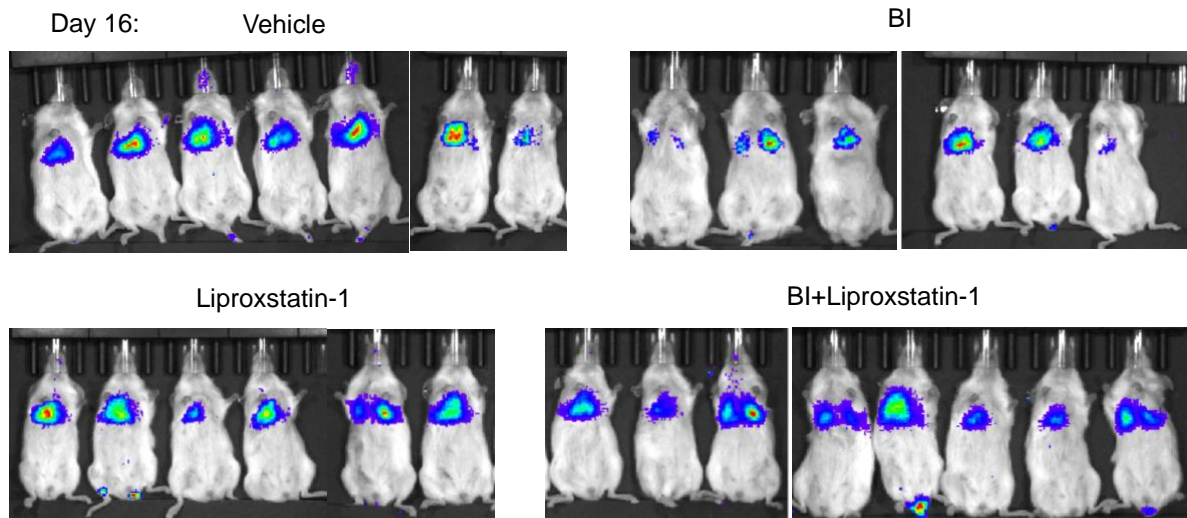
This study employed a tail-vein injection of  $1 \times 10^5$  LM2 cells, labelled with luciferase, into NOD/SCID mice. The subsequent day, tumor cell colonization was visualized using the Spectrum-CT in vivo imaging system (IVIS) instrument, following administration of luciferin (**Fig. 3.4A**). Treatment commenced on the following day with Liproxstatin-1 administered daily by intraperitoneal (i.p) injections at a dosage of 10 mgs/kg and BI delivered orally four times weekly at a dosage of 15mgs/kg. Analysis of the regions of interest (ROI) on Day 16 across the four treatment

groups (Vehicle, Liproxstatin-1, BI, and BI+Liproxstatin-1) revealed a marked reduction in lung metastatic colonization in the BI-treated group relative to the controls. This shows the therapeutic potential of targeting TRPC6 to impair metastatic progression (**Fig. 3.4 B, C**).

A.



B.



C.

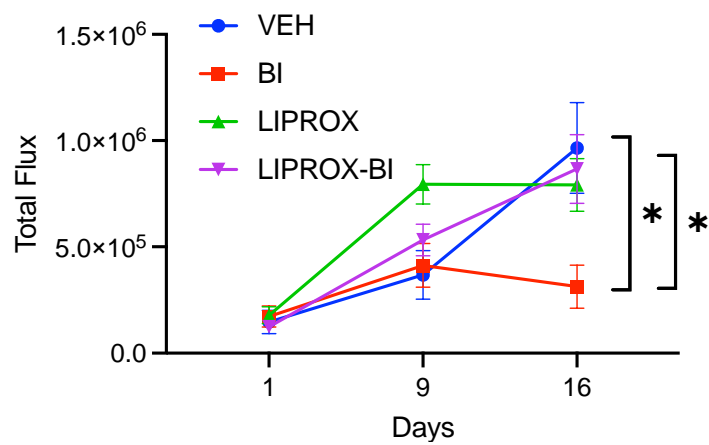


**Figure 3.4: TRPC6 inhibition prevents metastatic colonization of breast cancer cells in the lungs.** **A.** Images from of the mice on Day 1 after being injected with 100,000 LM2 cells labelled with luciferase on Day 0. **B.** Images from of the mice on Day 16 post-injection with of LM2 cells labelled with luciferase. **C.** Bioluminescent imaging quantification of the ROI in each treatment group. The signal is plotted as total flux (in photons/s) for each treatment group over a period of 16 days post injection.

## Discussion

In this Chapter, I demonstrate that TRPC6 promotes resistance to ferroptosis by maintaining high levels of reduced GSH. Mechanistically, TRPC6 alters cysteine metabolism by favoring intracellular cysteine biosynthesis over uptake through the X<sub>CT</sub> transporter. The enzyme CBS catalyzes the rate-limiting step in the intracellular cysteine biosynthesis, ultimately contributing to the maintenance of GSH pools. GSH is the substrate for the key antioxidant enzyme GPX4 that neutralizes membrane phospholipid peroxidation. Such mechanisms that enable GSH production in turn support GPX4 activity and resist cell death under ferroptotic stress. This discovery has clinical significance because TNBC exhibits a higher incidence of recurrence, relapse and metastasis compared to other subtypes. Several studies have pointed out that aggressive populations frequently encounter various oxidative stress environments during metastasis. Therefore, deciphering such protective mechanisms can facilitate targeting of aggressive populations, preventing metastatic dissemination and colonization.

The identification of treatment persister cells in TNBC as a rare population that is resistant to ferroptosis highlights a heterogeneous nature of ferroptotic sensitivity in TNBC. These resistant cells exhibit robust mechanisms of protection against oxidative stresses, contributing to their survival despite therapeutic challenges. By maintaining high levels of GSH derived from intracellular cysteine metabolism, TRPC6 shields these cells from ferroptosis-induced cell death.

However, it is important to recognize that there may be additional contributors to this resistance phenotype beyond cysteine metabolism and TRPC6 such as membrane lipid species and iron pool.

This study also sheds light on the metabolic heterogeneity presents in TNBC, revealing how the reprogramming of cysteine metabolism plays a crucial role in protecting aggressive cell populations from oxidative stresses. Ferroptosis, a pro-oxidant cell death mechanism, relies on three major regulatory axes: iron content that is key for the Fenton reaction to proceed, cysteine metabolism contributing directly to GSH pools and GPX4 activity, and lipid metabolism, which serves as the substrate for peroxidation. Extensive evidence suggests that PUFAs are preferred substrates for ferroptosis, while MUFAs drive resistance (86). Recent studies highlight metastasis as a pro-ferroptotic process, with cancer cells employing various strategies to counteract it. For instance, Piskanouva *et. al.* demonstrated that ROS limitation impedes metastasis, while subsequent studies by Sean Morrison's lab showed adaptations in metastatic cells that facilitate efficient dissemination and colonization (183-185). They found that melanoma cells utilize the lymphatic system for successful metastasis, exchanging PUFAS such as Palmitoic acid for MUFAs such as oleic acid (184). Our results add significantly to this literature by elucidating a novel mechanism of metabolic adaptation in metastatic cells that involves differential cysteine biosynthesis enabling survival under oxidative stress.

The role of cysteine metabolism in modulating ferroptosis resistance adds complexity to our current understanding of ferroptosis regulation, particularly through the enzyme CBS. While CBS KD sensitizes persister cells to ferroptosis, its impact on cellular hydrogen sulfide levels and subsequent activation of the enzyme sulfide quinone oxidoreductase (SQOR) suggests a multifaceted role in ferroptosis regulation. Moreover, recent research from the Kim lab demonstrates that SQOR prevents ferroptosis in cancer cells by reducing ubiquinone to ubiquinol

in the mitochondria (186). Further, the moderate effect of CBS knockdown on cell viability suggests the presence of additional resistance mechanisms in persister cells that may operate independently of amino acid metabolism. However, our data supports previous studies that has observed a similar effect of preventing ferroptosis driven by CBS (180, 187).

Further exploration into the mechanisms of resistance in persister cells requires an unbiased approach encompassing lipidomics and metabolomics. By examining lipid metabolism and cellular iron pools, we can gain insights into how these processes contribute to resistance to ferroptosis. Additionally, investigating the regulation of membrane phospholipid composition by TRPC6 through lipidomic analysis, with or without TRPC6 inhibition, will provide valuable information on its role in modulating the ferroptotic response of persister cells.

## Materials and Methods

**Cells and reagents:** CAL-51 cells were obtained from the Leibniz Institute DSMZ, Germany and HCC1806 cells were purchased from the American Type Culture Collection. The TRPC6 inhibitor BI-749327 was purchased from MedChem Express (Catalogue no. HY-111925), Liproxstatin-1 was purchased from Selleckchem. Luciferin was bought from Gold Biotechnology. Erastin, IKE, RSL3 were bought from MedChem. C11-Bodipy was bought from Sigma Aldrich. GSH kit fluorometric kit was bought from Abcam and colorimetric was bought from Cayman Chemicals.

**shRNAs and expression constructs:** The following lentiviral shRNAs were obtained from our core facility: TRPC6 (TRCN0000431016, TRCN0000044106) and CBS (TRCN0000308284, TRCN0000075999, TRCN0000045360). The quiescent reporter plasmid pCDH-EF1-mVenus-p27K was bought from Addgene (plasmid #176651). Lipofectamine 3000 (Thermo Fisher Scientific) was used for plasmid transfections.

**Cell-based assays:** For flow cytometry, cells were incubated detached from the plate and resuspended in PBS and sorted against the FITC channel to isolate p27<sup>high</sup> cells. To assay cell viability, cells were seeded at a density of  $5 \times 10^3$  cells per well. After 24 hours, cells were treated with either BI-749327 or IKE as described in the figure legends and viability was assessed using Promega CTG. Viability assay in organoids was measured using the Promega 3D CTG. The luminescence measured and normalized to the control.

**Biochemical assays:** mRNA quantification was accomplished using an RNA isolation kit (BS88133, Bio Basic Inc.), and complementary DNAs (cDNAs) were produced using an Azura

cDNA synthesis kit (AZ-1996, Azura Genomics). Azura View GreenFast qPCR Blue Mix LR was used as the qPCR Master Mix (AZ-1996, Azura Genomics).

**RNA sequencing:** RNA was extracted from the indicated cells using a Qiagen RNeasy Micro Kit (74004) and sent to Quick Biology for quantification, sequencing, and analysis.

Quick Biology Sequencing method: Library for RNA-Seq was prepared according to KAPA Stranded mRNA Hyper prep polyA selected kit with 201-300 bp insert size (KAPA Biosystems, Wilmington, MA) using 250 ng total RNAs as input. Final library quality and quantity was analyzed by Agilent Technologies 4200 station and Qubit 3.0 (Thermo Fisher Scientific Inc, Waltham, MA) Fluorometer. 150 bp paired-end reads were sequenced on Illumina HiSeqX (Illumina Inc., San Diego, CA). Each sample had a sequencing depth of 20-30 million. RNASeq analysis was performed with OneStopRNAseq workflow (61). Paired-end reads were aligned to human primary genome hg38, with star\_2.5.3a (62), annotated with GENCODE GRCh38.p12 annotation release 34 (63). Aligned exon fragments with mapping quality higher than 20 were counted toward gene expression with featureCounts\_1.5.2 (64). Differential expression (DE) analysis was performed with DESeq2\_1.20.0 (65). Within DE analysis, 'ashr' was used to create log2 Fold Change (LFC) shrinkage for each comparison (66). Significant DE genes (DEGs) were filtered with the criteria  $FDR < 0.05$ . Gene set enrichment analysis was performed with GSEA (67).

**Animal studies: For the in-vivo metastasis experiment,** Tail-vein injection was performed with 100,000 cells in 100ul PBS (using a 1 ml syringe and attach a 26-gauge needle) into NSG mice. Mice were monitored for 3 weeks, and lung metastasis was measured using the intensity of the Bioluminescence signal. Once the mouse started losing weight they were euthanized, and the

tumors collected for histological analysis. The mice were divided into 4 groups of 7-8 mice each. All mouse procedures were done under the guidance of the University of Massachusetts Medical School Institutional Animal Care and Use Committee in accordance with the institutional and regulatory guidelines.

**Bioluminescent imaging of tumor cells:** The tumor cells were injected on Day 0 and the imaging was performed from Day 1 onwards at a frequency of twice a week. In each imaging session a total of 150mg of Luciferin per kg body weight was administered via two injections into the peritoneal cavity. In this study, animals were imaged 10 minutes after Luciferin injection to ensure consistent photon flux. The IVIS Spectrum in-vivo imaging system uses a back-thinned charge coupled device cooled to  $-90^{\circ}\text{C}$  to achieve maximum sensitivity. The stage is maintained at constant temperature of  $37^{\circ}\text{C}$  to maintain body temperature in the animals. The bioluminescent signal is expressed in photons per second and displayed as an intensity map. The image display is adjusted to provide optimal contrast and resolution in the image without affecting quantitation.

**Analysis of the images:** The Spectral Instruments imaging Software also known as Aura was used for the quantification of the bioluminescent signals. Luminescence from the cells was measured in the lungs using a ROI tool. Measurement data are displayed in the table that was then plotted in Prism.

## CHAPTER IV: DISCUSSION

### Overview

In this thesis, I sought to uncover new factors associated with BCSCs that contribute to the aggressive nature of TNBC. To this end, I discovered that TRPC6, a calcium channel, is enriched in BCSCs and that it contributes to self-renewal and tumor initiation. More specifically, TRPC6-mediated calcium signaling influences gene expression changes through pathways distinct from the known effects of calcium-dependent NFAT/CREB transcriptional regulation. TRPC6 suppresses the splicing protein ESRP1, leading to an enrichment of the integrin  $\alpha 6B$  splice variant and subsequent suppression of MYC expression that maintains a quiescent CSC state. This finding also highlights a non-genetic mechanism of creating transcriptomic diversity that impacts response to therapy. These findings add to the limited understanding of TRP channels in the biology of breast cancers. Importantly, TRPC6 has the potential to be a biomarker for CSCs within heterogeneous TNBC tumors. My work also established a role for TRPC6 in therapy resistance by sustaining persister cells that is linked to its ability to maintain a quiescent CSC state.

An unexpected observation I made was that inhibition of TRPC6 positively enriches the transcriptional signature associated with ferroptosis, an iron-dependent form of cell death. The treatment persister cells that express very high levels of TRPC6 are resistant to ferroptosis. In pursuit of the mechanism involved, I found that the treatment persister cells resist ferroptosis by maintaining high levels of GSH. Ferroptosis is driven by several metabolic processes, including glutathione, iron, cysteine metabolism (179, 181), and lipid metabolism (99, 101, 188). My data demonstrates that ferroptosis resistant cells reprogram their cysteine metabolism, resulting in a reducing environment with GSH levels that sustain GPX4 activity. Specifically, persister cells

synthesize GSH mainly from intracellular cysteine biosynthesis, catalyzed by the enzyme CBS making them less dependent on extracellular cystine. In contrast, cells that are more sensitive to ferroptosis are dependent on extracellular cystine, indicating a metabolic diversity within TNBC populations. I also investigated the hypothesis that the unique metabolic adaptation displayed by persister cells can be exploited to impede metastasis by targeting TRPC6. Indeed, inhibition of TRPC6 with a small molecule inhibited metastatic colonization in the lungs by inducing ferroptosis. These findings add to our current understanding of the role of oxidative stress in tumorigenesis.

## TRPC6 and calcium signaling in breast cancer

Chapter II describes how TRPC6-mediated calcium signaling sustains self-renewal and promotes chemoresistant persister cell state in TNBC and maintains treatment persister cells. Previously, TRPC6's role in multi-drug resistance has been observed in Hepatocellular Carcinoma (HCC) (189) but the mechanism is not well understood. These findings bear on the more general issue of TRPC6 and calcium signaling in cancer. Most studies on TRPC6 have focused on its role in podocytes (see Introduction) (119, 190-195). However, its contribution to epithelial cells and cancer has not been investigated as intensely. The existing evidence has revealed that tumor tissues exhibit elevated expression of certain calcium channels, particularly TRP channels, compared to normal tissue (196). However, the functional role of these channels in cancer remains unclear. Very few studies have rigorously investigated the causal relationship between TRP channels and tumor progression, leaving a gap in our understanding. Notably, TRPC6 has been identified as a regulator SOCE in triple-negative breast cancers (TNBCs) (44). This finding is significant, as it addresses previous debates regarding the potential SOCE function of TRP channels, particularly in transformed cells. However, it prompts further inquiry into the downstream consequences of TRPC6-driven SOCE maintenance and TRPC6 specificity. Research by Chigurupati *et al.* revealed that hypoxia activates Notch1 signaling, leading to increased levels of TRPC6. This increase in TRPC6 boosts intracellular calcium in tumor cells, a key event that is closely associated with the activation of the calcineurin NFAT pathway (197). Another study showed, in human glioma cells, TRPC6 is essential for regulating hydroxylation, and thus the stability, of Hypoxia Inducible Factor-1 $\alpha$  (HIF-1 $\alpha$ ), triggered by the IGF-1R-PLC $\gamma$ -IP3R pathway (198). Recently, there have been more efforts in deciphering the specificity of calcium signaling in cancer and understanding its functional role during tumorigenesis. Takahashi *et al.* showed that TRPA1-mediated calcium

signaling prevents apoptosis-mediated cell death by protecting them against ROS (199). This previously unrecognized role of calcium signaling in stress response expands our current knowledge and prompts further investigation into its functional roles and underlying mechanisms. Understanding the mechanism of contextual utilization of these pathways by tumors is crucial for developing effective therapeutics. Tumor progression involves multiple steps and requires coordinated efforts from diverse clonal populations to overcome various limitations, including those imposed by growth and environmental stresses such as hypoxia, nutrient deprivation, and chemotherapy. In that context, Greg Semenza's lab showed that in fact calcium mediated signaling enriches for stem cells in breast cancers upon chemotherapy treatment (66). My findings build upon these studies by demonstrating that TRPC6-mediated calcium signaling maintains a quiescent treatment persister state through MYC suppression.

### **Splicing: Developmental mechanism to generate transcriptomic heterogeneity**

A major finding in this thesis is that TRPC6 regulates alternative mRNA splicing by repressing ESRP1. Alternative splicing enables a single gene to produce multiple protein isoforms through the selective inclusion or exclusion of exons and introns. This process contributes to significant transcriptomic and proteomic diversity. Several studies have elucidated that alternative splicing is dysregulated in almost all types of cancer (200). In fact, this dysregulation directly affects numerous cellular processes, many of which correspond to the hallmarks of cancer, including the evasion of apoptosis, tissue invasion, metastasis, altered cellular metabolism, genome instability, and drug resistance. Alternative splicing is a complex process orchestrated by the spliceosome; a sizable molecular machine made up of units called small nuclear ribonucleoproteins (snRNPs). These units, named U1, U2, U4/6 and U5, work alongside over 150 additional proteins to

accurately identify and splice specific sites within the pre-mRNA (201, 202). This intricate system ensures that a single gene can give rise to multiple protein variants, enhancing cellular diversity. Mutations, mostly those that are Loss-of-Function (LoF) types, occurring mostly in the genes of the A, C and U2 complexes, Serine and arginine-rich (SR) proteins, and heterogeneous nuclear ribonucleoproteins (hnRNPs) are significant contributors to cancer development. A comprehensive study across 33 cancer types identified 119 splicing factor-related gene mutations as likely oncogenic drivers (203). Most hotspot mutations affected the core components of the U2 complex— splicing factor 3b subunit 1 (SF3B1) and U2 small nuclear RNA auxiliary factor 1 (U2AF1)—and the splicing factor serine and arginine rich splicing factor 2 (SRSF2). For instance, the SF3B1K700E mutation impairs the recognition of intronic branch point sequences, causing shifts in 3' splice site selection (204, 205). This mutation, notably, results in amplified Notch pathway activity due to the production of a different Dishevelled segment polarity protein 2 (DVL2) splice variant (206).

My findings on TRPC6 and mRNA splicing are best discussed on the context of cellular plasticity. Cellular plasticity, especially the ability of tumor cells to change from one type to another—a process known as trans-differentiation—is crucial for cancer development and progression. The epithelial-to-mesenchymal transition (EMT) is a key example, where cells lose their epithelial characteristics and gain mesenchymal traits, facilitating tumor cell migration and invasion. Alternative splicing plays a key role in EMT, influencing various levels of this transition. Research has uncovered specific alternative splicing patterns linked to the EMT in breast cancer (135, 207). A set of 25 alternative splicing events was identified, marking tumors with significant EMT activity. Several studies have focused on the role of specific splicing factors and alternative splicing events in controlling the epithelial-to-mesenchymal transition (EMT). Factors such as

ESRP1, hnRNPM, serine and arginine rich splicing factor 1 (SRSF1) and RNA binding fox-1 homolog 2 (RBFOX2) are linked to EMT processes. ESRP1 regulates a splicing pattern unique to epithelial cells and is reduced by EMT activators Zeb1 and Snail. It has been found that ESRP1 and hnRNPM oppositely affect splicing during EMT, leading to changes that promote an EMT-related splicing pattern. For instance, ESRP1 affects the splicing of the TCF4 gene, resulting in a variant that reduces Wnt signaling activity that is crucial for the epithelial trait (208). RBFOX2, which increases with EMT, regulates splicing events associated with the mesenchymal state (72, 209-212).

Recent studies suggest that dysregulated alternative splicing fosters conditions that enhance tumor heterogeneity and cellular plasticity, which are key factors influencing a patient's response to therapy. For instance, in case of colorectal cancer, there are four molecular subtypes (CMSs). Gene expression patterns, specifically deregulation of transcript variants, have been successful at identifying high-risk subgroups within colorectal cancer. This shows the alternative splicing could serve as a prognostic tool, particularly within high-risk categories (213). RAC1B splice variants acts a marker for a particular colorectal cancer subgroup, which has poor prognosis and increased Wnt signaling activity (214). These insights demonstrate the complex connection between gene transcription, splicing events, and cancer progression. In pancreatic cancer research, classifications based on alternative splicing have proven to be more reliable in predicting patient survival than classifications based solely on gene expression levels (215). It highlights the critical role of alternative splicing in identifying key biomarkers and understanding the progression of disease.

I focused my efforts on understanding the impact of TRPC6-mediated mRNA splicing on the splicing of the integrin  $\alpha 6$  splice, which is regulated by ESRP1. My results related to cellular plasticity because the  $\alpha 6A$  splice variant is associated with a more differentiated non-CSC state,

while the  $\alpha 6B$ , which is generated by TRPC6-mediated mRNA splicing, is associated with a more mesenchymal state, and has a causal role in stemness and in sustaining persister cells. The depth of our RNA-Seq did not allow me to rigorously sequence exon-exon junctions that is necessary to effectively quantitate expression of different transcript variants. Thus, I could not capture the global effects of modulating ESRP1. However, it is obvious that suppressing a key splicing protein, such as ESRP1, would have effects beyond integrin  $\alpha 6$ . Failing to consider the broader downstream consequences of this suppression is a significant limitation of this study. Figure 3.2 shows that p27<sup>high</sup> persister cells have very little ESRP1 and p27<sup>low</sup> has high levels of ESRP1. This system offers an unbiased approach to examine transcriptomic heterogeneity influenced by ESRP1, providing further insight into inherent transcript variation between the two populations (chemosensitive vs chemoresistant). These findings are crucial for gaining a comprehensive understanding of the tumor, enabling better prediction of the functional roles of clonal populations. It is also worth discussing the role of alternative mRNA splicing in regulating cellular metabolism and promoting survival and fitness of cancer cells. Alternative splicing plays a crucial role in regulating nutrient metabolism through the mammalian target of rapamycin complex 1 (mTORC1), a key factor in cell growth and the synthesis of nucleotides, proteins, and lipids. This process controls the activity of protein S6 Kinase (S6K), which exists in two isoforms with opposite effects on mTORC1: one inhibits mTORC1, while the other activates it, enhancing its cancer-promoting actions. The splicing of S6K is regulated by SRSF1, which in turn influences mTORC1 activity. This relationship underlines the significant role of this splicing process in cellular metabolism and its potential as a therapeutic target (216).

Historically, ESRP1 in breast cancer has been linked with EMT, showing specifically how high ESRP1 levels enrich for epithelial specific transcript variants. Beyond the canonical targets of

ESRP1-mediated alternative splicing, there have been reports that ESRP1 can alternatively splice metabolic genes in certain contexts as seen in ER+ breast cancer model (217). Thus, our data introduces a novel concept of how a calcium channel drives functional heterogeneity and maintains stem-like state through mRNA splicing. TRPC6's ability to orchestrate a differential splicing pattern highlights an underappreciated role of generating novel transcriptomic diversity through non-genetic mechanisms. Considering the role of tumor heterogeneity in predicting clinical outcome of TNBC, we need to investigate all the roads that generate transcriptomic diversity in malignant cells.

### **Therapy persister cells: Nature and Mechanisms**

In this thesis, I have demonstrated a novel mechanism of therapy resistance in TNBC. The TRPC6-mediated suppression of ESRP1 is crucial to suppress MYC downstream, consequently promoting chemoresistance. Further investigations revealed that cells resistant to paclitaxel, characterized by high TRPC6 levels, can be sensitized to chemotherapy by overexpressing ESRP1. ESRP1 is known to preferentially enrich for transcripts that are associated with a more differentiated cell type. This poses a critical question of what the nature is of the treatment persister cell population that has a unique profile of high TRPC6 and low ESRP1 expression.

To this end, we examined expression of genes that are established markers of the epithelial and mesenchymal state. Inhibition of TRPC6 in these stem-like populations did not completely cause a reversion of the cell type from one (mesenchymal) to the other (epithelial); in fact, they retained markers of both. This brings us to explore the idea that the TRPC6<sup>high</sup> stem-like treatment persister

cells are in somewhat of a hybrid epithelial and mesenchymal state (E/M). Recent studies have increasingly highlighted the presence of a hybrid E/M state in cancer cells, particularly in breast cancer. Initial work on EMT painted a black and white picture of loss of epithelial and gain of mesenchymal markers induced by major players such as TGF-beta (73). Most of these experiments were performed *in-vitro* and in certain genetic mouse models of breast cancer *in-vivo* (MMTV-PyMT, and Neu) (218). Weinberg's group characterised this hybrid E/M cell state using their human mammary epithelial (HMLER) cell culture model (219). These cells were transformed with SV40, and HRASV12 oncogene and hTERT for immortalization (126). Several others have since then implicated that hybrid/partial EMT cells promote aggressive traits such as chemoresistance and metastasis.

To us, this concept of a hybrid E/M state is further emphasized by a recent study, Pitaressii et al., where they observed that calcium signaling promotes an E/M state (114). In a pathological context, recent work by Augimeri et al. analyzed patient samples from TNBC that have shown therapy resistance and metastasis. Their study revealed breast cancer cells with the markers of mesenchymal stem cells as well as epithelial state in the samples that have recurrence and/or metastasis (220). This clinical evidence further solidifies our inquisition as to whether the TRPC6-mediated treatment persister cells are in a hybrid E/M state. Preliminary analysis of the gene expression levels of different epithelial and mesenchymal markers showed enrichment in the TRPC6<sup>high</sup> stem-like population (data include in appendix). Besides gene expression analysis, it is essential to observe staining patterns of the epithelial and mesenchymal markers on the treatment persister cells. Visualization of these epithelial and mesenchymal markers by immunofluorescence on tumor cells is a more accurate way of determining their cell state.

It is also important to note that my study has only addressed the mechanisms of pre-existing treatment resistant populations. Multi-omics approaches provide valuable insights into resistance mechanisms, capturing both pre-existing and acquired resistance (221, 222). These methods offer understanding not only of chemoresistance but also of resistance to targeted therapies. For instance, Tyrosine Kinase Inhibitors (TKIs) have notably improved the mortality rate in EGFR-driven lung adenocarcinoma. However, long-term efficacy is reduced due to the emergence of acquired resistance to these TKIs. Katerina Politi's group adopted a systematic approach to identify markers and mechanisms of acquired resistance. Exome sequencing of the resistant clones did not reveal any significant mutational signature, specifically not on EGFR, which could have explained the emergence of TKI resistance. Thus, they could completely rule out genetic mechanisms but instead turned their focus on epigenetic mechanisms. There have also been reports that inhibition of the histone demethylase KDM5A can limit the growth of TKI resistant populations (223). Combining RNA-Seq with ATAC-Seq revealed a distinct signature of open chromatin regions shared amongst the resistant clones mechanistically driven by the SWI/SNF complex in creating the resistant state (224). The epigenetic mechanisms underlying global resistance in breast cancer are not extensively studied. In my thesis, I have discovered that calcium plays a central role in promoting resistance (BAPTA data on Cal51-R). Recent studies have elucidated potential roles of calcium signaling in epigenetic modulation, that is driven by calcium-dependent activation of Protein Arginine Deiminase 2 (PAD2) enzyme that citrullinates histone arginine residues (225). Thus, it would be exciting to perform a similar assay for transposase-accessible chromatin with sequencing (ATAC-Seq) to look at resistant and sensitive population with and without BAPTA treatment. Overall, this highlights our limited understanding of treatment-resistant populations and their unique adaptations that promote survival.

In this study, I delineate how TRPC6-induced chemoresistance in TNBC is driven by a mechanism of MYC suppression. This observation bears resemblance to a developmental process known as embryonic diapause that is also caused by MYC suppression (226). This pathway seems to be exploited by TNBC to promote chemoresistance. Cancer cells often hijack developmental pathways during tumorigenesis, and my study highlights yet another instance of this similarity, which likely impacts clinical outcomes. Given that embryonic diapause state is marked with suppressed activity of biosynthetic and bioenergetic processes, it will be interesting to look at the metabolic landscape of resistant cells. Such information will help identify the unique metabolic adaptations in these aggressive populations and reveal therapeutic targets.

### **Metabolic adaptations during tumorigenesis**

Metabolic reprogramming is fundamental to both tumorigenesis and therapy resistance. My data indicates that treatment persister cells utilize intracellular cysteine pools to generate GSH, which shields them from oxidative stress and enhances survival during challenging conditions such as chemotherapy and dissemination.

As expected, a growing tumor has very high demands for bioenergetics and macromolecules. It is known that tumor cells reprogram modes of nutrients acquisition and metabolism to provide macromolecules and energetic equivalents to support tumor growth. The reprogramming of core nutrient metabolism has been recognized as a hallmark of cancer (227). Although most of cancer research has focused on discovering oncogenes and then tumor suppressors, tumor metabolism is the oldest area of cancer research.

The underlying goal of metabolic rewiring in cancer is to improve cell fitness and aid in tumorigenesis. There are distinct challenges at different stages of tumor development. These metabolic pathways aim to support two activities overall - cell survival during stressful conditions and provision of macromolecules and energetics to support the growth of a tumor. Warburg effect, also known as aerobic glycolysis, serves as an exemplary illustration of metabolic pathway reprogramming in cancer. Otto Warburg's observations in the 1920s revealed that tumor slices and ascites cancer cells consistently metabolize glucose and generate lactate irrespective of oxygen levels (228). This increase in glycolysis supplies intermediates into other pathways such as Tricarboxylic Acid (TCA) cycle and Pentose Phosphate Pathway (PPP) which are essential for synthesis of fatty acids, proteins, and nucleotides. Their integration into biosynthetic pathways necessitates the replenishment of carbon to sustain intermediate pools. Hence anapleurotic pathways play a crucial role in cancer maintain a steady supply of substrates for the major anabolic pathways (229-233).

**Oncogene driven metabolism:** Following stimulation by growth factors, normal cells initiate the activation of Phosphatidylinositol 3-kinase (PI3K) and its downstream pathways, including AKT and mTOR. This cascade promotes an extensive anabolic program characterized by increase in glycolytic flux and fatty acid synthesis, facilitated by the activation HIF-1 and Sterol regulatory element binding protein (SREBP), respectively (234). Conversely, tumor cells frequently harbor mutations that confer the PI3K-AKT-mTOR network with the ability to sustain elevated signaling levels independently of extrinsic growth factor stimulation (235). Within this network lie numerous extensively studied oncogenes and tumor suppressors, with the aberrant activation of this pathway representing one of the most prevalent molecular alterations observed across a spectrum of cancer types. Another frequently dysregulated pathway in cancer involves the

acquisition of MYC gain of function through mechanisms such as chromosomal translocations, gene amplification and single-nucleotide polymorphisms. MYC upregulates the expression of numerous genes implicated in anabolic growth, encompassing transporters and enzymes associated with glycolysis, fatty acid synthesis, glutaminolysis, serine metabolism and mitochondrial metabolism (236-240). In 50% of human cancers, the TP53 gene, encoding the p53 protein, undergoes mutation. Conventionally, p53's tumor-suppressive capabilities are attributed to its roles in overseeing DNA repair, orchestrating cell cycle arrest, inducing senescence and instigating apoptosis. However, recent inquiries propose a departure from this conventional understanding, suggesting that p53's tumor-suppressive actions may extend beyond its classical functions. Instead, emerging evidence indicates a significant involvement in the regulation of metabolism and oxidative stress (91, 241). Notably, the absence of functional p53 results in an augmented glycolytic flux, thereby promoting anabolic processes and sustaining redox equilibrium—both critical in fostering tumorigenesis (242). Thus, oncogenic signaling aids to tumor growth by reprogramming metabolic pathways that supply macromolecules and energetics.

**Tumor metabolism reprogramming to support high biosynthesis demands:** Anabolic pathways are the backbone of tumorigenesis and tumor metabolism, facilitating the synthesis of macromolecules essential for cell division and tumor progression. Typically, these pathways involve the uptake of basic nutrients, such as sugars and essential amino acids, from the extracellular environment. Subsequently, these nutrients undergo conversion into biosynthetic intermediates through core metabolic pathways including glycolysis, PPP, TCA cycle and nonessential amino acid synthesis.

**Protein biosynthesis** is intricately regulated and requires both essential and nonessential amino acids. In response to growth factor signaling, cancer cells and other cell types, take up amino acids

from the extracellular environment (243). This step is crucial as it contributes to the activation of the mTOR signaling pathway, particularly mTORC1. Activation of mTORC1 is triggered by the availability of amino acids, thereby initiating protein synthesis by influencing translation and ribosome biogenesis (244). The bulk of nonessential amino acids are generated via transamination reactions, wherein the amino group is transferred from glutamate to a ketoacid. Tumor cells show dependence on glutamine, which also shows increased uptake. The enzyme mitochondrial amidohydrolase glutaminase catalyzes the conversion of glutamine to glutamate (245). This glutamate pool acts as a source for the synthesis of non-essential amino acids in the tumor cells.

mTORC1 stimulates both the uptake of glutamine and the activity of glutaminase, ensuring a sufficient supply of glutamate. Additionally, when the intracellular glutamine reservoir exceeds cellular requirements, glutamine is exported in exchange for essential amino acids, thereby activating mTORC1 activity that feeds back into protein synthesis (246).

**Fatty acid synthesis:** Due to the rapid cell proliferation that requires membrane biosynthesis, tumor cells upregulate fatty acid synthesis and consequent cellular signaling pathways to support that. This process requires acetyl-CoA and reducing power, typically supplied by cytosolic NADPH. In most cultured cells, glucose serves as the principal source of acetyl-CoA for fatty acid synthesis (247, 248). However, in scenarios where access to glucose-derived acetyl-CoA is constrained by factors such as hypoxia or mitochondrial dysfunction, alternative carbon sources such as glutamine and acetate have been shown to serve as viable alternatives (249-252). Recent isotopic tracing experiments aimed at assessing cytosolic NADPH pools suggest that the predominant source of NADPH utilized for fatty acid synthesis originates from the PPP (253, 254). SREBP-1 transcription factor is the master regulator of genes involved in fatty acid synthesis (255). SREBP-1 not only oversees the expression of enzymes responsible for the conversion of

acetyl-CoA into fatty acids but also the regulation of enzymes within the PPP and pathways involved in the conversion of acetate and glutamine into acetyl-CoA (256). During periods of lipid abundance, SREBP-1's transcriptional activity is repressed through its retention within the ER. Conversely, in instances of sterol depletion, proteolytic cleavage liberates the transcriptionally active domain, allowing it to translocate to the nucleus and bind to sterol response elements within the promoters of lipogenic genes (257). Cancer cells that have an unusually high demand for fatty acid synthesis find ways to activate SREBP-1. Beyond this, cancer cells also uptake fatty acids and lipids from the microenvironment to meet the biosynthetic demands. The PI3K-AKT pathway stimulation drives this pool towards lipogenesis and away from beta-oxidation. This describes an instance when the cells prioritize biosynthesis over energetics (258). This process becomes particularly important during times of metabolic stress, when cells struggle to meet the increased demands for building materials driven by oncogenes.

**Nucleotide biosynthesis**, such as purines and pyrimidines biosynthesis, are the basis of cell division which is further exacerbated in tumor cells. The process of synthesizing the phosphoribosyl amine backbone of these molecules begins with ribose-5-phosphate, an intermediate of the PPP, via an amide donation reaction involving glutamine as a substrate (259). Following this, purine and pyrimidine bases are synthesized from various nonessential amino acids and methyl groups derived from the one-carbon/folate pool. Moreover, the TCA cycle contributes oxaloacetate, which undergoes transamination to produce aspartate, an essential intermediate for the synthesis of both purine and pyrimidine bases. After this process, ribonucleotides are converted to deoxynucleotides by ribonucleotide reductase, requiring a source of NADPH. Robust mechanisms of feedback inhibition are extensively documented to regulate nucleotide accumulation, thus averting excessive levels. It is evident that nucleotide biosynthesis represents

a vulnerable point in cancer cells, as nucleoside analogs and antifolates have been fundamental components of chemotherapy treatments for many years (260).

Overall, these findings summarize how cancer cells tailor their metabolic processes for various essential functions, such as biosynthesis, energy production, and generating reducing agents to counteract oxidative stress. My findings contribute a new perspective to this adaptability, highlighting metabolic diversity within TNBC. Specifically, I demonstrate that treatment persister cells uniquely adjust their cysteine metabolism to enhance their glutathione levels, in contrast to other tumor cells. This observation also tells us that cancer cells have metabolic plasticity - depending on the environmental conditions and demands, it can utilize metabolite pools differently to achieve different functions. The overall goal is always to increase fitness in terms of survival or support exponential growth.

These basic discoveries in the field of tumor metabolism have been made possible primarily due to the emergence of technology allowing for precise measurements of metabolites. Scientists approach this in two ways - metabolomics, which gives a broad measurement of the metabolite abundance, and metabolic flux, which gives information about the activity of that particular pathway (261). Metabolomics primarily employs Mass Spectrometry (MS) and Nuclear Magnetic Resonance (NMR). Metabolic flux analysis requires the following  $^{13}\text{C}$ ,  $^{15}\text{N}$  and  $^2\text{H}$  isotope tracers which are usually made available to the cells as a nutrient source (such as  $^{13}\text{C}$ -glucose). The metabolites from those cells are then measured similarly by MS and NMR. This allows us to trace that isotope to different metabolites. Using the quantification from MS or NMR, we can now infer activity of the respective pathways. However, considering the radioactive nature of these flux experiments, they are usually limited to *in-vitro* systems.

Recent studies have started utilizing stable isotopes to explore metabolism within intact tumors. These isotopes, as they do not undergo radioactive decay, are safe for administration to both animals and human subjects. Administration of  $^{13}\text{C}$ -labeled nutrients systemically, either through boluses or continuous infusions, has been found to result in significant labeling of glycolytic and TCA cycle intermediates within tumors. For instance, in mice with orthotopic transplants of high-grade human gliomas, continuous infusion of  $^{13}\text{C}$ -glucose led to steady-state labeling of metabolites from the TCA cycle within the tumor, allowing for the evaluation of various metabolic pathways (262). Combining metabolomics and metabolic flux analysis with functional genomics helps pinpoint and comprehend metabolic weaknesses in cancer cells.

### **Oxidative stress and ROS: Is it good or bad for tumor progression?**

A clinically significant discovery from this thesis is that treatment persister cells exhibit protection against ROS, facilitated by TRPC6. This channel maintains high levels of GSH to counteract oxidative stress, promoting cell survival under stressful conditions. Our findings suggest that ROS can exert an anti-tumor effect, while aggressive populations employ antioxidant mechanisms to overcome it. This contradicts the conventional notion of ROS primarily promoting aggressive traits and aiding in tumorigenesis.

Traditionally, ROS were regarded as a toxic metabolic byproduct stemming from cellular respiration and protein folding. Contrary to that, research conducted over the last two decades have revealed a previously underestimated function of ROS in cellular signaling. At minimal concentrations, ROS promotes cell proliferation and aiding cellular adaptation to metabolic challenges by reversible oxidation of the cysteine residues on proteins (263). However, if when ROS levels are high, it gets converted to  $\text{OH}\cdot$  which leads to cell death due to macromolecular

damage. To prevent cell death from cancer, cells often upregulate ROS neutralizing enzymes, which is contrary to what cancer biologists initially thought. To the extent that antioxidants were considered as a feasible therapeutic approach in cancer patients. One example is cancer cells enhancing their antioxidant capacity by activating the transcription factor NRF2 (96, 264, 265). Upon activation, NRF2 stimulates the transcription of numerous antioxidant proteins, such as GPXs and Thioredoxins (TXNs), along with enzymes responsible for GSH synthesis and the import of cysteine via the cysteine/glutamate antiporter. These basic findings suggest that maintenance of Redox homeostasis is essential during tumorigenesis, and it can achieve different functions at different levels. These studies highlight a key double-edged sword property of ROS in tumorigenesis - they can be both pro and anti-tumorigenic depending on the amount of ROS and other environmental conditions (such as chemotherapy, dissemination, and starvation). Tumors utilize it differently at different stages of growth. In the initial stages, limited ROS pools trigger signaling pathways that indeed promote growth and migratory behaviors.

### **Metastatic cascade and the metabolic challenges**

Metastasis is the single most aggressive characteristic of tumors that drives most of the cancer-associated mortality rates. Breast cancers, specifically TNBC, show a high incidence rate of metastasis to lungs, brain, and liver. Although this results in lethal outcome, it is a very inefficient process by which only a fraction of cells that start the process successfully colonize the distant sites. Metastasis is a multi-step process involving cancer cells leaving the primary tumor, entering the bloodstream and lymphatic system, and finally colonizing the distant organ. Thus, the cancer cells traverse through diverse metabolic environments both in time and space compared to the primary site. Circulating tumor cells (CTCs) in blood with abundant oxygen and iron encounter a

huge oxidative stress pressure (97, 266). This observation contradicts the initial dogma in the field that overwhelming increase in ROS induces migratory behaviors and enables metastasis (263, 267). There have been recent studies in mouse models of cancer that support the new paradigm that ROS limits metastasis (183). Supplementation of antioxidants like N-acetylcysteine, vitamin E and certain dietary compounds (such as vitamin C,  $\beta$ -carotene, retinyl palmitate and canthaxanthin) promotes metastasis in mouse models of KRAS-driven lung cancer metastasis and BRAFV600E-driven melanoma (268, 269). As we have discussed, ferroptosis mediated cell death is caused by overwhelming phospholipid membrane peroxidation that requires iron and ROS. Taking this in context of the metabolic vulnerabilities of metastatic cells, strengthens our approach of impeding metastasis of breast cancer cells by inducing ferroptosis.

### **Novel methods of targeting aggressive traits of breast cancer**

There has been a justified huge interest in immunotherapy. Immunotherapy has the potential to completely abolish recurrence or even metastasis by educating the immune system (specifically T cells) that are poised to mount an immune response specifically to the cancer cells (270). Thus, ideally, they should be able to remove the residual cells after conventional therapy as well as from metastatic sites (271). Unfortunately, attempt to enhance anti-tumor immunity using checkpoint blockade anti-PD-1 has proven to be insufficient. Most times, tumors are immunologically cold and do not present enough antigens for immune cells to mount a response (272). In other cases, even though the initial anti-PD-1 treatments mount an immune response, chronic stimulation leads to exhaustion of the effector T cells (273). Specifically for breast cancer, immunotherapy has not been a successful avenue as evident from the mortality rates associated with resistance and metastasis (274).

The metastatic process remains poorly understood. It remains unclear whether any cell in the tumor can metastasize successfully, or if there are pre-existing clones that are better equipped to colonize distant sites. It is evident that cells with plasticity to adapt and rewire their signaling pathways and metabolic pathways would successfully colonize distal sites. We also understand now that ROS is limiting for the metastatic process and utilization of pro-oxidant approaches to kill metastatic cells have been employed. Within this context, ferroptosis is considered a promising strategy for targeting aggressive, metastatic cancer cells due to the inherent protection against ferroptosis in normal cells. This selectivity presents an opportunity for therapies that can specifically target cancer cells. Nevertheless, the implementation of such targeting strategies is complex. Effective therapeutic application of ferroptosis inducers requires the identification of specific biomarkers for the cancer type in question. Following biomarker identification, the delivery of ferroptosis-inducing drugs through antibodies targeted to the tumor must be accomplished. However, the process of targeting tumors with antibodies is inefficient (275). The antibodies must have very high affinity and specificity for the tumor to avoid unintended effects on normal tissue that could lead to severe consequences. Additionally, there is the challenge of optimal drug concentrations; while normal cells are usually resistant to ferroptosis, the drug concentrations used in animal studies could potentially cause acute inhibition of GPX4 (an enzyme that protects cells from oxidative damage) and lead to harmful side effects in normal cells. This delicate balance highlights the complexities of using ferroptosis as a therapeutic approach and necessitates further research to refine these strategies for clinical use (276).

Another important aspect to consider is the effect of ferroptotic drugs on immune cells. Research from Kim et. al. demonstrates that ferroptosis in Pathologically activated Neutrophils (PMNs), termed Myeloid-Derived Suppressor cells (PMN-MDSCs) within the TME results in greater

immunosuppression by transforming non-suppressive neutrophils into suppressive ones. This process is linked to an increased release of immunosuppressive molecules like Prostaglandin E2 (PGE2), which impairs T cell function, creating an immunosuppressive environment for the tumor (277). In a different study Yang et. al., looked at the diversity of ferroptosis traits in TNBC through multiomics analysis, showing that the luminal androgen receptor (LAR) subtype's vulnerability to ferroptosis via GPX4 inhibition. Their most significant finding was GPX4 inhibition not only induces tumor cell death but also bolsters antitumor immunity. Furthermore, it emphasizes the therapeutic effectiveness of pairing GPX4 inhibitors with anti-PD1 immunotherapy, suggesting a potent treatment strategy for TNBC (278). Thus, the effect of ferroptotic drugs on the immune system is unclear. This brings up a crucial problem in modeling tumors *in-vivo*. In this study we used PDX xenograft or TNBC cell lines in immunocompromised mice which fails to address how immune cells are being impacted during tumorigenesis or even by our drug treatments such as BI or IKE. In pancreatic cancer, tumor-associated macrophages have been implicated in promoting resistance to gemcitabine. These macrophages increase the expression of cytidine deaminase (CDA), an enzyme that deactivates gemcitabine, thus rendering it ineffective against tumor cells (279). Thus, it would be inaccurate to discount the role of an immunocompetent microenvironment in therapy resistance and metastasis.

The use of animal studies to model cancer and test therapies presents significant challenges. When tumors are modeled in immunocompromised mice, we fail to account for the critical interactions between tumor cells and the immune system that can influence both immune cell function and tumor growth, which can greatly influence both immune cell behavior and tumor development. The significance of immune-competent models in cancer research is supported by findings from the Agudo lab. Their work with a transgenic mouse model, featuring Jedi T-cells targeting GFP-

labeled tumor cells, showed that quiescent stem-like tumor cells could evade destruction by activated T-cells (280). While syngeneic models shed light on tumor-immune interactions, they do not capture the genetic complexity found in human cancers. On the other hand, xenografting patient-derived organoids (PDOs) into humanized mouse models can encompass the genetic diversity pertinent to human conditions. Choosing the optimal model is not straightforward but it is essential for identifying viable therapeutic targets. Data from our PDX mouse models of breast cancer are able to capture the complexity of human breast tumors. This provides a strong basis for targeting TRPC6 to counteract tumor intrinsic mechanisms of chemoresistance.

## Concluding Remarks

In my thesis, I adopted an unbiased approach to uncover novel proteins implicated in stemness and chemoresistance. Among these proteins, I identified TRPC6, a calcium channel crucial for maintaining stemness in TNBC. Given the high incidence of therapy resistance in TNBC, particularly associated with stem cells, I explored the relationship between TRPC6 and treatment persistence. Here I have shown that TRPC6-mediated calcium signaling suppresses the splicing protein ESRP1. This suppression by TRPC6 sustains the expression of the integrin  $\alpha 6B$  splice variant. Furthermore, my findings demonstrate the causal role of TRPC6 in promoting resistance to Paclitaxel. Utilizing a PDX model of TNBC, I show that inhibiting TRPC6 in combination with Paclitaxel significantly reduces tumor growth. Mechanistic insights provided in my thesis offer efficient ways to target treatment persister cells that drive recurrence and relapse.

In Chapter II, the thesis delineates a pathway whereby TRPC6-mediated activation of TAZ induces a quiescent state, presenting a paradox to the established view that activation of the Hippo pathway effector proteins YAP/TAZ typically promotes a proliferative phenotype. This observation raises a critical question: how can these findings be reconciled with the known functions of YAP and TAZ in cellular processes, including tumorigenesis and development? Indeed, YAP and TAZ are pivotal in regulating diverse cellular functions and have been implicated in both the promotion of stemness in triple-negative breast cancer and various other cellular outcomes in different cancers.

This divergence in function following YAP/TAZ activation may be attributable to the mode of upstream activation. For instance, besides LATS, which is a well-recognized inducer of YAP/TAZ inactivation, non-canonical pathways exist that can activate YAP/TAZ independent of LATS also exist. A study by Dupont et. al., presents significant insights into the activation mechanisms of

YAP and TAZ independent of LATS. Particularly, they showed that ECM stiffness emerges as a crucial physical factor in the activation and localization of YAP and TAZ, with stiffer environments promoting activation and nuclear presence of these regulators (141, 281). Given the various methods of activating TAZ, it's possible that each specific way of turning it on affects downstream consequences of YAP/TAZ activation differently, thus explaining the phenotypic diversity observed downstream. In my experimental model, I have noted that TRPC6 activates TAZ via a Rho-dependent mechanism that involves contractility. Thus I speculate whether the effects of TAZ are not merely due to its activation but it is worth looking at the context and manner of this activation while analyzing downstream effects.

Further complexity arises from the interaction of TAZ with gene regulatory elements. When TAZ forms complexes with TEAD and binds to gene regulatory elements, it can either induce or repress gene expression. Interestingly, genome-wide association studies suggest that YAP/TAZ predominantly binds to enhancer regions, which interact with AP-1 complexes to modulate gene expression, typically enhancing it. However, TAZ is also capable of binding near or at promoters, potentially exerting repressive effects on gene expression. This duality hints at a regulatory flexibility where enhancer binding might represent TAZ's primary function, but under conditions of acute activation, TAZ might bind to promoter sites, leading to gene repression and inducing a quiescent state.

Such hypotheses about the regulatory mechanisms of TAZ suggest that further genome-wide studies, such as Cut and Tag or Hi-C, under varying conditions of upstream activation or with mutants like constitutively active TAZ (4SA-TAZ), are essential to elucidate the specific patterns and conditions that determine whether YAP/TAZ activation leads to gene expression induction or

repression. This approach will provide deeper insights into the complex role of YAP/TAZ in cellular physiology and pathology.

In the mechanistic exploration of TRPC6-mediated signaling pathways detailed in this dissertation, it is crucial to recognize the involvement of key factors such as MYC, which plays a significant role in tumorigenesis. Notably, in several cancers characterized by MYC-driven mechanisms, patients typically exhibit poor prognosis. However, our findings diverge from the expected role of MYC, as we demonstrate that its suppression is instrumental in promoting a lethal, treatment-resistant phenotype in our models. Importantly, while MYC is recognized as one of the Yamanaka factors that enhances stemness (282)—a feature supported by extensive literature indicating MYC enrichment in cancer stem cell populations—our data present a paradox. We observe a suppressed MYC signature in quiescent, stem-like cells within triple-negative breast cancer models discussed in Chapter II, raising questions about the role of MYC in maintaining stemness in this context.

To elucidate this inconsistency, it becomes essential to dissect the tumor-initiating, stem-like population at the single-cell level and to employ unbiased pathway enrichment analyses to examine how these characteristics distribute within stem-like populations. Indeed, seminal research by John Dick's lab on acute myeloid leukemia (AML) using sc-RNA Seq revealed the presence of two distinct stem-like populations: one proliferative and the other slow-cycling and quiescent. Similarly, recent work by O'Connor et. al. mirrored these findings in T-cell acute lymphoblastic leukemia (T-ALL). He identified a subpopulation of leukemia-initiating cells (L-ICs) that exhibit chemotolerance and are linked to relapse. Utilizing sc-RNA Seq and nucleosome labeling, they discovered that this specific subset possesses a restricted cell cycle profile, expresses stemness and quiescence genes, and expands during leukemia progression, contributing to minimal residual disease (283).

Integrating these insights, our analysis suggests that in the quiescent stem-like populations we study, TRPC6 mechanistically suppresses MYC. This finding has significant clinical implications, providing mechanistic insights into an aggressive, treatment-persistent population and offering novel strategies for targeting these cells to enhance their responsiveness to therapeutic agents.

Ultimately, our model highlights the dual roles of tumorigenic factors such as MYC and TAZ, underscoring the necessity to dissect their functions across various clonal tumor populations rather than considering them in aggregate.

The optimal strategy to validate our findings involves implementing a single-cell approach on TNBC PDX tumors, categorizing them into cohorts that are either treatment-naive or subjected to short-term treatment with BI and PTX. This experimental design would require careful optimization of treatment durations to capture the clonal dynamics over time, ensuring that cellular viability is maintained for sequencing. This methodology would facilitate a comprehensive analysis of the clonal populations in the PDX. It would allow for the identification of distinct populations and using pathway enrichment analyses to ascertain whether the TRPC6-mediated signaling pathway is preferentially active in a slow-cycling population marked by high TAZ and low MYC transcriptomic signatures. By confirming these mechanistic details, such an approach would not only corroborate the findings presented in our study but also expand our understanding of whether targeting this pathway could be leveraged for therapeutic advantage.

Moreover, identifying this pathway and its key players, along with their transcriptomic signatures, could aid in the identification of patients likely to exhibit resistance mediated by these pathways. Achieving this would require a comprehensive approach, involving single-cell sequencing of TNBC PDX and applying deconvolution analyses to resolve bulk-sequencing data from patient

tumors at a quasi-single-cell resolution. This approach could be instrumental in pinpointing reliable biomarkers for patients predisposed to poor outcomes, recurrence, and relapse.

One of the key findings in Chapter III, is how treatment persister cells utilize trans-sulfuration (TSS) pathway to drive GSH that has a causal role in promoting survival under oxidative stress. Thus, in this light of our own observations, it is essential for us to discuss the functional importance of Cysteine metabolism in tumor development.

Cysteine serves as a cornerstone for numerous cellular functions, playing a particularly vital role within cancer cell biology. Comprehending the mechanisms by which cells regulate their cysteine reserves—whether through environmental absorption or internal generation via the TSS—is essential to decode the multifaceted roles of this amino acid and its impact on cellular processes. Cysteine, a thiol-containing amino acid, is crucial for synthesizing key metabolites across various biological processes. It provides sulfur to produce iron-sulfur (FeS) clusters (181) and coenzyme A (CoA) (284, 285), fundamental to metabolic enzymes. It's integral to thioredoxins' Cys-Gly-Pro-Cys motif, preserving protein thiol/disulfide equilibrium (286, 287). As a precursor for glutathione (GSH), the main antioxidant in mammalian cells, cysteine is vital for FeS protein activity and mitochondrial mRNA translation through mitochondrial GSH (288, 289). Cysteine also regulates ferroptosis—an iron-dependent cell death caused by lipid peroxidation, significant in various health and disease contexts (80), with GSH as a cofactor for GPX4, an enzyme inhibiting ferroptosis. Thus, cysteine is indispensable for diverse pathophysiological pathways.

**Roads to Cysteine:** Cancer cells usually bring in cystine through a specific transport system (xCT) but this uses up other important molecules inside the cell, which could lead to more problems for the cell, like oxidative stress (290-293). Even though cancer cells can find other ways to get

cysteine, such as breaking down GSH or eating proteins, these methods have their own issues. There isn't a lot of cysteine in proteins because it's so reactive (294), and while breaking down GSH outside the cell can provide some cysteine, it's not enough for the cell's needs (288). Intracellular GSH degradation also threatens redox balance and mitochondrial function, which rely on GSH. (295).

Amid these complexities, the trans-sulfuration (TSS) pathway emerges as an underexplored yet potentially significant player in cancer metabolism, with recent research highlighting its activation and critical role in de novo cysteine synthesis during tumor progression. While the uptake of cystine has been extensively studied, emerging research highlights TSS as a crucial mechanism for sustaining cysteine pools in cancer cells, especially under conditions of extracellular cystine scarcity. It is postulated that tumor cells, under conditions of pronounced oxidative stress due to accelerated proliferation and metastatic dissemination (183), may augment their dependence on endogenous cysteine production through the TSS pathway, particularly when extracellular cystine resources are scarce.

While some cancer cell lines maintain viability during cystine deprivation, robust proliferation under these conditions has not been demonstrated, even when the TSS pathway is essential for cell survival (180, 296-298). This holds true for neuroblastoma, Ewing sarcoma, and erastin-resistant ovarian cancer cells, where TSS supports survival but not growth under cystine limitation (292-294). Specifically, in Ewing sarcoma cells, Cystathione gamma-lyase (CTH) mediated cysteine synthesis combats ferroptosis during partial cystine deprivation, yet full deprivation remains lethal (292).

These findings indicate that TSS-driven cysteine synthesis, although crucial, does not sustain cellular proliferation. Factors such as the reduced substrate S-adenosylhomocysteine (SAH), produced by glycine N-methyltransferase (GNMT), may curtail this synthesis in certain cancers (293). Augmenting GNMT expression or supplementing with homocysteine can restore cell survival and division under cystine starvation (292-294). Additionally, PARK7, which supports SAH hydrolase under oxidative stress, is key for TSS function and ferroptosis resistance in non-small cell lung cancer (NSCLC) cells treated with erastin (299). These studies, conducted with adequate methionine and serine, confirm the critical roles of intermediate metabolites and enzymes in modulating TSS activity in cancer cells.

Collectively, these studies propose that *de novo* cysteine synthesis via TSS may act as a flexible, short-term response to stress in some cancer types when extracellular cystine is scarce. This implies that tumor cells could dynamically alternate between cystine import and TSS to manage cysteine levels, adjusting to immediate cystine availability. This ability to switch metabolic strategies may confer an adaptive advantage on cancer cells, helping them survive the fluctuating conditions of metastasis or nutrient-poor environments in the body, which present more variable challenges than the constant cystine starvation conditions created in the lab.

An important finding in my Chapter III of the thesis is TSS pathway is integral for cell survival under oxidative stress within quiescent and slow-cycling cancer cell populations characterized by elevated TRPC6 levels. This underscores the necessity for a nuanced assessment of TSS's role in tumor development, particularly considering the heterogeneity of clonal populations. It suggests that TSS-related GSH production contributes to ferroptosis resistance, yet the cysteine pools are unlikely to support high proliferation demands and hence mostly utilized my stem-like quiescent clonal populations as supported by other studies as well.

The precise mechanisms by which quiescent cells enhance TSS pathway and the role TRPC6 plays in this enhancement demand further exploration. Chapter II of my thesis shows that TRPC6's role in maintaining a quiescent treatment persist state is achieved by suppressing MYC. This raises questions about the possible interaction between TRPC6 and TSS: does TRPC6 direct cell fate by driving stem-like quiescent cells to enter a survival state through epigenetic changes or by suppressing MYC? Alternatively, might MYC suppression itself alter the balance between using the xCT transporter and activating TSS for the cell's cysteine needs?

It is noteworthy that such a reduction in biosynthetic and bioenergetic processes is also seen during Embryonic Diapause, suggesting that cancer cells might co-opt existing developmental pathways to overcome nutrient scarcity or stress, such as that induced by chemotherapy, rather than creating entirely new mechanisms. Our study specifically sheds light on pre-existing quiescent clones that exhibit resistance to treatment, which seem to be innately equipped to utilize the TSS pathway for their cysteine supply. It's critical to note, our model does not account for temporal heterogeneity, and thus it may not fully capture the spectrum or nature of acquired persistence and the specific role metabolic flexibility in enabling it.

Considering the evidence of stress response in tumors, I propose that cysteine metabolism may demonstrate a form of metabolic plasticity, equipping cells with the capability to rapidly adapt to environmental fluctuations. This includes swift responses to oxidative stress encountered during metastasis or to cysteine depletion during periods of accelerated tumor growth. Hence, to truly grasp the metabolic intricacies of cancer, one must investigate beyond the immediate metabolic landscape of tumor clonal populations, but also consider the progressive changes and adaptations that occur over time and in response to diverse conditions that mirror the natural progression of tumor development. Embracing this comprehensive perspective is essential to accurately identify

the vulnerabilities of cancer cells at various stages, which is a fundamental step toward developing more precise and effective therapeutic interventions.

While my *in-vitro* findings affirm the TSS pathway's role in supporting survival amid oxidative stress, we have yet to establish if metastasizing cancer cells exploit this pathway to survive and colonise in new organs. In Chapter III, a critical observation was that BI treatment diminished the spread of breast cancer cells to the lungs. This result provides a valuable model to dissect the TSS pathway's involvement in the metastasis of TNBC, potentially offering fresh perspectives on the metabolic needs of TNBC during metastasis.

Such insights are pivotal to grasp the intrinsic mechanisms and pathways that drive metastasis. The implications of these findings could be broadened by employing varied models of spontaneous and induced metastasis to ascertain whether cancer cells undergo reprogramming for survival, or if certain pre-existing clones possess inherent advantages in redox regulation—or if it's a combination of both. Delving deeper into the TSS pathway and identifying targeted interventions might pave the way to even selectively trigger ferroptosis in tumor cells. A strategic focus on this pathway may allow us to minimize unintended impacts on immune cell populations that do not rely on TSS, thereby enhancing the specificity and safety of these pro-oxidant therapeutic approaches.

In Chapter III, I show that TRPC6 inhibition can sensitize resistant cells to ferroptosis. However, one might speculate the need for that considering, how TRPC6 inhibition synergizes with PTX to induce cell death. While TRPC6 and chemotherapy have shown potential in sensitizing these aggressive populations, chemotherapy's broad effects can significantly harm normal cells, particularly immune cells. This is a clinical concern, especially with the growing appreciation of

immunotherapy, as chemotherapy may adversely impact the efficacy of immunotherapeutic approaches.

My findings reveal that the p27<sup>high</sup> persister population, characterized by high TRPC6 levels, demonstrates protection against oxidative stress. This contradicts certain studies suggesting that chemoresistant cells are susceptible to ferroptosis. I have found that TRPC6 inhibition sensitizes the persister cells to ferroptosis and its overexpression is sufficient to promote resistance in otherwise sensitive TNBC. This led me to investigate whether we can exploit TRPC6 inhibition during metastasis to overwhelm the cells with oxidative stress that could potentially impede successful metastasis to distant organs. Using a tail-vein model of breast cancer cell metastasis to the lungs, we show that TRPC6 inhibition significantly reduces metastatic growth in the lungs and that it can be rescued with Ferroptosis inhibitor Liproxstatin-1. This crucial finding not only unveils new therapeutic paths for targeting TRPC6 in clinical contexts of metastasis but also reinforces the role of ROS in limiting metastasis. However, our findings supported by others, prove that indeed pro-oxidant strategies are an effective way to reduce successful metastasis.

I initially identified TRPC6 from a stem-cell model of breast cancer. To understand the subtype specificity of TRPC6, I used organoids derived from PDXs of ER<sup>+</sup> and TNBC and specimens from patient tumors. There was clear distinction showing specificity of TRPC6 expression TNBC organoids and staining in a few patient samples. However, it's important to note that there is currently limited clinical evidence supporting the targeting of TRPC6. In analyses of public databases comprising gene expression data from patient samples across diverse tumor types, including both primary and metastatic tumors, TRPC6 is not well represented. Although there is a slight statistical enrichment of the channel in TNBC compared to other subtypes and its metastatic sites (as illustrated in the appendix) compared to primary tumors, these differences are subtle at

best and not particularly promising. Given this, it is reasonable to question the potential clinical benefit of targeting this pathway to selectively address aggressive populations.

While it may appear reasonable to question the clinical benefit of targeting TRPC6, it is essential to note that TRPC6 is clonally expressed in a rare population within the TNBC cell lines and organoids we have examined. This could explain the lack of representation in public gene expression data sets that are bulk RNA-Seq datasets from patient tumors. Establishing a robust clinical correlation is indeed imperative for translation of these findings. While single-cell RNA-Seq data could address this issue, it's currently unavailable for patient tumors. An alternative approach would involve obtaining single-cell RNA-Seq data from TNBC PDXs and leveraging deconvolution analysis of bulk RNA-Seq data from patient tumors to achieve some degree of clonal resolution. By combining these strategies, we can gain a more definitive understanding of TRPC6's presence in patient tumors, its frequency, and the transcriptomic signature of the respective clonal population. Conducting such analysis and validation in TNBC organoids will offer a compelling rationale for therapeutically targeting TRPC6 to mitigate resistance and metastasis.

In summary, my thesis suggests a new method to enhance TNBC responsiveness to chemotherapy. Most importantly, it shows that inhibiting TRPC6 can reduce lung metastatic colonization by inducing ferroptosis in the TNBC cells.

## APPENDIX

In this thesis I have determined the molecular mechanisms of TRPC6-mediated calcium signaling in promoting chemoresistance and ferroptosis resistance. Yet, it remains to be understood how the channel impacts intracellular calcium dynamics, how it gets activated, and specially how TRPC6 expression is regulated in the BCSCs. In this section I will briefly highlight some preliminary data that may help answer the above questions.

### **C-X-C motif chemokine receptor 4 (CXCR4) activates TRPC6-mediated calcium uptake:**

Given the established role of TRPC6 sustaining stemness and fostering aggressive phenotypes in TNBC, the specific mechanism by which TRPC6 may affect calcium dynamics remains unclear. To determine whether TRPC6 is involved in the modulation of calcium dynamics in TNBC cells, I employed the calcium-sensitive dye Fluo-4 for semi-quantitative measurements of intracellular calcium levels in both Cal51 control cells and TRPC6 KD cells. This study was designed to specifically examine extracellular calcium uptake, following the precedent set by prior research highlighting TRPC6's role in SOCE. The cells were treated in a calcium-free Hanks' Balanced Salt Solution (HBSS) buffer and incubated with the dye under these conditions. Time-lapse imaging was initiated at the point of reintroduction of complete HBSS media (time-point 0), to capture the dynamic changes in calcium levels, with images captured at 3-second intervals. The analysis of Fluo-4 fluorescence provided a semi-quantitative view of intracellular calcium dynamics. For a more precise quantification of calcium concentrations, the Fura-2 assay would be required, although it was not utilized in the current study. The observed data, indicated by the Mean Fluorescence Intensity (MFI) of the Fluo-4 dye, suggests that TRPC6 deficiency results in

diminished calcium uptake, demonstrating the channel's significant role in calcium uptake in TNBC cells (**Fig. A.1A**).

As elucidated in the introduction, cellular maintenance of a calcium gradient is an energetically demanding process, which illustrates the necessity for tight regulation of calcium trafficking within the cell (refer to Introduction for details). TRP channels are commonly activated by GPCRs, prompting an investigation into the possible activators of TRPC6. The RNA-Seq analysis of a breast cancer stem-cell-enriched model highlighted CXCR4 as significantly upregulated within the stem cell cohort. Given the established role of CXCR4 in maintaining stemness and facilitating metastasis in breast cancer (300), I investigated whether the interaction between CXCR4 and its ligand C-X-C chemokine ligand 12 (CXCL12) could be activating TRPC6. Employing calcium imaging with Fluo-4, I assessed the mean fluorescence intensity (MFI) changes in response to Plerixafor, a CXCR4 inhibitor. The data indicated a decrease in intracellular calcium levels upon Plerixafor treatment, comparable to the reduction observed with BI treatment. This effect was not intensified when Plerixafor was combined with BI, suggesting that CXCR4 is the upstream activator of TRPC6-mediated calcium uptake (**Fig. A.1B**). Further I measured the expression levels of ESRP1 upon Plerixafor treatment. The data provides supports the hypothesis that CXCR4 plays a functional role in TRPC6 activation and that its inhibition therefore causes a significant increase ESRP1 expression (**Fig. A.1C**). These findings are at an early stage and further research is needed to confirm the activation of TRPC6 by CXCR4 in TNBC stem cells. A potential approach would be to reduce CXCR4 levels using shRNA in cancer stem cells (transfected with empty vector or the TRPC6 pore-mutant) and then analyze the calcium dynamics to evaluate TRPC6 activity. Additionally, given the high secretion of CXCL12 by cancer cells, silencing this ligand

and assessing the subsequent calcium influx (in WT and TRPC6 pore-mutant CSCs) could provide further evidence supporting the role of CXCR4 in triggering TRPC6 in breast cancer stem cells.

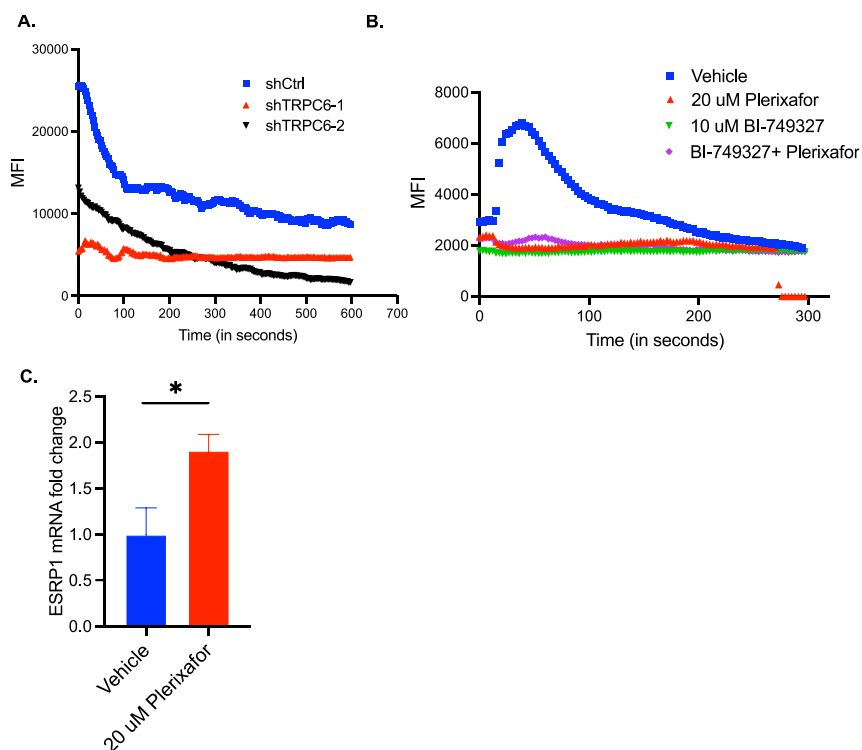


**Figure A1. CXCR4 activates TRPC6-mediated calcium uptake.** **A.** MFI of the Fluo-4 from 20 cells in the field was plotted from each image that was taken between 0-600 seconds in the Cal51 control and TRPC6 KD cells. **B.** MFI of the Fluo-4 from 20 cells in the field was plotted from each image that was taken between 0-300 seconds in the cells treated with either of the following: Vehicle (DMSO), BI (10 uM), Plerixafor (20 uM), BI+Plerixafor. **C.** qPCR data showing the expression levels of ESRP1 in Cal51 cells treated with Vehicle or Plerixafor for 24 hours.

**BCL11A regulates the expression of *TRPC6* in BCSCs.** In TNBC, *TRPC6* expression is notably variable and appears to correlate with a stem-like population, which led to an investigation into the regulatory mechanisms behind its expression. Utilizing ENCODE chromatin immunoprecipitation sequencing (ChIP-seq) data, we identified *BCL11A* as a significant regulator of *TRPC6* (139), a transcription factor implicated in various cancers' development including stemness and metastasis in TNBC (301, 302). My aim was to elucidate the role of *BCL11A* in the regulation of *TRPC6* expression in TNBC stem cells. I began by isolating the CSC population from the TNBC cell line, CAL-51 (Fig. 2A), and examined the differential binding of *BCL11A* to the *TRPC6* enhancer across CSC and non-CSC populations. Primers specific to the *TRPC6* enhancer region—where *BCL11A* binding had been indicated by ENCODE ChIP-seq data—were designed. Subsequent ChIP-qPCR experiments targeting *BCL11A* revealed a significant enrichment of the *TRPC6* enhancer sequence, corroborating our hypothesis as demonstrated by our qPCR results (Fig. 2B). Further, I knocked down *BCL11A* using two different shRNAs (Fig. 2C) and observed a significant downregulation of *TRPC6* in the *BCL11A* knockdown cells (Fig. 2D).

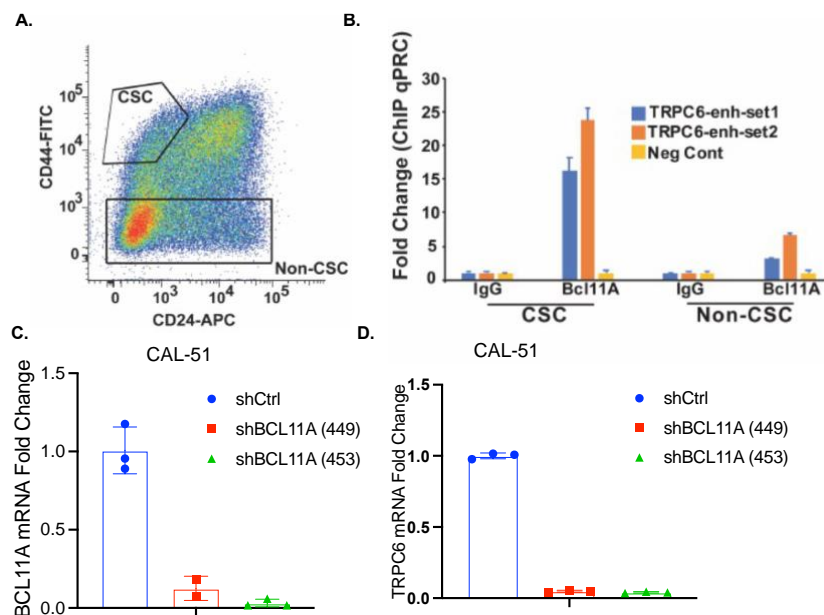


**Figure A2. BCL11A interacts with the TRPC6 gene.** A. CAL51 cells were FACS into CSC and non-CSC populations using CD44 and CD24. B. ChIP was performed using a BCL11A antibody and immunoprecipitated DNA was qPCR amplified using primers targeting either the TRPC6 proposed enhance

region or the C-terminal region (negative control). **C, D.** qPCR data showing the expression levels of BCL11A (C) and TRPC6 (D) in control and BCL11A KD Cal51 cells.

**TRPC6 is enriched in a hybrid E/M population.** The evidence linking stemness and metastasis to a state of partial EMT prompted the sorting of a TNBC cell line (HCC1806) into TRPC6-high and -low populations. The TRPC6-high group expressed both epithelial and mesenchymal markers, ITGB4 and CD44, respectively as well as other established markers of an E/M state such as FGFR1 (303). Additionally, cells sorted for CD44/ITGB4 expression showed that the CD44-high/ITGB4-high subset exhibited the highest levels of TRPC6. This suggests that elevated TRPC6 expression is indicative of a partial EMT state in these cells.

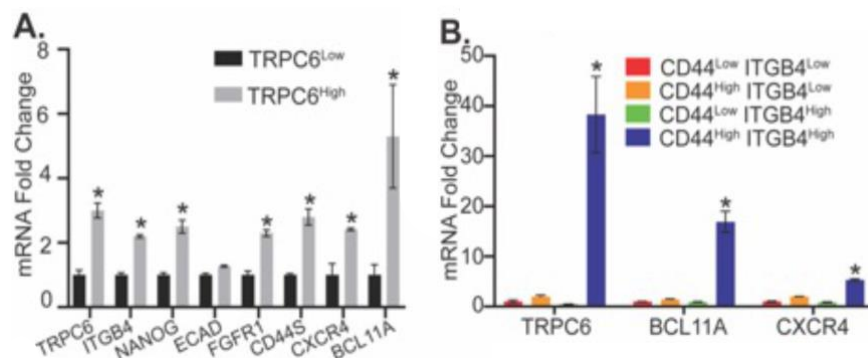


**Figure A3. TRPC6 is enriched in a hybrid E/M population:** **A.** qPCR data showing the expression levels of E/M markers in the TRPC6 high and low population that were sorted from CAL-51 cells. **B.** HCC-1806 TNBC cells were sorted based on CD44 and ITGB4 expression. qPCR data showing the expression levels of *TRPC6*, *BCL11A*, and *CXCR4* in the CD44<sup>high</sup>/ITGB4<sup>high</sup> populations compared to the others.

The data presented broadens our comprehension of TRPC6-driven calcium influx and its regulatory mechanisms, and sheds light on the specific cellular phenotypes associated with high TRPC6 expression, particularly the epithelial-mesenchymal (E/M) transitional state.

**TRPC6 expression in metastatic cell lines and clinical samples:** I analysed the expression levels of TRPC6 amongst the MDA-MB-231-cell variant specially to get a clue whether it has any association with aggressive variants. My data shows that TRPC6 expression is highest in the metastatic 231-LM2 variant that is known for its capacity to colonise the lungs. However, the most important basis for targeting any molecule in a clinical setting is get an idea of how it is expressed in patient samples. To do so, I looked at the expression levels of TRPC6 in primary and metastatic tumours of TNBC patients. The data I analysed is obtained from the metastatic breast cancer project dataset . The data shows mRNA expression of TRPC6 in primary tumours and if they had liver mets at the time of diagnosis (TRUE, FALSE). This suggests there is slight correlation between higher expression levels of TRPC6 and the occurrence of metastasis in patients.

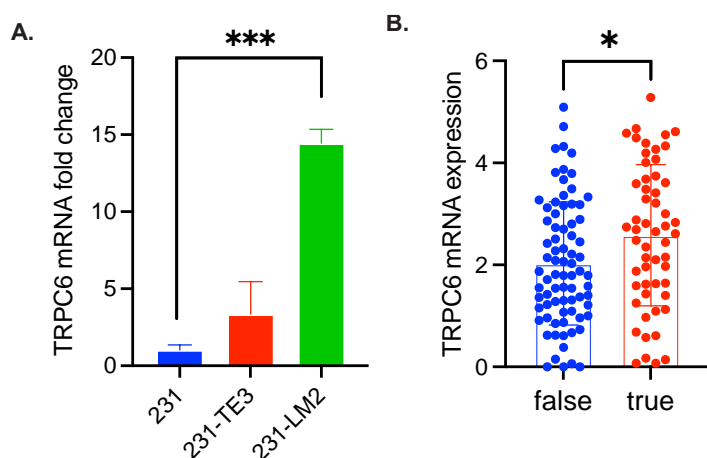


**Figure A4: TRPC6 expression in metastatic cell lines and clinical samples.** **A.** qPCR data showing expression levels of TRPC6 in the variants of MDA-MB-231 cell line. **B.** Data from the metastatic breast cancer project dataset was analysed to look at expression levels of TRPC6 and compare the incidence rate of metastasis amongst those patients.

## Materials and Methods

**Cells and reagents:** CAL-51 cells were obtained from the Leibniz Institute DSMZ, Germany and HCC1806 cells were purchased from the American Type Culture Collection. The TRPC6 inhibitor BI-749327 was purchased from MedChem Express (Catalogue no. HY-111925), Plerixafor was purchased from selleckchem (Catalogue no. S8030). The following Abs were used for flow cytometry: CD24–allophycocyanin (APC; ML5, BioLegend), CD44-FITC (IM7, BioLegend) and anti-rabbit FITC (MRM-47, BioLegend), anti-Rabbit-555 (Invitrogen-A32732), TRPC6 (18236-1-AP, Proteintech).

**shRNAs and expression constructs:** The following lentiviral shRNAs were obtained from our core facility: BCL11A (TRCN0000033449 and TRCN0000033453).

**Flow cytometry:** Antibody staining, and flow cytometry were accomplished as described in Chapter II. Flow activated sorting and data analysis were performed by Sony SH800 sorter and analyzed using FlowJo software.

**Real time qPCR:** mRNA quantification was accomplished using an RNA isolation kit (BS88133, Bio Basic Inc.), and complementary DNAs (cDNAs) were produced using an Azura cDNA synthesis kit (AZ-1996, Azura Genomics). Azura View GreenFast qPCR Blue Mix LR was used as the qPCR Master Mix (AZ-1996, Azura Genomics).

**Chromatin immunoprecipitation:** ChIP was performed using a ChIP-IT Express Chromatin Immunoprecipitation kit (Active Motif). Antibodies used were BCL11A (N-G2, Santa Cruz Biotechnology). The following qPCR primer sequence was used to amplify the region of the BCL11A peak in the TRPC6 enhancer identified in ENCODE: primers: 5'-GCTTACAGCTGGCTTCACTT-3' (forward) 5'-GGCCGAGAGAGAGAGAGATTT-3' (reverse) and the cDNA qPCR primer of TRPC6 used as the negative control.

## Bibliography

1. Rojas K, Stuckey A. Breast Cancer Epidemiology and Risk Factors. *Clin Obstet Gynecol.* 2016;59(4):651-72. Epub 2016/10/21. doi: 10.1097/GRF.0000000000000239. PubMed PMID: 27681694.
2. Stuckey A. Breast cancer: epidemiology and risk factors. *Clin Obstet Gynecol.* 2011;54(1):96-102. Epub 2011/02/01. doi: 10.1097/GRF.0b013e3182080056. PubMed PMID: 21278508.
3. Xu H, Xu B. Breast cancer: Epidemiology, risk factors and screening. *Chin J Cancer Res.* 2023;35(6):565-83. Epub 2024/01/11. doi: 10.21147/j.issn.1000-9604.2023.06.02. PubMed PMID: 38204449; PMCID: PMC10774137.
4. Makki J. Diversity of Breast Carcinoma: Histological Subtypes and Clinical Relevance. *Clin Med Insights Pathol.* 2015;8:23-31. Epub 2016/01/08. doi: 10.4137/CPath.S31563. PubMed PMID: 26740749; PMCID: PMC4689326.
5. Malhotra GK, Zhao X, Band H, Band V. Histological, molecular and functional subtypes of breast cancers. *Cancer Biol Ther.* 2010;10(10):955-60. Epub 2010/11/09. doi: 10.4161/cbt.10.10.13879. PubMed PMID: 21057215; PMCID: PMC3047091.
6. Perou CM, Sorlie T, Eisen MB, van de Rijn M, Jeffrey SS, Rees CA, Pollack JR, Ross DT, Johnsen H, Akslen LA, Fluge O, Pergamenschikov A, Williams C, Zhu SX, Lonning PE, Borresen-Dale AL, Brown PO, Botstein D. Molecular portraits of human breast tumours. *Nature.* 2000;406(6797):747-52. Epub 2000/08/30. doi: 10.1038/35021093. PubMed PMID: 10963602.
7. Cancer Genome Atlas N. Comprehensive molecular portraits of human breast tumours. *Nature.* 2012;490(7418):61-70. Epub 2012/09/25. doi: 10.1038/nature11412. PubMed PMID: 23000897; PMCID: PMC3465532.
8. Sorlie T, Perou CM, Tibshirani R, Aas T, Geisler S, Johnsen H, Hastie T, Eisen MB, van de Rijn M, Jeffrey SS, Thorsen T, Quist H, Matese JC, Brown PO, Botstein D, Lonning PE, Borresen-Dale AL. Gene expression patterns of breast carcinomas distinguish tumor subclasses with clinical implications. *Proc Natl Acad Sci U S A.* 2001;98(19):10869-74. Epub 2001/09/13. doi: 10.1073/pnas.191367098. PubMed PMID: 11553815; PMCID: PMC58566.
9. Falato C, Schettini F, Pascual T, Braso-Maristany F, Prat A. Clinical implications of the intrinsic molecular subtypes in hormone receptor-positive and HER2-negative metastatic breast cancer. *Cancer Treat Rev.* 2023;112:102496. Epub 2022/12/24. doi: 10.1016/j.ctrv.2022.102496. PubMed PMID: 36563600.
10. Prat A, Pineda E, Adamo B, Galvan P, Fernandez A, Gaba L, Diez M, Viladot M, Arance A, Munoz M. Clinical implications of the intrinsic molecular subtypes of breast cancer. *Breast.* 2015;24 Suppl 2:S26-35. Epub 2015/08/09. doi: 10.1016/j.breast.2015.07.008. PubMed PMID: 26253814.

11. Kreike B, van Kouwenhove M, Horlings H, Weigelt B, Peterse H, Bartelink H, van de Vijver MJ. Gene expression profiling and histopathological characterization of triple-negative/basal-like breast carcinomas. *Breast Cancer Res.* 2007;9(5):R65. Epub 2007/10/04. doi: 10.1186/bcr1771. PubMed PMID: 17910759; PMCID: PMC2242660.
12. Rakha EA, Elsheikh SE, Aleskandarany MA, Habashi HO, Green AR, Powe DG, El-Sayed ME, Benhasouna A, Brunet JS, Akslen LA, Evans AJ, Blamey R, Reis-Filho JS, Foulkes WD, Ellis IO. Triple-negative breast cancer: distinguishing between basal and nonbasal subtypes. *Clin Cancer Res.* 2009;15(7):2302-10. Epub 2009/03/26. doi: 10.1158/1078-0432.CCR-08-2132. PubMed PMID: 19318481.
13. Bertucci F, Finetti P, Cervera N, Esterni B, Hermitte F, Viens P, Birnbaum D. How basal are triple-negative breast cancers? *Int J Cancer.* 2008;123(1):236-40. Epub 2008/04/10. doi: 10.1002/ijc.23518. PubMed PMID: 18398844.
14. Lehmann BD, Bauer JA, Chen X, Sanders ME, Chakravarthy AB, Shyr Y, Pietenpol JA. Identification of human triple-negative breast cancer subtypes and preclinical models for selection of targeted therapies. *J Clin Invest.* 2011;121(7):2750-67. Epub 2011/06/03. doi: 10.1172/JCI45014. PubMed PMID: 21633166; PMCID: PMC3127435.
15. Sorlie T, Tibshirani R, Parker J, Hastie T, Marron JS, Nobel A, Deng S, Johnsen H, Pesich R, Geisler S, Demeter J, Perou CM, Lonning PE, Brown PO, Borresen-Dale AL, Botstein D. Repeated observation of breast tumor subtypes in independent gene expression data sets. *Proc Natl Acad Sci U S A.* 2003;100(14):8418-23. Epub 2003/06/28. doi: 10.1073/pnas.0932692100. PubMed PMID: 12829800; PMCID: PMC166244.
16. Dai X, Li T, Bai Z, Yang Y, Liu X, Zhan J, Shi B. Breast cancer intrinsic subtype classification, clinical use and future trends. *Am J Cancer Res.* 2015;5(10):2929-43. Epub 2015/12/23. PubMed PMID: 26693050; PMCID: PMC4656721.
17. Shah SP, Roth A, Goya R, Oloumi A, Ha G, Zhao Y, Turashvili G, Ding J, Tse K, Haffari G, Bashashati A, Prentice LM, Khattra J, Burleigh A, Yap D, Bernard V, McPherson A, Shumansky K, Crisan A, Giuliany R, Heravi-Moussavi A, Rosner J, Lai D, Birol I, Varhol R, Tam A, Dhalla N, Zeng T, Ma K, Chan SK, Griffith M, Moradian A, Cheng SW, Morin GB, Watson P, Gelmon K, Chia S, Chin SF, Curtis C, Rueda OM, Pharoah PD, Damaraju S, Mackey J, Hoon K, Harkins T, Tadigotla V, Sigaroudinia M, Gascard P, Tlsty T, Costello JF, Meyer IM, Eaves CJ, Wasserman WW, Jones S, Huntsman D, Hirst M, Caldas C, Marra MA, Aparicio S. The clonal and mutational evolution spectrum of primary triple-negative breast cancers. *Nature.* 2012;486(7403):395-9. Epub 2012/04/13. doi: 10.1038/nature10933. PubMed PMID: 22495314; PMCID: PMC3863681.
18. Thong T, Wang Y, Brooks MD, Lee CT, Scott C, Balzano L, Wicha MS, Colacino JA. Hybrid Stem Cell States: Insights Into the Relationship Between Mammary Development and Breast Cancer Using Single-Cell Transcriptomics. *Front Cell Dev Biol.* 2020;8:288. Epub 2020/05/28. doi: 10.3389/fcell.2020.00288. PubMed PMID: 32457901; PMCID: PMC7227401.

19. Visvader JE, Lindeman GJ. Cancer stem cells: current status and evolving complexities. *Cell Stem Cell*. 2012;10(6):717-28. Epub 2012/06/19. doi: 10.1016/j.stem.2012.05.007. PubMed PMID: 22704512.
20. Sin WC, Lim CL. Breast cancer stem cells-from origins to targeted therapy. *Stem Cell Investig*. 2017;4:96. Epub 2017/12/23. doi: 10.21037/sci.2017.11.03. PubMed PMID: 29270422; PMCID: PMC5723743.
21. Al-Hajj M, Wicha MS, Benito-Hernandez A, Morrison SJ, Clarke MF. Prospective identification of tumorigenic breast cancer cells. *Proc Natl Acad Sci U S A*. 2003;100(7):3983-8. Epub 2003/03/12. doi: 10.1073/pnas.0530291100. PubMed PMID: 12629218; PMCID: PMC153034.
22. Liu Y, Nenutil R, Appleyard MV, Murray K, Boylan M, Thompson AM, Coates PJ. Lack of correlation of stem cell markers in breast cancer stem cells. *Br J Cancer*. 2014;110(8):2063-71. Epub 2014/03/01. doi: 10.1038/bjc.2014.105. PubMed PMID: 24577057; PMCID: PMC3992489.
23. Dontu G, Wicha MS. Survival of mammary stem cells in suspension culture: implications for stem cell biology and neoplasia. *J Mammary Gland Biol Neoplasia*. 2005;10(1):75-86. Epub 2005/05/12. doi: 10.1007/s10911-005-2542-5. PubMed PMID: 15886888.
24. Elbaiomy MA, Akl T, Atwan N, Elsayed AA, Elzaafarany M, Shamaa S. Clinical Impact of Breast Cancer Stem Cells in Metastatic Breast Cancer Patients. *J Oncol*. 2020;2020:2561726. Epub 2020/07/21. doi: 10.1155/2020/2561726. PubMed PMID: 32684928; PMCID: PMC7336231.
25. Li X, Lewis MT, Huang J, Gutierrez C, Osborne CK, Wu MF, Hilsenbeck SG, Pavlick A, Zhang X, Chamness GC, Wong H, Rosen J, Chang JC. Intrinsic resistance of tumorigenic breast cancer cells to chemotherapy. *J Natl Cancer Inst*. 2008;100(9):672-9. Epub 2008/05/01. doi: 10.1093/jnci/djn123. PubMed PMID: 18445819.
26. Jiang G, Tu J, Zhou L, Dong M, Fan J, Chang Z, Zhang L, Bian X, Liu S. Single-cell transcriptomics reveal the heterogeneity and dynamic of cancer stem-like cells during breast tumor progression. *Cell Death Dis*. 2021;12(11):979. Epub 2021/10/23. doi: 10.1038/s41419-021-04261-y. PubMed PMID: 34675206; PMCID: PMC8531288.
27. Visvader JE. Keeping abreast of the mammary epithelial hierarchy and breast tumorigenesis. *Genes Dev*. 2009;23(22):2563-77. Epub 2009/11/26. doi: 10.1101/gad.1849509. PubMed PMID: 19933147; PMCID: PMC2779757.
28. Visvader JE, Stingl J. Mammary stem cells and the differentiation hierarchy: current status and perspectives. *Genes Dev*. 2014;28(11):1143-58. Epub 2014/06/04. doi: 10.1101/gad.242511.114. PubMed PMID: 24888586; PMCID: PMC4052761.

29. Goldstein M, Kastan MB. The DNA damage response: implications for tumor responses to radiation and chemotherapy. *Annu Rev Med.* 2015;66:129-43. Epub 2014/11/26. doi: 10.1146/annurev-med-081313-121208. PubMed PMID: 25423595.
30. Lagadec C, Vlashi E, Della Donna L, Dekmezian C, Pajonk F. Radiation-induced reprogramming of breast cancer cells. *Stem Cells.* 2012;30(5):833-44. Epub 2012/04/11. doi: 10.1002/stem.1058. PubMed PMID: 22489015; PMCID: PMC3413333.
31. Chaffer CL, Marjanovic ND, Lee T, Bell G, Klier CG, Reinhardt F, D'Alessio AC, Young RA, Weinberg RA. Poised chromatin at the ZEB1 promoter enables breast cancer cell plasticity and enhances tumorigenicity. *Cell.* 2013;154(1):61-74. Epub 2013/07/06. doi: 10.1016/j.cell.2013.06.005. PubMed PMID: 23827675; PMCID: PMC4015106.
32. Koren S, Reavie L, Couto JP, De Silva D, Stadler MB, Roloff T, Britschgi A, Eichlisberger T, Kohler H, Aina O, Cardiff RD, Bentires-Alj M. PIK3CA(H1047R) induces multipotency and multi-lineage mammary tumours. *Nature.* 2015;525(7567):114-8. Epub 2015/08/13. doi: 10.1038/nature14669. PubMed PMID: 26266975.
33. Pece S, Tosoni D, Confalonieri S, Mazzarol G, Vecchi M, Ronzoni S, Bernard L, Viale G, Pelicci PG, Di Fiore PP. Biological and molecular heterogeneity of breast cancers correlates with their cancer stem cell content. *Cell.* 2010;140(1):62-73. Epub 2010/01/16. doi: 10.1016/j.cell.2009.12.007. PubMed PMID: 20074520.
34. Collina F, Di Bonito M, Li Bergolis V, De Laurentiis M, Vitagliano C, Cerrone M, Nuzzo F, Cantile M, Botti G. Prognostic Value of Cancer Stem Cells Markers in Triple-Negative Breast Cancer. *Biomed Res Int.* 2015;2015:158682. Epub 2015/10/28. doi: 10.1155/2015/158682. PubMed PMID: 26504780; PMCID: PMC4609334.
35. Clapham DE. Calcium signaling. *Cell.* 2007;131(6):1047-58. Epub 2007/12/18. doi: 10.1016/j.cell.2007.11.028. PubMed PMID: 18083096.
36. Hoeflich KP, Ikura M. Calmodulin in action: diversity in target recognition and activation mechanisms. *Cell.* 2002;108(6):739-42. Epub 2002/04/17. doi: 10.1016/s0092-8674(02)00682-7. PubMed PMID: 11955428.
37. Meador WE, Means AR, Quijcho FA. Target enzyme recognition by calmodulin: 2.4 Å structure of a calmodulin-peptide complex. *Science.* 1992;257(5074):1251-5. Epub 1992/08/28. doi: 10.1126/science.1519061. PubMed PMID: 1519061.
38. Meador WE, Means AR, Quijcho FA. Modulation of calmodulin plasticity in molecular recognition on the basis of x-ray structures. *Science.* 1993;262(5140):1718-21. Epub 1993/12/10. doi: 10.1126/science.8259515. PubMed PMID: 8259515.
39. Hilgemann DW, Fine M, Linder ME, Jennings BC, Lin MJ. Massive endocytosis triggered by surface membrane palmitoylation under mitochondrial control in BHK fibroblasts. *Elife.* 2013;2:e01293. Epub 2013/11/28. doi: 10.7554/eLife.01293. PubMed PMID: 24282236; PMCID: PMC3839538.

40. Terlau H, Stuhmer W. Structure and function of voltage-gated ion channels. *Naturwissenschaften*. 1998;85(9):437-44. Epub 1998/11/05. doi: 10.1007/s001140050527. PubMed PMID: 9802045.
41. Ramsey IS, Delling M, Clapham DE. An introduction to TRP channels. *Annu Rev Physiol*. 2006;68:619-47. Epub 2006/02/08. doi: 10.1146/annurev.physiol.68.040204.100431. PubMed PMID: 16460286.
42. Hodeify R, Yu F, Courjaret R, Nader N, Dib M, Sun L, Adap E, Hubrack S, Machaca K. Regulation and Role of Store-Operated Ca(2+) Entry in Cellular Proliferation. In: Kozak JA, Putney JW, Jr., editors. *Calcium Entry Channels in Non-Excitable Cells*. Boca Raton (FL)2018. p. 215-40.
43. Parekh AB, Putney JW, Jr. Store-operated calcium channels. *Physiol Rev*. 2005;85(2):757-810. Epub 2005/03/25. doi: 10.1152/physrev.00057.2003. PubMed PMID: 15788710.
44. Jardin I, Diez-Bello R, Falcon D, Alvarado S, Regodon S, Salido GM, Smani T, Rosado JA. Melatonin downregulates TRPC6, impairing store-operated calcium entry in triple-negative breast cancer cells. *J Biol Chem*. 2021;296:100254. Epub 2021/01/01. doi: 10.1074/jbc.RA120.015769. PubMed PMID: 33380424; PMCID: PMC7948746.
45. Freichel M, Berlin M, Schurger A, Mathar I, Bacmeister L, Medert R, Frede W, Marx A, Segin S, Londono JEC. TRP Channels in the Heart. In: Emir TLR, editor. *Neurobiology of TRP Channels*. Boca Raton (FL)2017. p. 149-85.
46. Haws HJ, McNeil MA, Hansen MD. Control of cell mechanics by RhoA and calcium fluxes during epithelial scattering. *Tissue Barriers*. 2016;4(3):e1187326. Epub 2016/09/02. doi: 10.1080/21688370.2016.1187326. PubMed PMID: 27583192; PMCID: PMC4993584.
47. Dolmetsch RE, Xu K, Lewis RS. Calcium oscillations increase the efficiency and specificity of gene expression. *Nature*. 1998;392(6679):933-6. Epub 1998/05/15. doi: 10.1038/31960. PubMed PMID: 9582075.
48. Lewis RS. Calcium signaling mechanisms in T lymphocytes. *Annu Rev Immunol*. 2001;19:497-521. Epub 2001/03/13. doi: 10.1146/annurev.immunol.19.1.497. PubMed PMID: 11244045.
49. Feske S. Calcium signalling in lymphocyte activation and disease. *Nat Rev Immunol*. 2007;7(9):690-702. Epub 2007/08/19. doi: 10.1038/nri2152. PubMed PMID: 17703229.
50. Brouland JP, Gelebart P, Kovacs T, Enouf J, Grossmann J, Papp B. The loss of sarco/endoplasmic reticulum calcium transport ATPase 3 expression is an early event during the multistep process of colon carcinogenesis. *Am J Pathol*. 2005;167(1):233-42. Epub 2005/06/24. doi: 10.1016/S0002-9440(10)62968-9. PubMed PMID: 15972967; PMCID: PMC1603437.
51. Dhennin-Duthille I, Gautier M, Faouzi M, Guilbert A, Brevet M, Vaudry D, Ahidouch A, Sevestre H, Ouadid-Ahidouch H. High expression of transient receptor potential channels in

- human breast cancer epithelial cells and tissues: correlation with pathological parameters. *Cell Physiol Biochem*. 2011;28(5):813-22. Epub 2011/12/20. doi: 10.1159/000335795. PubMed PMID: 22178934.
52. Chodon D, Guilbert A, Dhennin-Duthille I, Gautier M, Telliez MS, Sevestre H, Ouadid-Ahidouch H. Estrogen regulation of TRPM8 expression in breast cancer cells. *BMC Cancer*. 2010;10:212. Epub 2010/05/21. doi: 10.1186/1471-2407-10-212. PubMed PMID: 20482834; PMCID: PMC2887400.
53. Liu J, Chen Y, Shuai S, Ding D, Li R, Luo R. TRPM8 promotes aggressiveness of breast cancer cells by regulating EMT via activating AKT/GSK-3beta pathway. *Tumour Biol*. 2014;35(9):8969-77. Epub 2014/06/07. doi: 10.1007/s13277-014-2077-8. PubMed PMID: 24903376.
54. Fixemer T, Wissenbach U, Flockerzi V, Bonkhoff H. Expression of the Ca<sup>2+</sup>-selective cation channel TRPV6 in human prostate cancer: a novel prognostic marker for tumor progression. *Oncogene*. 2003;22(49):7858-61. Epub 2003/10/31. doi: 10.1038/sj.onc.1206895. PubMed PMID: 14586412.
55. Raphael M, Lehen'kyi V, Vandenberghe M, Beck B, Khalimonchuk S, Vanden Abeele F, Farsetti L, Germain E, Bokhobza A, Mihalache A, Gosset P, Romanin C, Clezardin P, Skryma R, Prevarskaya N. TRPV6 calcium channel translocates to the plasma membrane via Orail-mediated mechanism and controls cancer cell survival. *Proc Natl Acad Sci U S A*. 2014;111(37):E3870-9. Epub 2014/08/31. doi: 10.1073/pnas.1413409111. PubMed PMID: 25172921; PMCID: PMC4169956.
56. Krapivinsky G, Krapivinsky L, Manasian Y, Clapham DE. The TRPM7 channel is cleaved to release a chromatin-modifying kinase. *Cell*. 2014;157(5):1061-72. Epub 2014/05/27. doi: 10.1016/j.cell.2014.03.046. PubMed PMID: 24855944; PMCID: PMC4156102.
57. Ardura JA, Alvarez-Carrion L, Gutierrez-Rojas I, Alonso V. Role of Calcium Signaling in Prostate Cancer Progression: Effects on Cancer Hallmarks and Bone Metastatic Mechanisms. *Cancers (Basel)*. 2020;12(5). Epub 2020/04/30. doi: 10.3390/cancers12051071. PubMed PMID: 32344908; PMCID: PMC7281772.
58. Asuthkar S, Velpula KK, Elustondo PA, Demirkhanyan L, Zakharian E. TRPM8 channel as a novel molecular target in androgen-regulated prostate cancer cells. *Oncotarget*. 2015;6(19):17221-36. Epub 2015/05/20. doi: 10.18632/oncotarget.3948. PubMed PMID: 25980497; PMCID: PMC4627303.
59. Bas E, Naziroglu M, Pecze L. ADP-Ribose and oxidative stress activate TRPM8 channel in prostate cancer and kidney cells. *Sci Rep*. 2019;9(1):4100. Epub 2019/03/13. doi: 10.1038/s41598-018-37552-0. PubMed PMID: 30858386; PMCID: PMC6411746.
60. Chen YF, Chen YT, Chiu WT, Shen MR. Remodeling of calcium signaling in tumor progression. *J Biomed Sci*. 2013;20:23. Epub 2013/04/19. doi: 10.1186/1423-0127-20-23. PubMed PMID: 23594099; PMCID: PMC3639169.

61. Chinigo G, Fiorio Pla A, Gkika D. TRP Channels and Small GTPases Interplay in the Main Hallmarks of Metastatic Cancer. *Front Pharmacol.* 2020;11:581455. Epub 2020/11/03. doi: 10.3389/fphar.2020.581455. PubMed PMID: 33132914; PMCID: PMC7550629.
62. Du GJ, Li JH, Liu WJ, Liu YH, Zhao B, Li HR, Hou XD, Li H, Qi XX, Duan YJ. The combination of TRPM8 and TRPA1 expression causes an invasive phenotype in lung cancer. *Tumour Biol.* 2014;35(2):1251-61. Epub 2013/09/17. doi: 10.1007/s13277-013-1167-3. PubMed PMID: 24037916.
63. Jung J, Cho KJ, Naji AK, Clemons KN, Wong CO, Villanueva M, Gregory S, Karagas NE, Tan L, Liang H, Rousseau MA, Tomasevich KM, Sikora AG, Levental I, van der Hoeven D, Zhou Y, Hancock JF, Venkatachalam K. HRAS-driven cancer cells are vulnerable to TRPML1 inhibition. *EMBO Rep.* 2019;20(4). Epub 2019/02/23. doi: 10.15252/embr.201846685. PubMed PMID: 30787043; PMCID: PMC6446245.
64. Lee H, Kim JW, Kim DK, Choi DK, Lee S, Yu JH, Kwon OB, Lee J, Lee DS, Kim JH, Min SH. Calcium Channels as Novel Therapeutic Targets for Ovarian Cancer Stem Cells. *Int J Mol Sci.* 2020;21(7). Epub 2020/04/02. doi: 10.3390/ijms21072327. PubMed PMID: 32230901; PMCID: PMC7177693.
65. Lehen'kyi V, Flourakis M, Skryma R, Prevarskaya N. TRPV6 channel controls prostate cancer cell proliferation via Ca(2+)/NFAT-dependent pathways. *Oncogene.* 2007;26(52):7380-5. Epub 2007/05/30. doi: 10.1038/sj.onc.1210545. PubMed PMID: 17533368.
66. Lu H, Chen I, Shimoda LA, Park Y, Zhang C, Tran L, Zhang H, Semenza GL. Chemotherapy-Induced Ca(2+) Release Stimulates Breast Cancer Stem Cell Enrichment. *Cell Rep.* 2017;18(8):1946-57. Epub 2017/02/24. doi: 10.1016/j.celrep.2017.02.001. PubMed PMID: 28228260.
67. Makena MR, Rao R. Subtype specific targeting of calcium signaling in breast cancer. *Cell Calcium.* 2020;85:102109. Epub 2019/11/30. doi: 10.1016/j.ceca.2019.102109. PubMed PMID: 31783287; PMCID: PMC6931135.
68. Miller BA. TRPM2 in Cancer. *Cell Calcium.* 2019;80:8-17. Epub 2019/03/30. doi: 10.1016/j.ceca.2019.03.002. PubMed PMID: 30925291; PMCID: PMC6545160.
69. Morales-Lazaro SL, Simon SA, Rosenbaum T. The role of endogenous molecules in modulating pain through transient receptor potential vanilloid 1 (TRPV1). *J Physiol.* 2013;591(13):3109-21. Epub 2013/04/25. doi: 10.1113/jphysiol.2013.251751. PubMed PMID: 23613529; PMCID: PMC3717213.
70. Zhu H, Zhang H, Jin F, Fang M, Huang M, Yang CS, Chen T, Fu L, Pan Z. Elevated Orai1 expression mediates tumor-promoting intracellular Ca<sup>2+</sup> oscillations in human esophageal squamous cell carcinoma. *Oncotarget.* 2014;5(11):3455-71. Epub 2014/05/07. doi: 10.18632/oncotarget.1903. PubMed PMID: 24797725; PMCID: PMC4116495.

71. Feng M, Grice DM, Faddy HM, Nguyen N, Leitch S, Wang Y, Muend S, Kenny PA, Sukumar S, Roberts-Thomson SJ, Monteith GR, Rao R. Store-independent activation of Orail by SPCA2 in mammary tumors. *Cell*. 2010;143(1):84-98. Epub 2010/10/05. doi: 10.1016/j.cell.2010.08.040. PubMed PMID: 20887894; PMCID: PMC2950964.
72. Ahuja N, Ashok C, Natua S, Pant D, Cherian A, Pandkar MR, Yadav P, Vishnu NSS, Mishra J, Samaiya A, Shukla S. Hypoxia-induced TGF-beta-RBFOX2-ESRP1 axis regulates human MENA alternative splicing and promotes EMT in breast cancer. *NAR Cancer*. 2020;2(3):zcaa021. Epub 2020/10/23. doi: 10.1093/narcan/zcaa021. PubMed PMID: 33089214; PMCID: PMC7116222.
73. Han G, Lu SL, Li AG, He W, Corless CL, Kulesz-Martin M, Wang XJ. Distinct mechanisms of TGF-beta1-mediated epithelial-to-mesenchymal transition and metastasis during skin carcinogenesis. *J Clin Invest*. 2005;115(7):1714-23. Epub 2005/06/07. doi: 10.1172/JCI24399. PubMed PMID: 15937546; PMCID: PMC1142114.
74. Mirzaei S, Ranjbar B, Tackallou SH, Aref AR. Hypoxia inducible factor-1alpha (HIF-1alpha) in breast cancer: The crosstalk with oncogenic and onco-suppressor factors in regulation of cancer hallmarks. *Pathol Res Pract*. 2023;248:154676. Epub 2023/07/17. doi: 10.1016/j.prp.2023.154676. PubMed PMID: 37454494.
75. Yin W, Liu Y, Liu X, Ma X, Sun B, Yu Z. Metformin inhibits epithelial-mesenchymal transition of oral squamous cell carcinoma via the mTOR/HIF-1alpha/PKM2/STAT3 pathway. *Oncol Lett*. 2021;21(1):31. Epub 2020/12/03. doi: 10.3892/ol.2020.12292. PubMed PMID: 33262823; PMCID: PMC7693125.
76. Dang DK, Makena MR, Llongueras JP, Prasad H, Ko M, Bandral M, Rao R. A Ca(2+)-ATPase Regulates E-cadherin Biogenesis and Epithelial-Mesenchymal Transition in Breast Cancer Cells. *Mol Cancer Res*. 2019;17(8):1735-47. Epub 2019/05/12. doi: 10.1158/1541-7786.MCR-19-0070. PubMed PMID: 31076498; PMCID: PMC6679749.
77. Davis FM, Azimi I, Faville RA, Peters AA, Jalink K, Putney JW, Jr., Goodhill GJ, Thompson EW, Roberts-Thomson SJ, Monteith GR. Induction of epithelial-mesenchymal transition (EMT) in breast cancer cells is calcium signal dependent. *Oncogene*. 2014;33(18):2307-16. Epub 2013/05/21. doi: 10.1038/onc.2013.187. PubMed PMID: 23686305; PMCID: PMC3917976.
78. Davis FM, Peters AA, Grice DM, Cabot PJ, Parat MO, Roberts-Thomson SJ, Monteith GR. Non-stimulated, agonist-stimulated and store-operated Ca<sup>2+</sup> influx in MDA-MB-468 breast cancer cells and the effect of EGF-induced EMT on calcium entry. *PLoS One*. 2012;7(5):e36923. Epub 2012/06/06. doi: 10.1371/journal.pone.0036923. PubMed PMID: 22666335; PMCID: PMC3364242.
79. Ge P, Wei L, Zhang M, Hu B, Wang K, Li Y, Liu S, Wang J, Li Y. TRPC1/3/6 inhibition attenuates the TGF-beta1-induced epithelial-mesenchymal transition in gastric cancer via the Ras/Raf1/ERK signaling pathway. *Cell Biol Int*. 2018;42(8):975-84. Epub 2018/03/24. doi: 10.1002/cbin.10963. PubMed PMID: 29570903.

80. Dixon SJ, Lemberg KM, Lamprecht MR, Skouta R, Zaitsev EM, Gleason CE, Patel DN, Bauer AJ, Cantley AM, Yang WS, Morrison B, 3rd, Stockwell BR. Ferroptosis: an iron-dependent form of nonapoptotic cell death. *Cell*. 2012;149(5):1060-72. Epub 2012/05/29. doi: 10.1016/j.cell.2012.03.042. PubMed PMID: 22632970; PMCID: PMC3367386.
81. Kerr JF, Wyllie AH, Currie AR. Apoptosis: a basic biological phenomenon with wide-ranging implications in tissue kinetics. *Br J Cancer*. 1972;26(4):239-57. Epub 1972/08/01. doi: 10.1038/bjc.1972.33. PubMed PMID: 4561027; PMCID: PMC2008650.
82. Hengartner MO. Programmed cell death in invertebrates. *Curr Opin Genet Dev*. 1996;6(1):34-8. Epub 1996/02/01. doi: 10.1016/s0959-437x(96)90007-6. PubMed PMID: 8791487.
83. Yang WS, Stockwell BR. Synthetic lethal screening identifies compounds activating iron-dependent, nonapoptotic cell death in oncogenic-RAS-harboring cancer cells. *Chem Biol*. 2008;15(3):234-45. Epub 2008/03/22. doi: 10.1016/j.chembiol.2008.02.010. PubMed PMID: 18355723; PMCID: PMC2683762.
84. Brown CW, Amante JJ, Chhoy P, Elaimy AL, Liu H, Zhu LJ, Baer CE, Dixon SJ, Mercurio AM. Prominin2 Drives Ferroptosis Resistance by Stimulating Iron Export. *Dev Cell*. 2019;51(5):575-86 e4. Epub 2019/11/19. doi: 10.1016/j.devcel.2019.10.007. PubMed PMID: 31735663; PMCID: PMC8316835.
85. Doll S, Proneth B, Tyurina YY, Panzilius E, Kobayashi S, Ingold I, Irmeler M, Beckers J, Aichler M, Walch A, Prokisch H, Trumbach D, Mao G, Qu F, Bayir H, Fullekrug J, Scheel CH, Wurst W, Schick JA, Kagan VE, Angeli JP, Conrad M. ACSL4 dictates ferroptosis sensitivity by shaping cellular lipid composition. *Nat Chem Biol*. 2017;13(1):91-8. Epub 2016/11/15. doi: 10.1038/nchembio.2239. PubMed PMID: 27842070; PMCID: PMC5610546.
86. Liang D, Feng Y, Zandkarimi F, Wang H, Zhang Z, Kim J, Cai Y, Gu W, Stockwell BR, Jiang X. Ferroptosis surveillance independent of GPX4 and differentially regulated by sex hormones. *Cell*. 2023;186(13):2748-64 e22. Epub 2023/06/03. doi: 10.1016/j.cell.2023.05.003. PubMed PMID: 37267948; PMCID: PMC10330611.
87. Yang WS, SriRamaratnam R, Welsch ME, Shimada K, Skouta R, Viswanathan VS, Cheah JH, Clemons PA, Shamji AF, Clish CB, Brown LM, Girotti AW, Cornish VW, Schreiber SL, Stockwell BR. Regulation of ferroptotic cancer cell death by GPX4. *Cell*. 2014;156(1-2):317-31. Epub 2014/01/21. doi: 10.1016/j.cell.2013.12.010. PubMed PMID: 24439385; PMCID: PMC4076414.
88. Doll S, Freitas FP, Shah R, Aldrovandi M, da Silva MC, Ingold I, Goya Grocin A, Xavier da Silva TN, Panzilius E, Scheel CH, Mourao A, Buday K, Sato M, Wanninger J, Vignane T, Mohana V, Rehberg M, Flatley A, Schepers A, Kurz A, White D, Sauer M, Sattler M, Tate EW, Schmitz W, Schulze A, O'Donnell V, Proneth B, Popowicz GM, Pratt DA, Angeli JPF, Conrad M. FSP1 is a glutathione-independent ferroptosis suppressor. *Nature*. 2019;575(7784):693-8. Epub 2019/10/22. doi: 10.1038/s41586-019-1707-0. PubMed PMID: 31634899.

89. Wu YC, Huang CS, Hsieh MS, Huang CM, Setiawan SA, Yeh CT, Kuo KT, Liu SC. Targeting of FSP1 regulates iron homeostasis in drug-tolerant persister head and neck cancer cells via lipid-metabolism-driven ferroptosis. *Aging (Albany NY)*. 2024;16(1):627-47. Epub 2024/01/11. doi: 10.18632/aging.205409. PubMed PMID: 38206305; PMCID: PMC10817390.
90. Kung CP, Murphy ME. The role of the p53 tumor suppressor in metabolism and diabetes. *J Endocrinol*. 2016;231(2):R61-R75. Epub 2016/09/11. doi: 10.1530/JOE-16-0324. PubMed PMID: 27613337; PMCID: PMC5148674.
91. Jiang L, Kon N, Li T, Wang SJ, Su T, Hibshoosh H, Baer R, Gu W. Ferroptosis as a p53-mediated activity during tumour suppression. *Nature*. 2015;520(7545):57-62. Epub 2015/03/25. doi: 10.1038/nature14344. PubMed PMID: 25799988; PMCID: PMC4455927.
92. Wang SJ, Li D, Ou Y, Jiang L, Chen Y, Zhao Y, Gu W. Acetylation Is Crucial for p53-Mediated Ferroptosis and Tumor Suppression. *Cell Rep*. 2016;17(2):366-73. Epub 2016/10/06. doi: 10.1016/j.celrep.2016.09.022. PubMed PMID: 27705786; PMCID: PMC5227654.
93. Arfin S, Jha NK, Jha SK, Kesari KK, Ruokolainen J, Roychoudhury S, Rathi B, Kumar D. Oxidative Stress in Cancer Cell Metabolism. *Antioxidants (Basel)*. 2021;10(5). Epub 2021/05/01. doi: 10.3390/antiox10050642. PubMed PMID: 33922139; PMCID: PMC8143540.
94. Azmanova M, Pitto-Barry A. Oxidative Stress in Cancer Therapy: Friend or Enemy? *Chembiochem*. 2022;23(10):e202100641. Epub 2022/01/12. doi: 10.1002/cbic.202100641. PubMed PMID: 35015324.
95. Barrera G, Cucci MA, Grattarola M, Dianzani C, Muzio G, Pizzimenti S. Control of Oxidative Stress in Cancer Chemoresistance: Spotlight on Nrf2 Role. *Antioxidants (Basel)*. 2021;10(4). Epub 2021/04/04. doi: 10.3390/antiox10040510. PubMed PMID: 33805928; PMCID: PMC8064392.
96. DeNicola GM, Karreth FA, Humpton TJ, Gopinathan A, Wei C, Frese K, Mangal D, Yu KH, Yeo CJ, Calhoun ES, Scrimieri F, Winter JM, Hruban RH, Iacobuzio-Donahue C, Kern SE, Blair IA, Tuveson DA. Oncogene-induced Nrf2 transcription promotes ROS detoxification and tumorigenesis. *Nature*. 2011;475(7354):106-9. Epub 2011/07/08. doi: 10.1038/nature10189. PubMed PMID: 21734707; PMCID: PMC3404470.
97. Hayes JD, Dinkova-Kostova AT, Tew KD. Oxidative Stress in Cancer. *Cancer Cell*. 2020;38(2):167-97. Epub 2020/07/11. doi: 10.1016/j.ccell.2020.06.001. PubMed PMID: 32649885; PMCID: PMC7439808.
98. Barrera G. Oxidative stress and lipid peroxidation products in cancer progression and therapy. *ISRN Oncol*. 2012;2012:137289. Epub 2012/11/03. doi: 10.5402/2012/137289. PubMed PMID: 23119185; PMCID: PMC3483701.
99. Pope LE, Dixon SJ. Regulation of ferroptosis by lipid metabolism. *Trends Cell Biol*. 2023;33(12):1077-87. Epub 2023/07/06. doi: 10.1016/j.tcb.2023.05.003. PubMed PMID: 37407304; PMCID: PMC10733748.

100. Yoshimura Y, Uchiyama K, Ohsawa K, Imaeda K, Ohtani Y, Tamura K. Oxygen dependence of lipid peroxidation in mice. *J Toxicol Sci.* 1991;16(1):1-9. Epub 1991/02/01. doi: 10.2131/jts.16.1. PubMed PMID: 1895348.
101. Stockwell BR, Jiang X, Gu W. Emerging Mechanisms and Disease Relevance of Ferroptosis. *Trends Cell Biol.* 2020;30(6):478-90. Epub 2020/05/16. doi: 10.1016/j.tcb.2020.02.009. PubMed PMID: 32413317; PMCID: PMC7230071.
102. Bersuker K, Hendricks JM, Li Z, Magtanong L, Ford B, Tang PH, Roberts MA, Tong B, Maimone TJ, Zoncu R, Bassik MC, Nomura DK, Dixon SJ, Olzmann JA. The CoQ oxidoreductase FSP1 acts parallel to GPX4 to inhibit ferroptosis. *Nature.* 2019;575(7784):688-92. Epub 2019/10/22. doi: 10.1038/s41586-019-1705-2. PubMed PMID: 31634900; PMCID: PMC6883167.
103. Hendricks JM, Doubravsky CE, Wehri E, Li Z, Roberts MA, Deol KK, Lange M, Lasheras-Otero I, Momper JD, Dixon SJ, Bersuker K, Schaletzky J, Olzmann JA. Identification of structurally diverse FSP1 inhibitors that sensitize cancer cells to ferroptosis. *Cell Chem Biol.* 2023;30(9):1090-103 e7. Epub 2023/05/14. doi: 10.1016/j.chembiol.2023.04.007. PubMed PMID: 37178691; PMCID: PMC10524360.
104. Kim JW, Kim MJ, Han TH, Lee JY, Kim S, Kim H, Oh KJ, Kim WK, Han BS, Bae KH, Ban HS, Bae SH, Lee SC, Lee H, Lee EW. FSP1 confers ferroptosis resistance in KEAP1 mutant non-small cell lung carcinoma in NRF2-dependent and -independent manner. *Cell Death Dis.* 2023;14(8):567. Epub 2023/08/27. doi: 10.1038/s41419-023-06070-x. PubMed PMID: 37633973; PMCID: PMC10460413.
105. Li J, Wang H. [Kelch-like ech-associated protein 1/nuclear factor E2-related factor 2/antioxidant response element pathway alleviates ferroptosis in sepsis by regulating oxidative stress]. *Zhonghua Wei Zhong Bing Ji Jiu Yi Xue.* 2021;33(7):881-4. Epub 2021/08/21. doi: 10.3760/cma.j.cn121430-20210130-00180. PubMed PMID: 34412763.
106. Muller F, Lim JKM, Bebbler CM, Seidel E, Tishina S, Dahlhaus A, Stroh J, Beck J, Yapici FI, Nakayama K, Torres Fernandez L, Bragelmann J, Leprivier G, von Karstedt S. Elevated FSP1 protects KRAS-mutated cells from ferroptosis during tumor initiation. *Cell Death Differ.* 2023;30(2):442-56. Epub 2022/11/29. doi: 10.1038/s41418-022-01096-8. PubMed PMID: 36443441; PMCID: PMC9950476.
107. Nakamura T, Hipp C, Santos Dias Mourao A, Borggrafe J, Aldrovandi M, Henkelmann B, Wanninger J, Mishima E, Lytton E, Emler D, Proneth B, Sattler M, Conrad M. Phase separation of FSP1 promotes ferroptosis. *Nature.* 2023;619(7969):371-7. Epub 2023/06/29. doi: 10.1038/s41586-023-06255-6. PubMed PMID: 37380771; PMCID: PMC10338336 M.C. and B.P. are co-founders and shareholders of ROSCUE Therapeutics GmbH. The other authors declare no competing interests.
108. Nakamura T, Mishima E, Yamada N, Mourao ASD, Trumbach D, Doll S, Wanninger J, Lytton E, Sennhenn P, Nishida Xavier da Silva T, Angeli JPF, Sattler M, Proneth B, Conrad M. Integrated chemical and genetic screens unveil FSP1 mechanisms of ferroptosis regulation. *Nat*

Struct Mol Biol. 2023;30(11):1806-15. Epub 2023/11/14. doi: 10.1038/s41594-023-01136-y. PubMed PMID: 37957306; PMCID: PMC10643123 other authors declare no competing interests.

109. Prevarskaya N, Ouadid-Ahidouch H, Skryma R, Shuba Y. Remodelling of Ca<sup>2+</sup> transport in cancer: how it contributes to cancer hallmarks? *Philos Trans R Soc Lond B Biol Sci.* 2014;369(1638):20130097. Epub 2014/02/05. doi: 10.1098/rstb.2013.0097. PubMed PMID: 24493745; PMCID: PMC3917351.

110. Roderick HL, Cook SJ. Ca<sup>2+</sup> signalling checkpoints in cancer: remodelling Ca<sup>2+</sup> for cancer cell proliferation and survival. *Nat Rev Cancer.* 2008;8(5):361-75. Epub 2008/04/25. doi: 10.1038/nrc2374. PubMed PMID: 18432251.

111. Thankamony AP, Saxena K, Murali R, Jolly MK, Nair R. Cancer Stem Cell Plasticity – A Deadly Deal. *Front Mol Biosci.* 2020;7. doi: 10.3389/fmolb.2020.00079.

112. Brabletz T. To differentiate or not — routes towards metastasis. *Nature Reviews Cancer.* 2012;12(6):425-36. doi: 10.1038/nrc3265.

113. Luo M, Shang L, Brooks MD, Jiagge E, Zhu Y, Buschhaus JM, Conley S, Fath MA, Davis A, Gheordunescu E, Wang Y, Harouaka R, Lozier A, Triner D, McDermott S, Merajver SD, Luker GD, Spitz DR, Wicha MS. Targeting Breast Cancer Stem Cell State Equilibrium through Modulation of Redox Signaling. *Cell metabolism.* 2018;28(1):69-86.e6. doi: 10.1016/j.cmet.2018.06.006.

114. Norgard RJ, Pitarresi JR, Maddipati R, Aiello-Couzo NM, Balli D, Li J, Yamazoe T, Wengyn MD, Millstein ID, Folkert IW, Rosario-Berrios DN, Kim IK, Bassett JB, Payne R, Berry CT, Feng X, Sun K, Cioffi M, Chakraborty P, Jolly MK, Gutkind JS, Lyden D, Freedman BD, Foscett JK, Rustgi AK, Stanger BZ. Calcium signaling induces a partial EMT. *EMBO Rep.* 2021;22(9):e51872. Epub 2021/07/30. doi: 10.15252/embr.202051872. PubMed PMID: 34324787; PMCID: PMC8419705.

115. Liu M, Inoue K, Leng T, Guo S, Xiong ZG. TRPM7 channels regulate glioma stem cell through STAT3 and Notch signaling pathways. *Cell Signal.* 2014;26(12):2773-81. Epub 2014/09/07. doi: 10.1016/j.cellsig.2014.08.020. PubMed PMID: 25192910; PMCID: PMC4405379.

116. Hu Z, Cao X, Fang Y, Liu G, Xie C, Qian K, Lei X, Cao Z, Du H, Cheng X, Xu X. Transient receptor potential vanilloid-type 2 targeting on stemness in liver cancer. *Biomed Pharmacother.* 2018;105:697-706. Epub 2018/06/16. doi: 10.1016/j.biopha.2018.06.029. PubMed PMID: 29906748.

117. Terrie E, Deliot N, Benzidane Y, Harnois T, Cousin L, Bois P, Oliver L, Arnault P, Vallette F, Constantin B, Coronas V. Store-Operated Calcium Channels Control Proliferation and Self-Renewal of Cancer Stem Cells from Glioblastoma. *Cancers (Basel).* 2021;13(14). Epub 2021/07/25. doi: 10.3390/cancers13143428. PubMed PMID: 34298643; PMCID: PMC8307764.

118. Daya HA, Kouba S, Ouled-Haddou H, Benzerdjeb N, Telliez MS, Dayen C, Sevestre H, Garcon L, Hague F, Ouadid-Ahidouch H. Orai3-Mediates Cisplatin-Resistance in Non-Small Cell Lung Cancer Cells by Enriching Cancer Stem Cell Population through PI3K/AKT Pathway. *Cancers (Basel)*. 2021;13(10). Epub 2021/06/03. doi: 10.3390/cancers13102314. PubMed PMID: 34065942; PMCID: PMC8150283.
119. Dietrich A, Gudermann T. TRPC6: physiological function and pathophysiological relevance. *Handb Exp Pharmacol*. 2014;222:157-88. Epub 2014/04/24. doi: 10.1007/978-3-642-54215-2\_7. PubMed PMID: 24756706.
120. Geng Y, Amante JJ, Goel HL, Zhang X, Walker MR, Luther DC, Mercurio AM, Rotello VM. Differentiation of Cancer Stem Cells through Nanoparticle Surface Engineering. *ACS Nano*. 2020;14(11):15276-85. Epub 2020/11/10. doi: 10.1021/acsnano.0c05589. PubMed PMID: 33164505.
121. Azimi I, Milevskiy MJG, Chalmers SB, Yapa K, Robitaille M, Henry C, Baillie GJ, Thompson EW, Roberts-Thomson SJ, Monteith GR. ORAI1 and ORAI3 in Breast Cancer Molecular Subtypes and the Identification of ORAI3 as a Hypoxia Sensitive Gene and a Regulator of Hypoxia Responses. *Cancers (Basel)*. 2019;11(2). Epub 2019/02/14. doi: 10.3390/cancers11020208. PubMed PMID: 30754719; PMCID: PMC6406924.
122. Jardin I, Diez-Bello R, Lopez JJ, Redondo PC, Salido GM, Smani T, Rosado JA. TRPC6 Channels Are Required for Proliferation, Migration and Invasion of Breast Cancer Cell Lines by Modulation of Orai1 and Orai3 Surface Exposure. *Cancers (Basel)*. 2018;10(9). Epub 2018/09/19. doi: 10.3390/cancers10090331. PubMed PMID: 30223530; PMCID: PMC6162527.
123. Atala A. Re: Ion Channel TRPM8 Promotes Hypoxic Growth of Prostate Cancer Cells via an O<sub>2</sub>-Independent and RACK1-Mediated Mechanism of HIF-1alpha Stabilization. *J Urol*. 2015;194(1):260. Epub 2015/06/20. doi: 10.1016/j.juro.2015.04.027. PubMed PMID: 26088253.
124. Alaimo A, De Felice D, Genovesi S, Lorenzoni M, Lunardi A. Tune the channel: TRPM8 targeting in prostate cancer. *Oncoscience*. 2021;8:97-100. Epub 2021/09/14. doi: 10.18632/oncoscience.543. PubMed PMID: 34514058; PMCID: PMC8428510.
125. Ross JB, Huh D, Noble LB, Tavazoie SF. Identification of molecular determinants of primary and metastatic tumour re-initiation in breast cancer. *Nat Cell Biol*. 2015;17(5):651-64. Epub 2015/04/14. doi: 10.1038/ncb3148. PubMed PMID: 25866923; PMCID: PMC4609531.
126. Elenbaas B, Spirio L, Koerner F, Fleming MD, Zimonjic DB, Donaher JL, Popescu NC, Hahn WC, Weinberg RA. Human breast cancer cells generated by oncogenic transformation of primary mammary epithelial cells. *Genes Dev*. 2001;15(1):50-65. Epub 2001/01/13. doi: 10.1101/gad.828901. PubMed PMID: 11156605; PMCID: PMC312602.
127. Walker MR, Goel HL, Mukhopadhyay D, Chhoy P, Karner ER, Clark JL, Liu H, Li R, Zhu JL, Chen S, Mahal LK, Bensing BA, Mercurio AM. O-linked alpha2,3 sialylation defines stem cell populations in breast cancer. *Sci Adv*. 2022;8(1):eabj9513. Epub 2022/01/08. doi: 10.1126/sciadv.abj9513. PubMed PMID: 34995107; PMCID: PMC8741191.

128. Riehle M, Buscher AK, Gohlke BO, Kassmann M, Kolatsi-Joannou M, Brasen JH, Nagel M, Becker JU, Winyard P, Hoyer PF, Preissner R, Krautwurst D, Gollasch M, Weber S, Harteneck C. TRPC6 G757D Loss-of-Function Mutation Associates with FSGS. *J Am Soc Nephrol*. 2016;27(9):2771-83. Epub 2016/02/20. doi: 10.1681/ASN.2015030318. PubMed PMID: 26892346; PMCID: PMC5004639.
129. Lin BL, Matera D, Doerner JF, Zheng N, Del Camino D, Mishra S, Bian H, Zeveleva S, Zhen X, Blair NT, Chong JA, Hessler DP, Bedja D, Zhu G, Muller GK, Ranek MJ, Pantages L, McFarland M, Netherton MR, Berry A, Wong D, Rast G, Qian HS, Weldon SM, Kuo JJ, Sauer A, Sarko C, Moran MM, Kass DA, Pullen SS. In vivo selective inhibition of TRPC6 by antagonist BI 749327 ameliorates fibrosis and dysfunction in cardiac and renal disease. *Proc Natl Acad Sci U S A*. 2019;116(20):10156-61. Epub 2019/04/28. doi: 10.1073/pnas.1815354116. PubMed PMID: 31028142; PMCID: PMC6525474.
130. Hu Y, Smyth GK. ELDA: extreme limiting dilution analysis for comparing depleted and enriched populations in stem cell and other assays. *J Immunol Methods*. 2009;347(1-2):70-8. Epub 2009/07/02. doi: 10.1016/j.jim.2009.06.008. PubMed PMID: 19567251.
131. Yin L, Duan JJ, Bian XW, Yu SC. Triple-negative breast cancer molecular subtyping and treatment progress. *Breast Cancer Res*. 2020;22(1):61. Epub 2020/06/11. doi: 10.1186/s13058-020-01296-5. PubMed PMID: 32517735; PMCID: PMC7285581.
132. Won KA, Spruck C. Triple-negative breast cancer therapy: Current and future perspectives (Review). *Int J Oncol*. 2020;57(6):1245-61. Epub 2020/11/12. doi: 10.3892/ijo.2020.5135. PubMed PMID: 33174058; PMCID: PMC7646583.
133. Zhou HM, Zhang JG, Zhang X, Li Q. Targeting cancer stem cells for reversing therapy resistance: mechanism, signaling, and prospective agents. *Signal Transduct Target Ther*. 2021;6(1):62. Epub 2021/02/17. doi: 10.1038/s41392-020-00430-1. PubMed PMID: 33589595; PMCID: PMC7884707.
134. Guillen KP, Fujita M, Butterfield AJ, Scherer SD, Bailey MH, Chu Z, DeRose YS, Zhao L, Cortes-Sanchez E, Yang CH, Toner J, Wang G, Qiao Y, Huang X, Greenland JA, Vahrenkamp JM, Lum DH, Factor RE, Nelson EW, Matsen CB, Poretta JM, Rosenthal R, Beck AC, Buys SS, Vaklavas C, Ward JH, Jensen RL, Jones KB, Li Z, Oesterreich S, Dobrolecki LE, Pathi SS, Woo XY, Berrett KC, Wadsworth ME, Chuang JH, Lewis MT, Marth GT, Gertz J, Varley KE, Welm BE, Welm AL. A human breast cancer-derived xenograft and organoid platform for drug discovery and precision oncology. *Nat Cancer*. 2022;3(2):232-50. Epub 2022/03/01. doi: 10.1038/s43018-022-00337-6. PubMed PMID: 35221336; PMCID: PMC8882468.
135. Shapiro IM, Cheng AW, Flytzanis NC, Balsamo M, Condeelis JS, Oktay MH, Burge CB, Gertler FB. An EMT-driven alternative splicing program occurs in human breast cancer and modulates cellular phenotype. *PLoS Genet*. 2011;7(8):e1002218. Epub 2011/08/31. doi: 10.1371/journal.pgen.1002218. PubMed PMID: 21876675; PMCID: PMC3158048.

136. Zhang H, Brown RL, Wei Y, Zhao P, Liu S, Liu X, Deng Y, Hu X, Zhang J, Gao XD, Kang Y, Mercurio AM, Goel HL, Cheng C. CD44 splice isoform switching determines breast cancer stem cell state. *Genes Dev.* 2019;33(3-4):166-79. Epub 2019/01/30. doi: 10.1101/gad.319889.118. PubMed PMID: 30692202; PMCID: PMC6362815.
137. Goel HL, Gritsko T, Pursell B, Chang C, Shultz LD, Greiner DL, Norum JH, Toftgard R, Shaw LM, Mercurio AM. Regulated splicing of the alpha6 integrin cytoplasmic domain determines the fate of breast cancer stem cells. *Cell Rep.* 2014;7(3):747-61. Epub 2014/04/29. doi: 10.1016/j.celrep.2014.03.059. PubMed PMID: 24767994; PMCID: PMC4038359.
138. Chang C, Goel HL, Gao H, Pursell B, Shultz LD, Greiner DL, Ingerpau S, Patarroyo M, Cao S, Lim E, Mao J, McKee KK, Yurchenco PD, Mercurio AM. A laminin 511 matrix is regulated by TAZ and functions as the ligand for the alpha6Bbeta1 integrin to sustain breast cancer stem cells. *Genes Dev.* 2015;29(1):1-6. Epub 2015/01/07. doi: 10.1101/gad.253682.114. PubMed PMID: 25561492; PMCID: PMC4281560.
139. Roopra A. MAGIC: A tool for predicting transcription factors and cofactors driving gene sets using ENCODE data. *PLoS Comput Biol.* 2020;16(4):e1007800. Epub 2020/04/07. doi: 10.1371/journal.pcbi.1007800. PubMed PMID: 32251445; PMCID: PMC7162552.
140. Vassilev A, Kaneko KJ, Shu H, Zhao Y, DePamphilis ML. TEAD/TEF transcription factors utilize the activation domain of YAP65, a Src/Yes-associated protein localized in the cytoplasm. *Genes Dev.* 2001;15(10):1229-41. Epub 2001/05/19. doi: 10.1101/gad.888601. PubMed PMID: 11358867; PMCID: PMC313800.
141. Dupont S, Morsut L, Aragona M, Enzo E, Giulitti S, Cordenonsi M, Zanconato F, Le Digabel J, Forcato M, Bicciato S, Elvassore N, Piccolo S. Role of YAP/TAZ in mechanotransduction. *Nature.* 2011;474(7350):179-83. Epub 2011/06/10. doi: 10.1038/nature10137. PubMed PMID: 21654799.
142. Tian D, Jacobo SM, Billing D, Rozkalne A, Gage SD, Anagnostou T, Pavenstadt H, Hsu HH, Schlondorff J, Ramos A, Greka A. Antagonistic regulation of actin dynamics and cell motility by TRPC5 and TRPC6 channels. *Sci Signal.* 2010;3(145):ra77. Epub 2010/10/28. doi: 10.1126/scisignal.2001200. PubMed PMID: 20978238; PMCID: PMC3071756.
143. Dhimolea E, de Matos Simoes R, Kansara D, Al'Khafaji A, Bouyssou J, Weng X, Sharma S, Raja J, Awate P, Shirasaki R, Tang H, Glassner BJ, Liu Z, Gao D, Bryan J, Bender S, Roth J, Scheffer M, Jeselsohn R, Gray NS, Georgakoudi I, Vazquez F, Tsherniak A, Chen Y, Welm A, Duy C, Melnick A, Bartholdy B, Brown M, Culhane AC, Mitsiades CS. An Embryonic Diapause-like Adaptation with Suppressed Myc Activity Enables Tumor Treatment Persistence. *Cancer Cell.* 2021;39(2):240-56 e11. Epub 2021/01/09. doi: 10.1016/j.ccell.2020.12.002. PubMed PMID: 33417832; PMCID: PMC8670073.
144. Dai L, Ye S, Li HW, Chen DF, Wang HL, Jia SN, Lin C, Yang JS, Yang F, Nagasawa H, Yang WJ. SETD4 Regulates Cell Quiescence and Catalyzes the Trimethylation of H4K20 during Diapause Formation in *Artemia*. *Mol Cell Biol.* 2017;37(7). Epub 2016/12/30. doi: 10.1128/MCB.00453-16. PubMed PMID: 28031330; PMCID: PMC5359430.

145. Ye S, Ding YF, Jia WH, Liu XL, Feng JY, Zhu Q, Cai SL, Yang YS, Lu QY, Huang XT, Yang JS, Jia SN, Ding GP, Wang YH, Zhou JJ, Chen YD, Yang WJ. SET Domain-Containing Protein 4 Epigenetically Controls Breast Cancer Stem Cell Quiescence. *Cancer Res.* 2019;79(18):4729-43. Epub 2019/07/17. doi: 10.1158/0008-5472.CAN-19-1084. PubMed PMID: 31308046.
146. Oki T, Nishimura K, Kitaura J, Togami K, Maehara A, Izawa K, Sakaue-Sawano A, Niida A, Miyano S, Aburatani H, Kiyonari H, Miyawaki A, Kitamura T. A novel cell-cycle-indicator, mVenus-p27K-, identifies quiescent cells and visualizes G0-G1 transition. *Sci Rep.* 2014;4:4012. Epub 2014/02/07. doi: 10.1038/srep04012. PubMed PMID: 24500246; PMCID: PMC3915272.
147. Fluegen G, Avivar-Valderas A, Wang Y, Padgen MR, Williams JK, Nobre AR, Calvo V, Cheung JF, Bravo-Cordero JJ, Entenberg D, Castracane J, Verkhusha V, Keely PJ, Condeelis J, Aguirre-Ghiso JA. Phenotypic heterogeneity of disseminated tumour cells is preset by primary tumour hypoxic microenvironments. *Nat Cell Biol.* 2017;19(2):120-32. Epub 2017/01/24. doi: 10.1038/ncb3465. PubMed PMID: 28114271; PMCID: PMC5342902.
148. Mehterov N, Kazakova M, Sbirkov Y, Vladimirov B, Belev N, Yaneva G, Todorova K, Hayrabedyan S, Sarafian V. Alternative RNA Splicing-The Trojan Horse of Cancer Cells in Chemotherapy. *Genes (Basel).* 2021;12(7). Epub 2021/08/07. doi: 10.3390/genes12071085. PubMed PMID: 34356101; PMCID: PMC8306420.
149. Hu X, Harvey SE, Zheng R, Lyu J, Grzeskowiak CL, Powell E, Piwnica-Worms H, Scott KL, Cheng C. The RNA-binding protein AKAP8 suppresses tumor metastasis by antagonizing EMT-associated alternative splicing. *Nat Commun.* 2020;11(1):486. Epub 2020/01/26. doi: 10.1038/s41467-020-14304-1. PubMed PMID: 31980632; PMCID: PMC6981122.
150. Krebs J. The influence of calcium signaling on the regulation of alternative splicing. *Biochim Biophys Acta.* 2009;1793(6):979-84. Epub 2009/01/10. doi: 10.1016/j.bbamcr.2008.12.006. PubMed PMID: 19133299.
151. Lee JA, Xing Y, Nguyen D, Xie J, Lee CJ, Black DL. Depolarization and CaM kinase IV modulate NMDA receptor splicing through two essential RNA elements. *PLoS Biol.* 2007;5(2):e40. Epub 2007/02/15. doi: 10.1371/journal.pbio.0050040. PubMed PMID: 17298178; PMCID: PMC1790950.
152. Xie J, Black DL. A CaMK IV responsive RNA element mediates depolarization-induced alternative splicing of ion channels. *Nature.* 2001;410(6831):936-9. Epub 2001/04/20. doi: 10.1038/35073593. PubMed PMID: 11309619.
153. Xie J, Jan C, Stoilov P, Park J, Black DL. A consensus CaMK IV-responsive RNA sequence mediates regulation of alternative exons in neurons. *RNA.* 2005;11(12):1825-34. Epub 2005/11/30. doi: 10.1261/rna.2171205. PubMed PMID: 16314456; PMCID: PMC1370871.
154. Warzecha CC, Jiang P, Amirikian K, Dittmar KA, Lu H, Shen S, Guo W, Xing Y, Carstens RP. An ESRP-regulated splicing programme is abrogated during the epithelial-

mesenchymal transition. *EMBO J.* 2010;29(19):3286-300. Epub 2010/08/17. doi: 10.1038/emboj.2010.195. PubMed PMID: 20711167; PMCID: PMC2957203.

155. Tamura RN, Cooper HM, Collo G, Quaranta V. Cell type-specific integrin variants with alternative alpha chain cytoplasmic domains. *Proc Natl Acad Sci U S A.* 1991;88(22):10183-7. Epub 1991/11/15. doi: 10.1073/pnas.88.22.10183. PubMed PMID: 1946438; PMCID: PMC52892.

156. Hogervorst F, Kuikman I, van Kessel AG, Sonnenberg A. Molecular cloning of the human alpha 6 integrin subunit. Alternative splicing of alpha 6 mRNA and chromosomal localization of the alpha 6 and beta 4 genes. *Eur J Biochem.* 1991;199(2):425-33. Epub 1991/07/15. doi: 10.1111/j.1432-1033.1991.tb16140.x. PubMed PMID: 2070796.

157. Verheijden KAT, Sonneveld R, Bakker-van Bebbber M, Wetzels JFM, van der Vlag J, Nijenhuis T. The Calcium-Dependent Protease Calpain-1 Links TRPC6 Activity to Podocyte Injury. *J Am Soc Nephrol.* 2018;29(8):2099-109. Epub 2018/06/30. doi: 10.1681/ASN.2016111248. PubMed PMID: 29954830; PMCID: PMC6065075.

158. Regoli M, Bendayan M. Alterations in the expression of the alpha 3 beta 1 integrin in certain membrane domains of the glomerular epithelial cells (podocytes) in diabetes mellitus. *Diabetologia.* 1997;40(1):15-22. Epub 1997/01/01. doi: 10.1007/s001250050637. PubMed PMID: 9028713.

159. Rao A. Signaling to gene expression: calcium, calcineurin and NFAT. *Nat Immunol.* 2009;10(1):3-5. Epub 2008/12/18. doi: 10.1038/ni0109-3. PubMed PMID: 19088731.

160. Ren XD, Kiosses WB, Schwartz MA. Regulation of the small GTP-binding protein Rho by cell adhesion and the cytoskeleton. *EMBO J.* 1999;18(3):578-85. Epub 1999/02/02. doi: 10.1093/emboj/18.3.578. PubMed PMID: 9927417; PMCID: PMC1171150.

161. Goel HL, Pursell B, Shultz LD, Greiner DL, Brekken RA, Vander Kooi CW, Mercurio AM. P-Rex1 Promotes Resistance to VEGF/VEGFR-Targeted Therapy in Prostate Cancer. *Cell Rep.* 2016;14(9):2193-208. Epub 2016/03/01. doi: 10.1016/j.celrep.2016.02.016. PubMed PMID: 26923603; PMCID: PMC4791963.

162. Li R, Hu K, Liu H, Green MR, Zhu LJ. OneStopRNAseq: A Web Application for Comprehensive and Efficient Analyses of RNA-Seq Data. *Genes (Basel).* 2020;11(10). Epub 2020/10/08. doi: 10.3390/genes11101165. PubMed PMID: 33023248; PMCID: PMC7650687.

163. Dobin A, Davis CA, Schlesinger F, Drenkow J, Zaleski C, Jha S, Batut P, Chaisson M, Gingeras TR. STAR: ultrafast universal RNA-seq aligner. *Bioinformatics.* 2013;29(1):15-21. Epub 2012/10/30. doi: 10.1093/bioinformatics/bts635. PubMed PMID: 23104886; PMCID: PMC3530905.

164. Harrow J, Frankish A, Gonzalez JM, Tapanari E, Diekhans M, Kokocinski F, Aken BL, Barrell D, Zadissa A, Searle S, Barnes I, Bignell A, Boychenko V, Hunt T, Kay M, Mukherjee G, Rajan J, Despacio-Reyes G, Saunders G, Steward C, Harte R, Lin M, Howald C, Tanzer A,

- Derrien T, Chrast J, Walters N, Balasubramanian S, Pei B, Tress M, Rodriguez JM, Ezkurdia I, van Baren J, Brent M, Haussler D, Kellis M, Valencia A, Reymond A, Gerstein M, Guigo R, Hubbard TJ. GENCODE: the reference human genome annotation for The ENCODE Project. *Genome Res.* 2012;22(9):1760-74. Epub 2012/09/08. doi: 10.1101/gr.135350.111. PubMed PMID: 22955987; PMCID: PMC3431492.
165. Liao Y, Smyth GK, Shi W. featureCounts: an efficient general purpose program for assigning sequence reads to genomic features. *Bioinformatics.* 2014;30(7):923-30. Epub 2013/11/15. doi: 10.1093/bioinformatics/btt656. PubMed PMID: 24227677.
166. Love MI, Huber W, Anders S. Moderated estimation of fold change and dispersion for RNA-seq data with DESeq2. *Genome Biol.* 2014;15(12):550. Epub 2014/12/18. doi: 10.1186/s13059-014-0550-8. PubMed PMID: 25516281; PMCID: PMC4302049.
167. Stephens M. False discovery rates: a new deal. *Biostatistics.* 2017;18(2):275-94. Epub 2016/10/21. doi: 10.1093/biostatistics/kxw041. PubMed PMID: 27756721; PMCID: PMC5379932.
168. Subramanian A, Tamayo P, Mootha VK, Mukherjee S, Ebert BL, Gillette MA, Paulovich A, Pomeroy SL, Golub TR, Lander ES, Mesirov JP. Gene set enrichment analysis: a knowledge-based approach for interpreting genome-wide expression profiles. *Proc Natl Acad Sci U S A.* 2005;102(43):15545-50. Epub 2005/10/04. doi: 10.1073/pnas.0506580102. PubMed PMID: 16199517; PMCID: PMC1239896.
169. Sachs N, de Ligt J, Kopper O, Gogola E, Bounova G, Weeber F, Balgobind AV, Wind K, Gracanin A, Begthel H, Korving J, van Boxtel R, Duarte AA, Lelieveld D, van Hoeck A, Ernst RF, Blokzijl F, Nijman IJ, Hoogstraat M, van de Ven M, Egan DA, Zinzalla V, Moll J, Boj SF, Voest EE, Wessels L, van Diest PJ, Rottenberg S, Vries RGJ, Cuppen E, Clevers H. A Living Biobank of Breast Cancer Organoids Captures Disease Heterogeneity. *Cell.* 2018;172(1-2):373-86 e10. Epub 2017/12/12. doi: 10.1016/j.cell.2017.11.010. PubMed PMID: 29224780.
170. Feng Q, Hao S, Fang P, Zhang P, Sheng X. Role of GPX4 inhibition-mediated ferroptosis in the chemoresistance of ovarian cancer to Taxol in vitro. *Mol Biol Rep.* 2023;50(12):10189-98. Epub 2023/11/04 21:51. doi: 10.1007/s11033-023-08856-w. PubMed PMID: 37924448.
171. Dixon SJ, Patel DN, Welsch M, Skouta R, Lee ED, Hayano M, Thomas AG, Gleason CE, Tatonetti NP, Slusher BS, Stockwell BR. Pharmacological inhibition of cystine-glutamate exchange induces endoplasmic reticulum stress and ferroptosis. *Elife.* 2014;3:e02523. Epub 2014/05/23. doi: 10.7554/eLife.02523. PubMed PMID: 24844246; PMCID: PMC4054777.
172. Mukhopadhyay D, Goel HL, Xiong C, Goel S, Kumar A, Li R, Zhu LJ, Clark JL, Brehm MA, Mercurio AM. The calcium channel TRPC6 promotes chemotherapy-induced persistence by regulating integrin alpha6 mRNA splicing. *Cell Rep.* 2023;42(11):113347. Epub 2023/11/01. doi: 10.1016/j.celrep.2023.113347. PubMed PMID: 37910503; PMCID: PMC10872598.

173. Poreba M, Strozyk A, Salvesen GS, Drag M. Caspase substrates and inhibitors. *Cold Spring Harb Perspect Biol.* 2013;5(8):a008680. Epub 2013/06/22. doi: 10.1101/cshperspect.a008680. PubMed PMID: 23788633; PMCID: PMC3721276.
174. Villa P, Kaufmann SH, Earnshaw WC. Caspases and caspase inhibitors. *Trends Biochem Sci.* 1997;22(10):388-93. Epub 1997/11/14. doi: 10.1016/s0968-0004(97)01107-9. PubMed PMID: 9357314.
175. Drummen GP, van Liebergen LC, Op den Kamp JA, Post JA. C11-BODIPY(581/591), an oxidation-sensitive fluorescent lipid peroxidation probe: (micro)spectroscopic characterization and validation of methodology. *Free Radic Biol Med.* 2002;33(4):473-90. Epub 2002/08/06. doi: 10.1016/s0891-5849(02)00848-1. PubMed PMID: 12160930.
176. Mills GC. Hemoglobin catabolism. I. Glutathione peroxidase, an erythrocyte enzyme which protects hemoglobin from oxidative breakdown. *J Biol Chem.* 1957;229(1):189-97. Epub 1957/11/01. PubMed PMID: 13491573.
177. Takebe G, Yarimizu J, Saito Y, Hayashi T, Nakamura H, Yodoi J, Nagasawa S, Takahashi K. A comparative study on the hydroperoxide and thiol specificity of the glutathione peroxidase family and selenoprotein P. *J Biol Chem.* 2002;277(43):41254-8. Epub 2002/08/20. doi: 10.1074/jbc.M202773200. PubMed PMID: 12185074.
178. Stipanuk MH, Dominy JE, Jr., Lee JI, Coloso RM. Mammalian cysteine metabolism: new insights into regulation of cysteine metabolism. *J Nutr.* 2006;136(6 Suppl):1652S-9S. Epub 2006/05/17. doi: 10.1093/jn/136.6.1652S. PubMed PMID: 16702335.
179. Cunningham A, Oudejans LL, Geugien M, Pereira-Martins DA, Wierenga ATJ, Erdem A, Sternadt D, Huls G, Schuringa JJ. The nonessential amino acid cysteine is required to prevent ferroptosis in acute myeloid leukemia. *Blood Adv.* 2024;8(1):56-69. Epub 2023/10/31. doi: 10.1182/bloodadvances.2023010786. PubMed PMID: 37906522; PMCID: PMC10784682 interests.
180. Liu N, Lin X, Huang C. Activation of the reverse transsulfuration pathway through NRF2/CBS confers erastin-induced ferroptosis resistance. *Br J Cancer.* 2020;122(2):279-92. Epub 2019/12/11. doi: 10.1038/s41416-019-0660-x. PubMed PMID: 31819185; PMCID: PMC7052275.
181. Poltorack CD, Dixon SJ. Understanding the role of cysteine in ferroptosis: progress & paradoxes. *FEBS J.* 2022;289(2):374-85. Epub 2021/03/28. doi: 10.1111/febs.15842. PubMed PMID: 33773039; PMCID: PMC8473584.
182. Minn AJ, Gupta GP, Siegel PM, Bos PD, Shu W, Giri DD, Viale A, Olshen AB, Gerald WL, Massague J. Genes that mediate breast cancer metastasis to lung. *Nature.* 2005;436(7050):518-24. Epub 2005/07/29. doi: 10.1038/nature03799. PubMed PMID: 16049480; PMCID: PMC1283098.

183. Piskounova E, Agathocleous M, Murphy MM, Hu Z, Huddleston SE, Zhao Z, Leitch AM, Johnson TM, DeBerardinis RJ, Morrison SJ. Oxidative stress inhibits distant metastasis by human melanoma cells. *Nature*. 2015;527(7577):186-91. Epub 2015/10/16. doi: 10.1038/nature15726. PubMed PMID: 26466563; PMCID: PMC4644103.
184. Ubellacker JM, Tasdogan A, Ramesh V, Shen B, Mitchell EC, Martin-Sandoval MS, Gu Z, McCormick ML, Durham AB, Spitz DR, Zhao Z, Mathews TP, Morrison SJ. Lymph protects metastasizing melanoma cells from ferroptosis. *Nature*. 2020;585(7823):113-8. Epub 2020/08/21. doi: 10.1038/s41586-020-2623-z. PubMed PMID: 32814895; PMCID: PMC7484468.
185. Gill JG, Piskounova E, Morrison SJ. Cancer, Oxidative Stress, and Metastasis. *Cold Spring Harb Symp Quant Biol*. 2016;81:163-75. Epub 2017/01/14. doi: 10.1101/sqb.2016.81.030791. PubMed PMID: 28082378.
186. Lee N, Park SJ, Lange M, Tseyang T, Doshi MB, Kim TY, Song Y, Kim DI, Greer PL, Olzmann JA, Spinelli JB, Kim D. Selenium reduction of ubiquinone via SQOR suppresses ferroptosis. *Nat Metab*. 2024;6(2):343-58. Epub 2024/02/14. doi: 10.1038/s42255-024-00974-4. PubMed PMID: 38351124.
187. Wang L, Cai H, Hu Y, Liu F, Huang S, Zhou Y, Yu J, Xu J, Wu F. A pharmacological probe identifies cystathionine beta-synthase as a new negative regulator for ferroptosis. *Cell Death Dis*. 2018;9(10):1005. Epub 2018/09/28. doi: 10.1038/s41419-018-1063-2. PubMed PMID: 30258181; PMCID: PMC6158189.
188. Naowarojna N, Wu TW, Pan Z, Li M, Han JR, Zou Y. Dynamic Regulation of Ferroptosis by Lipid Metabolism. *Antioxid Redox Signal*. 2023;39(1-3):59-78. Epub 2023/03/29. doi: 10.1089/ars.2023.0278. PubMed PMID: 36974367.
189. Wen L, Liang C, Chen E, Chen W, Liang F, Zhi X, Wei T, Xue F, Li G, Yang Q, Gong W, Feng X, Bai X, Liang T. Regulation of Multi-drug Resistance in hepatocellular carcinoma cells is TRPC6/Calcium Dependent. *Sci Rep*. 2016;6:23269. Epub 2016/03/25. doi: 10.1038/srep23269. PubMed PMID: 27011063; PMCID: PMC4806320.
190. Chen S, He FF, Wang H, Fang Z, Shao N, Tian XJ, Liu JS, Zhu ZH, Wang YM, Wang S, Huang K, Zhang C. Calcium entry via TRPC6 mediates albumin overload-induced endoplasmic reticulum stress and apoptosis in podocytes. *Cell Calcium*. 2011;50(6):523-9. Epub 2011/10/01. doi: 10.1016/j.ceca.2011.08.008. PubMed PMID: 21959089.
191. Farmer LK, Rollason R, Whitcomb DJ, Ni L, Goodliff A, Lay AC, Birnbaumer L, Heesom KJ, Xu SZ, Saleem MA, Welsh GI. TRPC6 Binds to and Activates Calpain, Independent of Its Channel Activity, and Regulates Podocyte Cytoskeleton, Cell Adhesion, and Motility. *J Am Soc Nephrol*. 2019;30(10):1910-24. Epub 2019/08/17. doi: 10.1681/ASN.2018070729. PubMed PMID: 31416818; PMCID: PMC6779362.
192. Ilatovskaya DV, Palygin O, Chubinskiy-Nadezhdin V, Negulyaev YA, Ma R, Birnbaumer L, Staruschenko A. Angiotensin II has acute effects on TRPC6 channels in

- podocytes of freshly isolated glomeruli. *Kidney Int.* 2014;86(3):506-14. Epub 2014/03/22. doi: 10.1038/ki.2014.71. PubMed PMID: 24646854; PMCID: PMC4149864.
193. Ji T, Zhang C, Ma L, Wang Q, Zou L, Meng K, Zhang R, Jiao J. TRPC6-Mediated Ca<sup>2+</sup> Signaling is Required for Hypoxia-Induced Autophagy in Human Podocytes. *Cell Physiol Biochem.* 2018;48(4):1782-92. Epub 2018/08/06. doi: 10.1159/000492351. PubMed PMID: 30078002.
194. Kim EY, Anderson M, Dryer SE. Insulin increases surface expression of TRPC6 channels in podocytes: role of NADPH oxidases and reactive oxygen species. *Am J Physiol Renal Physiol.* 2012;302(3):F298-307. Epub 2011/10/28. doi: 10.1152/ajprenal.00423.2011. PubMed PMID: 22031853; PMCID: PMC3287354.
195. Kim EY, Anderson M, Wilson C, Hagmann H, Benzing T, Dryer SE. NOX2 interacts with podocyte TRPC6 channels and contributes to their activation by diacylglycerol: essential role of podocin in formation of this complex. *Am J Physiol Cell Physiol.* 2013;305(9):C960-71. Epub 2013/08/21. doi: 10.1152/ajpcell.00191.2013. PubMed PMID: 23948707.
196. Prevarskaya N, Zhang L, Barritt G. TRP channels in cancer. *Biochim Biophys Acta.* 2007;1772(8):937-46. Epub 2007/07/10. doi: 10.1016/j.bbadis.2007.05.006. PubMed PMID: 17616360.
197. Chigurupati S, Venkataraman R, Barrera D, Naganathan A, Madan M, Paul L, Pattisapu JV, Kyriazis GA, Sugaya K, Bushnev S, Lathia JD, Rich JN, Chan SL. Receptor channel TRPC6 is a key mediator of Notch-driven glioblastoma growth and invasiveness. *Cancer Res.* 2010;70(1):418-27. Epub 2009/12/24. doi: 10.1158/0008-5472.CAN-09-2654. PubMed PMID: 20028870.
198. Li S, Wang J, Wei Y, Liu Y, Ding X, Dong B, Xu Y, Wang Y. Crucial role of TRPC6 in maintaining the stability of HIF-1alpha in glioma cells under hypoxia. *J Cell Sci.* 2015;128(17):3317-29. Epub 2015/07/19. doi: 10.1242/jcs.173161. PubMed PMID: 26187851.
199. Takahashi N, Chen HY, Harris IS, Stover DG, Selfors LM, Bronson RT, Deraedt T, Cichowski K, Welm AL, Mori Y, Mills GB, Brugge JS. Cancer Cells Co-opt the Neuronal Redox-Sensing Channel TRPA1 to Promote Oxidative-Stress Tolerance. *Cancer Cell.* 2018;33(6):985-1003 e7. Epub 2018/05/29. doi: 10.1016/j.ccell.2018.05.001. PubMed PMID: 29805077; PMCID: PMC6100788.
200. Other-Gee Pohl S, Myant KB. Alternative RNA splicing in tumour heterogeneity, plasticity and therapy. *Dis Model Mech.* 2022;15(1). Epub 2022/01/12. doi: 10.1242/dmm.049233. PubMed PMID: 35014671; PMCID: PMC8764416.
201. Cherry S, Lynch KW. Alternative splicing and cancer: insights, opportunities, and challenges from an expanding view of the transcriptome. *Genes Dev.* 2020;34(15-16):1005-16. Epub 2020/08/05. doi: 10.1101/gad.338962.120. PubMed PMID: 32747477; PMCID: PMC7397854.

202. Wilkinson ME, Charenton C, Nagai K. RNA Splicing by the Spliceosome. *Annu Rev Biochem.* 2020;89:359-88. Epub 2019/12/04. doi: 10.1146/annurev-biochem-091719-064225. PubMed PMID: 31794245.
203. Seiler M, Peng S, Agrawal AA, Palacino J, Teng T, Zhu P, Smith PG, Cancer Genome Atlas Research N, Buonamici S, Yu L. Somatic Mutational Landscape of Splicing Factor Genes and Their Functional Consequences across 33 Cancer Types. *Cell Rep.* 2018;23(1):282-96 e4. Epub 2018/04/05. doi: 10.1016/j.celrep.2018.01.088. PubMed PMID: 29617667; PMCID: PMC5933844.
204. Darman RB, Seiler M, Agrawal AA, Lim KH, Peng S, Aird D, Bailey SL, Bhavsar EB, Chan B, Colla S, Corson L, Feala J, Fekkes P, Ichikawa K, Keaney GF, Lee L, Kumar P, Kunii K, MacKenzie C, Matijevic M, Mizui Y, Myint K, Park ES, Puyang X, Selvaraj A, Thomas MP, Tsai J, Wang JY, Warmuth M, Yang H, Zhu P, Garcia-Manero G, Furman RR, Yu L, Smith PG, Buonamici S. Cancer-Associated SF3B1 Hotspot Mutations Induce Cryptic 3' Splice Site Selection through Use of a Different Branch Point. *Cell Rep.* 2015;13(5):1033-45. Epub 2015/11/14. doi: 10.1016/j.celrep.2015.09.053. PubMed PMID: 26565915.
205. Zhang J, Ali AM, Lieu YK, Liu Z, Gao J, Rabadan R, Raza A, Mukherjee S, Manley JL. Disease-Causing Mutations in SF3B1 Alter Splicing by Disrupting Interaction with SUGP1. *Mol Cell.* 2019;76(1):82-95 e7. Epub 2019/09/03. doi: 10.1016/j.molcel.2019.07.017. PubMed PMID: 31474574; PMCID: PMC7065273.
206. Wang L, Brooks AN, Fan J, Wan Y, Gambe R, Li S, Hergert S, Yin S, Freeman SS, Levin JZ, Fan L, Seiler M, Buonamici S, Smith PG, Chau KF, Cibulskis CL, Zhang W, Rassenti LZ, Ghia EM, Kipps TJ, Fernandes S, Bloch DB, Kotliar D, Landau DA, Shukla SA, Aster JC, Reed R, DeLuca DS, Brown JR, Neuberg D, Getz G, Livak KJ, Meyerson MM, Kharchenko PV, Wu CJ. Transcriptomic Characterization of SF3B1 Mutation Reveals Its Pleiotropic Effects in Chronic Lymphocytic Leukemia. *Cancer Cell.* 2016;30(5):750-63. Epub 2016/11/08. doi: 10.1016/j.ccell.2016.10.005. PubMed PMID: 27818134; PMCID: PMC5127278.
207. Qiu Y, Lyu J, Dunlap M, Harvey SE, Cheng C. A combinatorially regulated RNA splicing signature predicts breast cancer EMT states and patient survival. *RNA.* 2020;26(9):1257-67. Epub 2020/05/30. doi: 10.1261/rna.074187.119. PubMed PMID: 32467311; PMCID: PMC7430667.
208. Weise A, Bruser K, Elfert S, Wallmen B, Wittel Y, Wohrle S, Hecht A. Alternative splicing of Tcf7l2 transcripts generates protein variants with differential promoter-binding and transcriptional activation properties at Wnt/beta-catenin targets. *Nucleic Acids Res.* 2010;38(6):1964-81. Epub 2010/01/02. doi: 10.1093/nar/gkp1197. PubMed PMID: 20044351; PMCID: PMC2847248.
209. Braeutigam C, Rago L, Rolke A, Waldmeier L, Christofori G, Winter J. The RNA-binding protein Rbfox2: an essential regulator of EMT-driven alternative splicing and a mediator of cellular invasion. *Oncogene.* 2014;33(9):1082-92. Epub 2013/02/26. doi: 10.1038/onc.2013.50. PubMed PMID: 23435423.

210. Ehrmann I, Dalgliesh C, Liu Y, Danilenko M, Crosier M, Overman L, Arthur HM, Lindsay S, Clowry GJ, Venables JP, Fort P, Elliott DJ. The tissue-specific RNA binding protein T-STAR controls regional splicing patterns of neurexin pre-mRNAs in the brain. *PLoS Genet.* 2013;9(4):e1003474. Epub 2013/05/03. doi: 10.1371/journal.pgen.1003474. PubMed PMID: 23637638; PMCID: PMC3636136.
211. Venables JP, Brosseau JP, Gadea G, Klinck R, Prinos P, Beaulieu JF, Lapointe E, Durand M, Thibault P, Tremblay K, Rousset F, Tazi J, Abou Elela S, Chabot B. RBFOX2 is an important regulator of mesenchymal tissue-specific splicing in both normal and cancer tissues. *Mol Cell Biol.* 2013;33(2):396-405. Epub 2012/11/15. doi: 10.1128/MCB.01174-12. PubMed PMID: 23149937; PMCID: PMC3554129.
212. Venables JP, Lapasset L, Gadea G, Fort P, Klinck R, Irimia M, Vignal E, Thibault P, Prinos P, Chabot B, Abou Elela S, Roux P, Lemaitre JM, Tazi J. MBNL1 and RBFOX2 cooperate to establish a splicing programme involved in pluripotent stem cell differentiation. *Nat Commun.* 2013;4:2480. Epub 2013/09/21. doi: 10.1038/ncomms3480. PubMed PMID: 24048253.
213. Xiong Y, Deng Y, Wang K, Zhou H, Zheng X, Si L, Fu Z. Profiles of alternative splicing in colorectal cancer and their clinical significance: A study based on large-scale sequencing data. *EBioMedicine.* 2018;36:183-95. Epub 2018/09/24. doi: 10.1016/j.ebiom.2018.09.021. PubMed PMID: 30243491; PMCID: PMC6197784.
214. Gudino V, Cammareri P, Billard CV, Myant KB. Negative regulation of TGFbeta-induced apoptosis by RAC1B enhances intestinal tumourigenesis. *Cell Death Dis.* 2021;12(10):873. Epub 2021/09/27. doi: 10.1038/s41419-021-04177-7. PubMed PMID: 34564693; PMCID: PMC8464603.
215. Tan DJ, Mitra M, Chiu AM, Collier HA. Intron retention is a robust marker of intertumoral heterogeneity in pancreatic ductal adenocarcinoma. *NPJ Genom Med.* 2020;5(1):55. Epub 2020/12/15. doi: 10.1038/s41525-020-00159-4. PubMed PMID: 33311498; PMCID: PMC7733475.
216. Ben-Hur V, Denichenko P, Siegfried Z, Maimon A, Krainer A, Davidson B, Karni R. S6K1 alternative splicing modulates its oncogenic activity and regulates mTORC1. *Cell Rep.* 2013;3(1):103-15. Epub 2013/01/01. doi: 10.1016/j.celrep.2012.11.020. PubMed PMID: 23273915; PMCID: PMC5021319.
217. Gokmen-Polar Y, Neelamraju Y, Goswami CP, Gu Y, Gu X, Nallamotheu G, Vieth E, Janga SC, Ryan M, Badve SS. Splicing factor ESRP1 controls ER-positive breast cancer by altering metabolic pathways. *EMBO Rep.* 2019;20(2). Epub 2019/01/23. doi: 10.15252/embr.201846078. PubMed PMID: 30665944; PMCID: PMC6362360.
218. Siegel PM, Shu W, Cardiff RD, Muller WJ, Massague J. Transforming growth factor beta signaling impairs Neu-induced mammary tumorigenesis while promoting pulmonary metastasis. *Proc Natl Acad Sci U S A.* 2003;100(14):8430-5. Epub 2003/06/17. doi: 10.1073/pnas.0932636100. PubMed PMID: 12808151; PMCID: PMC166246.

219. Kroger C, Afeyan A, Mraz J, Eaton EN, Reinhardt F, Khodor YL, Thiru P, Bieri B, Ye X, Burge CB, Weinberg RA. Acquisition of a hybrid E/M state is essential for tumorigenicity of basal breast cancer cells. *Proc Natl Acad Sci U S A*. 2019;116(15):7353-62. Epub 2019/03/27. doi: 10.1073/pnas.1812876116. PubMed PMID: 30910979; PMCID: PMC6462070.
220. Augimeri G, Gonzalez ME, Paoli A, Eido A, Choi Y, Burman B, Djomehri S, Karthikeyan SK, Varambally S, Buschhaus JM, Chen YC, Mauro L, Bonofiglio D, Nesvizhskii AI, Luker GD, Ando S, Yoon E, Kleer CG. A hybrid breast cancer/mesenchymal stem cell population enhances chemoresistance and metastasis. *JCI Insight*. 2023;8(18). Epub 2023/08/22. doi: 10.1172/jci.insight.164216. PubMed PMID: 37607007; PMCID: PMC10561721.
221. Kinnel B, Singh SK, Oprea-Ilies G, Singh R. Targeted Therapy and Mechanisms of Drug Resistance in Breast Cancer. *Cancers (Basel)*. 2023;15(4). Epub 2023/02/26. doi: 10.3390/cancers15041320. PubMed PMID: 36831661; PMCID: PMC9954028.
222. Kim C, Gao R, Sei E, Brandt R, Hartman J, Hatschek T, Crosetto N, Foukakis T, Navin NE. Chemoresistance Evolution in Triple-Negative Breast Cancer Delineated by Single-Cell Sequencing. *Cell*. 2018;173(4):879-93 e13. Epub 2018/04/24. doi: 10.1016/j.cell.2018.03.041. PubMed PMID: 29681456; PMCID: PMC6132060.
223. White JC, Pucci P, Crea F. The role of histone lysine demethylases in cancer cells' resistance to tyrosine kinase inhibitors. *Cancer Drug Resist*. 2019;2(2):326-34. Epub 2019/06/19. doi: 10.20517/cdr.2019.16. PubMed PMID: 35582714; PMCID: PMC8992625.
224. de Miguel FJ, Gentile C, Feng WW, Silva SJ, Sankar A, Exposito F, Cai WL, Melnick MA, Robles-Oteiza C, Hinkley MM, Tsai JA, Hartley AV, Wei J, Wurtz A, Li F, Toki MI, Rimm DL, Homer R, Wilen CB, Xiao AZ, Qi J, Yan Q, Nguyen DX, Janne PA, Kadoch C, Politi KA. Mammalian SWI/SNF chromatin remodeling complexes promote tyrosine kinase inhibitor resistance in EGFR-mutant lung cancer. *Cancer Cell*. 2023;41(8):1516-34 e9. Epub 2023/08/05. doi: 10.1016/j.ccell.2023.07.005. PubMed PMID: 37541244.
225. Zheng L, Nagar M, Maurais AJ, Slade DJ, Parelkar SS, Coonrod SA, Weerapana E, Thompson PR. Calcium Regulates the Nuclear Localization of Protein Arginine Deiminase 2. *Biochemistry*. 2019;58(27):3042-56. Epub 2019/06/28. doi: 10.1021/acs.biochem.9b00225. PubMed PMID: 31243954; PMCID: PMC6691507.
226. Fenelon JC, Banerjee A, Murphy BD. Embryonic diapause: development on hold. *Int J Dev Biol*. 2014;58(2-4):163-74. Epub 2014/07/16. doi: 10.1387/ijdb.140074bm. PubMed PMID: 25023682.
227. Hanahan D, Weinberg RA. Hallmarks of cancer: the next generation. *Cell*. 2011;144(5):646-74. Epub 2011/03/08. doi: 10.1016/j.cell.2011.02.013. PubMed PMID: 21376230.
228. Koppenol WH, Bounds PL, Dang CV. Otto Warburg's contributions to current concepts of cancer metabolism. *Nat Rev Cancer*. 2011;11(5):325-37. Epub 2011/04/22. doi: 10.1038/nrc3038. PubMed PMID: 21508971.

229. Christen S, Lorendeau D, Schmieder R, Broekaert D, Metzger K, Veys K, Elia I, Buescher JM, Orth MF, Davidson SM, Grunewald TG, De Bock K, Fendt SM. Breast Cancer-Derived Lung Metastases Show Increased Pyruvate Carboxylase-Dependent Anaplerosis. *Cell Rep.* 2016;17(3):837-48. Epub 2016/10/13. doi: 10.1016/j.celrep.2016.09.042. PubMed PMID: 27732858.
230. Muir A, Danai LV, Gui DY, Waingarten CY, Lewis CA, Vander Heiden MG. Environmental cystine drives glutamine anaplerosis and sensitizes cancer cells to glutaminase inhibition. *Elife.* 2017;6. Epub 2017/08/23. doi: 10.7554/eLife.27713. PubMed PMID: 28826492; PMCID: PMC5589418.
231. Possemato R, Marks KM, Shaul YD, Pacold ME, Kim D, Birsoy K, Sethumadhavan S, Woo HK, Jang HG, Jha AK, Chen WW, Barrett FG, Stransky N, Tsun ZY, Cowley GS, Barretina J, Kalaany NY, Hsu PP, Ottina K, Chan AM, Yuan B, Garraway LA, Root DE, Mino-Kenudson M, Brachtel EF, Driggers EM, Sabatini DM. Functional genomics reveal that the serine synthesis pathway is essential in breast cancer. *Nature.* 2011;476(7360):346-50. Epub 2011/07/16. doi: 10.1038/nature10350. PubMed PMID: 21760589; PMCID: PMC3353325.
232. Sant'Anna-Silva ACB, Perez-Valencia JA, Sciacovelli M, Lalou C, Sarlak S, Tronci L, Nikitopoulou E, Meszaros AT, Frezza C, Rossignol R, Gnaiger E, Klocker H. Succinate Anaplerosis Has an Onco-Driving Potential in Prostate Cancer Cells. *Cancers (Basel).* 2021;13(7). Epub 2021/05/01. doi: 10.3390/cancers13071727. PubMed PMID: 33917317; PMCID: PMC8038717.
233. Singleton DC, Dechaume AL, Murray PM, Katt WP, Baguley BC, Leung EY. Pyruvate anaplerosis is a mechanism of resistance to pharmacological glutaminase inhibition in triple-receptor negative breast cancer. *BMC Cancer.* 2020;20(1):470. Epub 2020/05/27. doi: 10.1186/s12885-020-06885-3. PubMed PMID: 32450839; PMCID: PMC7333265.
234. Dibble CC, Manning BD. Signal integration by mTORC1 coordinates nutrient input with biosynthetic output. *Nat Cell Biol.* 2013;15(6):555-64. Epub 2013/06/04. doi: 10.1038/ncb2763. PubMed PMID: 23728461; PMCID: PMC3743096.
235. Yuan TL, Cantley LC. PI3K pathway alterations in cancer: variations on a theme. *Oncogene.* 2008;27(41):5497-510. Epub 2008/09/17. doi: 10.1038/onc.2008.245. PubMed PMID: 18794884; PMCID: PMC3398461.
236. Casciano JC, Perry C, Cohen-Nowak AJ, Miller KD, Vande Voorde J, Zhang Q, Chalmers S, Sandison ME, Liu Q, Hedley A, McBryan T, Tang HY, Gorman N, Beer T, Speicher DW, Adams PD, Liu X, Schlegel R, McCarron JG, Wakelam MJO, Gottlieb E, Kossenkov AV, Schug ZT. MYC regulates fatty acid metabolism through a multigenic program in claudin-low triple negative breast cancer. *Br J Cancer.* 2020;122(6):868-84. Epub 2020/01/17. doi: 10.1038/s41416-019-0711-3. PubMed PMID: 31942031; PMCID: PMC7078291.
237. Chen Y, Leon-Letelier RA, Abdel Sater AH, Vykoukal J, Dennison JB, Hanash S, Fahrman JF. c-MYC-Driven Polyamine Metabolism in Ovarian Cancer: From Pathogenesis to

- Early Detection and Therapy. *Cancers (Basel)*. 2023;15(3). Epub 2023/02/12. doi: 10.3390/cancers15030623. PubMed PMID: 36765581; PMCID: PMC9913358.
238. Dang CV. Therapeutic targeting of Myc-reprogrammed cancer cell metabolism. *Cold Spring Harb Symp Quant Biol*. 2011;76:369-74. Epub 2011/10/01. doi: 10.1101/sqb.2011.76.011296. PubMed PMID: 21960526.
239. Dang CV, Le A, Gao P. MYC-induced cancer cell energy metabolism and therapeutic opportunities. *Clin Cancer Res*. 2009;15(21):6479-83. Epub 2009/10/29. doi: 10.1158/1078-0432.CCR-09-0889. PubMed PMID: 19861459; PMCID: PMC2783410.
240. Stine ZE, Walton ZE, Altman BJ, Hsieh AL, Dang CV. MYC, Metabolism, and Cancer. *Cancer Discov*. 2015;5(10):1024-39. Epub 2015/09/19. doi: 10.1158/2159-8290.CD-15-0507. PubMed PMID: 26382145; PMCID: PMC4592441.
241. Li T, Kon N, Jiang L, Tan M, Ludwig T, Zhao Y, Baer R, Gu W. Tumor suppression in the absence of p53-mediated cell-cycle arrest, apoptosis, and senescence. *Cell*. 2012;149(6):1269-83. Epub 2012/06/12. doi: 10.1016/j.cell.2012.04.026. PubMed PMID: 22682249; PMCID: PMC3688046.
242. Kruiswijk F, Labuschagne CF, Vousden KH. p53 in survival, death and metabolic health: a lifeguard with a licence to kill. *Nat Rev Mol Cell Biol*. 2015;16(7):393-405. Epub 2015/07/01. doi: 10.1038/nrm4007. PubMed PMID: 26122615.
243. McCracken AN, Edinger AL. Nutrient transporters: the Achilles' heel of anabolism. *Trends Endocrinol Metab*. 2013;24(4):200-8. Epub 2013/02/14. doi: 10.1016/j.tem.2013.01.002. PubMed PMID: 23402769; PMCID: PMC3617053.
244. Laplante M, Sabatini DM. mTOR signaling in growth control and disease. *Cell*. 2012;149(2):274-93. Epub 2012/04/17. doi: 10.1016/j.cell.2012.03.017. PubMed PMID: 22500797; PMCID: PMC3331679.
245. Hensley CT, Wasti AT, DeBerardinis RJ. Glutamine and cancer: cell biology, physiology, and clinical opportunities. *J Clin Invest*. 2013;123(9):3678-84. Epub 2013/09/04. doi: 10.1172/JCI69600. PubMed PMID: 23999442; PMCID: PMC3754270.
246. Nicklin P, Bergman P, Zhang B, Triantafellow E, Wang H, Nyfeler B, Yang H, Hild M, Kung C, Wilson C, Myer VE, MacKeigan JP, Porter JA, Wang YK, Cantley LC, Finan PM, Murphy LO. Bidirectional transport of amino acids regulates mTOR and autophagy. *Cell*. 2009;136(3):521-34. Epub 2009/02/11. doi: 10.1016/j.cell.2008.11.044. PubMed PMID: 19203585; PMCID: PMC3733119.
247. Yoo H, Stephanopoulos G, Kelleher JK. Quantifying carbon sources for de novo lipogenesis in wild-type and IRS-1 knockout brown adipocytes. *J Lipid Res*. 2004;45(7):1324-32. Epub 2004/04/23. doi: 10.1194/jlr.M400031-JLR200. PubMed PMID: 15102881.
248. DeBerardinis RJ, Mancuso A, Daikhin E, Nissim I, Yudkoff M, Wehrli S, Thompson CB. Beyond aerobic glycolysis: transformed cells can engage in glutamine metabolism that exceeds

- the requirement for protein and nucleotide synthesis. *Proc Natl Acad Sci U S A*. 2007;104(49):19345-50. Epub 2007/11/23. doi: 10.1073/pnas.0709747104. PubMed PMID: 18032601; PMCID: PMC2148292.
249. Mullen AR, Wheaton WW, Jin ES, Chen PH, Sullivan LB, Cheng T, Yang Y, Linehan WM, Chandel NS, DeBerardinis RJ. Reductive carboxylation supports growth in tumour cells with defective mitochondria. *Nature*. 2011;481(7381):385-8. Epub 2011/11/22. doi: 10.1038/nature10642. PubMed PMID: 22101431; PMCID: PMC3262117.
250. Metallo CM, Gameiro PA, Bell EL, Mattaini KR, Yang J, Hiller K, Jewell CM, Johnson ZR, Irvine DJ, Guarente L, Kelleher JK, Vander Heiden MG, Iliopoulos O, Stephanopoulos G. Reductive glutamine metabolism by IDH1 mediates lipogenesis under hypoxia. *Nature*. 2011;481(7381):380-4. Epub 2011/11/22. doi: 10.1038/nature10602. PubMed PMID: 22101433; PMCID: PMC3710581.
251. Wise DR, Ward PS, Shay JE, Cross JR, Gruber JJ, Sachdeva UM, Platt JM, DeMatteo RG, Simon MC, Thompson CB. Hypoxia promotes isocitrate dehydrogenase-dependent carboxylation of alpha-ketoglutarate to citrate to support cell growth and viability. *Proc Natl Acad Sci U S A*. 2011;108(49):19611-6. Epub 2011/11/23. doi: 10.1073/pnas.1117773108. PubMed PMID: 22106302; PMCID: PMC3241793.
252. Schug ZT, Peck B, Jones DT, Zhang Q, Grosskurth S, Alam IS, Goodwin LM, Smethurst E, Mason S, Blyth K, McGarry L, James D, Shanks E, Kalna G, Saunders RE, Jiang M, Howell M, Lassailly F, Thin MZ, Spencer-Dene B, Stamp G, van den Broek NJ, Mackay G, Bulusu V, Kamphorst JJ, Tardito S, Strachan D, Harris AL, Aboagye EO, Critchlow SE, Wakelam MJ, Schulze A, Gottlieb E. Acetyl-CoA synthetase 2 promotes acetate utilization and maintains cancer cell growth under metabolic stress. *Cancer Cell*. 2015;27(1):57-71. Epub 2015/01/15. doi: 10.1016/j.ccell.2014.12.002. PubMed PMID: 25584894; PMCID: PMC4297291.
253. Fan J, Ye J, Kamphorst JJ, Shlomi T, Thompson CB, Rabinowitz JD. Quantitative flux analysis reveals folate-dependent NADPH production. *Nature*. 2014;510(7504):298-302. Epub 2014/05/09. doi: 10.1038/nature13236. PubMed PMID: 24805240; PMCID: PMC4104482.
254. Lewis CA, Parker SJ, Fiske BP, McCloskey D, Gui DY, Green CR, Vokes NI, Feist AM, Vander Heiden MG, Metallo CM. Tracing compartmentalized NADPH metabolism in the cytosol and mitochondria of mammalian cells. *Mol Cell*. 2014;55(2):253-63. Epub 2014/06/03. doi: 10.1016/j.molcel.2014.05.008. PubMed PMID: 24882210; PMCID: PMC4106038.
255. Horton JD, Goldstein JL, Brown MS. SREBPs: activators of the complete program of cholesterol and fatty acid synthesis in the liver. *J Clin Invest*. 2002;109(9):1125-31. Epub 2002/05/08. doi: 10.1172/JCI15593. PubMed PMID: 11994399; PMCID: PMC150968.
256. Duvel K, Yecies JL, Menon S, Raman P, Lipovsky AI, Souza AL, Triantafellow E, Ma Q, Gorski R, Cleaver S, Vander Heiden MG, MacKeigan JP, Finan PM, Clish CB, Murphy LO, Manning BD. Activation of a metabolic gene regulatory network downstream of mTOR complex 1. *Mol Cell*. 2010;39(2):171-83. Epub 2010/07/31. doi: 10.1016/j.molcel.2010.06.022. PubMed PMID: 20670887; PMCID: PMC2946786.

257. Goldstein JL, DeBose-Boyd RA, Brown MS. Protein sensors for membrane sterols. *Cell*. 2006;124(1):35-46. Epub 2006/01/18. doi: 10.1016/j.cell.2005.12.022. PubMed PMID: 16413480.
258. Deberardinis RJ, Lum JJ, Thompson CB. Phosphatidylinositol 3-kinase-dependent modulation of carnitine palmitoyltransferase 1A expression regulates lipid metabolism during hematopoietic cell growth. *J Biol Chem*. 2006;281(49):37372-80. Epub 2006/10/13. doi: 10.1074/jbc.M608372200. PubMed PMID: 17030509.
259. Stincone A, Prigione A, Cramer T, Wamelink MM, Campbell K, Cheung E, Olin-Sandoval V, Gruning NM, Kruger A, Tauqeer Alam M, Keller MA, Breitenbach M, Brindle KM, Rabinowitz JD, Ralser M. The return of metabolism: biochemistry and physiology of the pentose phosphate pathway. *Biol Rev Camb Philos Soc*. 2015;90(3):927-63. Epub 2014/09/23. doi: 10.1111/brv.12140. PubMed PMID: 25243985; PMCID: PMC4470864.
260. Vander Heiden MG. Targeting cancer metabolism: a therapeutic window opens. *Nat Rev Drug Discov*. 2011;10(9):671-84. Epub 2011/09/01. doi: 10.1038/nrd3504. PubMed PMID: 21878982.
261. Buescher JM, Antoniewicz MR, Boros LG, Burgess SC, Brunengraber H, Clish CB, DeBerardinis RJ, Feron O, Frezza C, Ghesquiere B, Gottlieb E, Hiller K, Jones RG, Kamphorst JJ, Kibbey RG, Kimmelman AC, Locasale JW, Lunt SY, Maddocks OD, Malloy C, Metallo CM, Meuillet EJ, Munger J, Noh K, Rabinowitz JD, Ralser M, Sauer U, Stephanopoulos G, St-Pierre J, Tennant DA, Wittmann C, Vander Heiden MG, Vazquez A, Vousden K, Young JD, Zamboni N, Fendt SM. A roadmap for interpreting (13)C metabolite labeling patterns from cells. *Curr Opin Biotechnol*. 2015;34:189-201. Epub 2015/03/04. doi: 10.1016/j.copbio.2015.02.003. PubMed PMID: 25731751; PMCID: PMC4552607.
262. Marin-Valencia I, Yang C, Mashimo T, Cho S, Baek H, Yang XL, Rajagopalan KN, Maddie M, Vemireddy V, Zhao Z, Cai L, Good L, Tu BP, Hatanpaa KJ, Mickey BE, Mates JM, Pascual JM, Maher EA, Malloy CR, Deberardinis RJ, Bachoo RM. Analysis of tumor metabolism reveals mitochondrial glucose oxidation in genetically diverse human glioblastomas in the mouse brain in vivo. *Cell Metab*. 2012;15(6):827-37. Epub 2012/06/12. doi: 10.1016/j.cmet.2012.05.001. PubMed PMID: 22682223; PMCID: PMC3372870.
263. Schieber M, Chandel NS. ROS function in redox signaling and oxidative stress. *Curr Biol*. 2014;24(10):R453-62. Epub 2014/05/23. doi: 10.1016/j.cub.2014.03.034. PubMed PMID: 24845678; PMCID: PMC4055301.
264. Jaramillo MC, Zhang DD. The emerging role of the Nrf2-Keap1 signaling pathway in cancer. *Genes Dev*. 2013;27(20):2179-91. Epub 2013/10/22. doi: 10.1101/gad.225680.113. PubMed PMID: 24142871; PMCID: PMC3814639.
265. Sporn MB, Liby KT. NRF2 and cancer: the good, the bad and the importance of context. *Nat Rev Cancer*. 2012;12(8):564-71. Epub 2012/07/20. doi: 10.1038/nrc3278. PubMed PMID: 22810811; PMCID: PMC3836441.

266. Gorrini C, Harris IS, Mak TW. Modulation of oxidative stress as an anticancer strategy. *Nat Rev Drug Discov.* 2013;12(12):931-47. Epub 2013/11/30. doi: 10.1038/nrd4002. PubMed PMID: 24287781.
267. Weinberg F, Hamanaka R, Wheaton WW, Weinberg S, Joseph J, Lopez M, Kalyanaraman B, Mutlu GM, Budinger GR, Chandel NS. Mitochondrial metabolism and ROS generation are essential for Kras-mediated tumorigenicity. *Proc Natl Acad Sci U S A.* 2010;107(19):8788-93. Epub 2010/04/28. doi: 10.1073/pnas.1003428107. PubMed PMID: 20421486; PMCID: PMC2889315.
268. Wiel C, Le Gal K, Ibrahim MX, Jahangir CA, Kashif M, Yao H, Ziegler DV, Xu X, Ghosh T, Mondal T, Kanduri C, Lindahl P, Sayin VI, Bergo MO. BACH1 Stabilization by Antioxidants Stimulates Lung Cancer Metastasis. *Cell.* 2019;178(2):330-45 e22. Epub 2019/07/02. doi: 10.1016/j.cell.2019.06.005. PubMed PMID: 31257027.
269. Kashif M, Yao H, Schmidt S, Chen X, Truong M, Tuksammel E, Liu Y, Bergo MO. ROS-lowering doses of vitamins C and A accelerate malignant melanoma metastasis. *Redox Biol.* 2023;60:102619. Epub 2023/02/13. doi: 10.1016/j.redox.2023.102619. PubMed PMID: 36774779; PMCID: PMC9945759.
270. Jin HT, Ahmed R, Okazaki T. Role of PD-1 in regulating T-cell immunity. *Curr Top Microbiol Immunol.* 2011;350:17-37. Epub 2010/11/10. doi: 10.1007/82\_2010\_116. PubMed PMID: 21061197.
271. Pennock ND, White JT, Cross EW, Cheney EE, Tamburini BA, Kedl RM. T cell responses: naive to memory and everything in between. *Adv Physiol Educ.* 2013;37(4):273-83. Epub 2013/12/03. doi: 10.1152/advan.00066.2013. PubMed PMID: 24292902; PMCID: PMC4089090.
272. Vinay DS, Ryan EP, Pawelec G, Talib WH, Stagg J, Elkord E, Lichtor T, Decker WK, Whelan RL, Kumara H, Signori E, Honoki K, Georgakilas AG, Amin A, Helferich WG, Boosani CS, Guha G, Ciriolo MR, Chen S, Mohammed SI, Azmi AS, Keith WN, Bilsland A, Bhakta D, Halicka D, Fujii H, Aquilano K, Ashraf SS, Newsheen S, Yang X, Choi BK, Kwon BS. Immune evasion in cancer: Mechanistic basis and therapeutic strategies. *Semin Cancer Biol.* 2015;35 Suppl:S185-S98. Epub 2015/03/31. doi: 10.1016/j.semcancer.2015.03.004. PubMed PMID: 25818339.
273. Speiser DE, Utzschneider DT, Oberle SG, Munz C, Romero P, Zehn D. T cell differentiation in chronic infection and cancer: functional adaptation or exhaustion? *Nat Rev Immunol.* 2014;14(11):768-74. Epub 2014/09/27. doi: 10.1038/nri3740. PubMed PMID: 25257362.
274. Debien V, De Caluwe A, Wang X, Piccart-Gebhart M, Tuohy VK, Romano E, Buisseret L. Immunotherapy in breast cancer: an overview of current strategies and perspectives. *NPJ Breast Cancer.* 2023;9(1):7. Epub 2023/02/14. doi: 10.1038/s41523-023-00508-3. PubMed PMID: 36781869; PMCID: PMC9925769 following authors declare no competing non-financial interests but the following competing financial interests: A.d.C.: Investigator-initiated trial

(funds paid to institution): AstraZeneca. M.P.-G.: Board Member (Scientific Board): Oncolytics; Consultant (honoraria): AstraZeneca, Camel-IDS, Crescendo Biologics, G1 Therapeutics, Genentech, Huya, Immunomedics, Lilly, Menarini, MSD, Novartis, Odonate, Oncolytics, Periphagen, Pfizer, Roche, Seattle Genetics, Immutep, NBE Therapeutics, SeaGen; Research grants to her Institute: AstraZeneca, Lilly, MSD, Novartis, Pfizer, Radius, Roche-Genentech, Servier, Synthron (outside the submitted work). V.K.T.: Funding from the Department of Defense Breakthrough Award, Level 3 Clinical Trial for Primary Immunoprevention of Triple-Negative Breast Cancer, Anixa Biosciences, Inc. V.K.T. holds personal equity in Anixa Biosciences, Inc. ER: Investigator-initiated trial (funds paid to institution): AstraZeneca, BMS, Roche, Replimmune. Consultancy/advisory board: AstraZeneca, Merck, Roche, Pierre Fabre. L.B.: Investigator-initiated trial (funds paid to institution): AstraZeneca. L.B. is supported by the Belgian "Fondation Contre le Cancer".

275. Chen Z, Kankala RK, Yang Z, Li W, Xie S, Li H, Chen AZ, Zou L. Antibody-based drug delivery systems for cancer therapy: Mechanisms, challenges, and prospects. *Theranostics*. 2022;12(8):3719-46. Epub 2022/06/07. doi: 10.7150/thno.72594. PubMed PMID: 35664074; PMCID: PMC9131265.

276. Zou Y, Schreiber SL. Progress in Understanding Ferroptosis and Challenges in Its Targeting for Therapeutic Benefit. *Cell Chem Biol*. 2020;27(4):463-71. Epub 2020/04/18. doi: 10.1016/j.chembiol.2020.03.015. PubMed PMID: 32302583; PMCID: PMC7346472.

277. Kim R, Hashimoto A, Markosyan N, Tyurin VA, Tyurina YY, Kar G, Fu S, Sehgal M, Garcia-Gerique L, Kossenkov A, Gebregziabher BA, Tobias JW, Hicks K, Halpin RA, Cveticic N, Deng H, Donthireddy L, Greenberg A, Nam B, Vonderheide RH, Nefedova Y, Kagan VE, Gabrilovich DI. Ferroptosis of tumour neutrophils causes immune suppression in cancer. *Nature*. 2022;612(7939):338-46. Epub 2022/11/18. doi: 10.1038/s41586-022-05443-0. PubMed PMID: 36385526; PMCID: PMC9875862.

278. Yang F, Xiao Y, Ding JH, Jin X, Ma D, Li DQ, Shi JX, Huang W, Wang YP, Jiang YZ, Shao ZM. Ferroptosis heterogeneity in triple-negative breast cancer reveals an innovative immunotherapy combination strategy. *Cell Metab*. 2023;35(1):84-100 e8. Epub 2022/10/19. doi: 10.1016/j.cmet.2022.09.021. PubMed PMID: 36257316.

279. Halbrook CJ, Pontious C, Kovalenko I, Lapienyte L, Dreyer S, Lee HJ, Thurston G, Zhang Y, Lazarus J, Sajjakulnukit P, Hong HS, Kremer DM, Nelson BS, Kemp S, Zhang L, Chang D, Biankin A, Shi J, Frankel TL, Crawford HC, Morton JP, Pasca di Magliano M, Lyssiotis CA. Macrophage-Released Pyrimidines Inhibit Gemcitabine Therapy in Pancreatic Cancer. *Cell Metab*. 2019;29(6):1390-9 e6. Epub 2019/03/05. doi: 10.1016/j.cmet.2019.02.001. PubMed PMID: 30827862; PMCID: PMC6602533.

280. Baldominos P, Barbera-Mourelle A, Barreiro O, Huang Y, Wight A, Cho JW, Zhao X, Estivill G, Adam I, Sanchez X, McCarthy S, Schaller J, Khan Z, Ruzo A, Pastorello R, Richardson ET, Dillon D, Montero-Llopis P, Barroso-Sousa R, Forman J, Shukla SA, Tolaney SM, Mittendorf EA, von Andrian UH, Wucherpfennig KW, Hemberg M, Agudo J. Quiescent cancer cells resist T cell attack by forming an immunosuppressive niche. *Cell*.

2022;185(10):1694-708 e19. Epub 2022/04/22. doi: 10.1016/j.cell.2022.03.033. PubMed PMID: 35447074.

281. Mohri Z, Del Rio Hernandez A, Krams R. The emerging role of YAP/TAZ in mechanotransduction. *J Thorac Dis.* 2017;9(5):E507-E9. Epub 2017/06/16. doi: 10.21037/jtd.2017.03.179. PubMed PMID: 28616323; PMCID: PMC5465147.

282. Takahashi K, Yamanaka S. Induction of pluripotent stem cells from mouse embryonic and adult fibroblast cultures by defined factors. *Cell.* 2006;126(4):663-76. Epub 2006/08/15. doi: 10.1016/j.cell.2006.07.024. PubMed PMID: 16904174.

283. O'Connor KW, Kishimoto K, Kuzma IO, Wagner KP, Selway JS, Roderick JE, Karna KK, Gallagher KM, Hu K, Liu H, Li R, Brehm MA, Zhu LJ, Curtis DJ, Tremblay CS, Kelliher MA. The role of quiescent thymic progenitors in TAL/LMO2-induced T-ALL chemotolerance. *Leukemia.* 2024. Epub 2024/03/30. doi: 10.1038/s41375-024-02232-8. PubMed PMID: 38553571.

284. Badgley MA, Kremer DM, Maurer HC, DelGiorno KE, Lee HJ, Purohit V, Sagalovskiy IR, Ma A, Kapilian J, Firl CEM, Decker AR, Sastra SA, Palermo CF, Andrade LR, Sajjakulnukit P, Zhang L, Tolstyka ZP, Hirschhorn T, Lamb C, Liu T, Gu W, Seeley ES, Stone E, Georgiou G, Manor U, Iuga A, Wahl GM, Stockwell BR, Lyssiotis CA, Olive KP. Cysteine depletion induces pancreatic tumor ferroptosis in mice. *Science.* 2020;368(6486):85-9. Epub 2020/04/04. doi: 10.1126/science.aaw9872. PubMed PMID: 32241947; PMCID: PMC7681911.

285. Gout I. Coenzyme A, protein CoAlation and redox regulation in mammalian cells. *Biochem Soc Trans.* 2018;46(3):721-8. Epub 2018/05/29. doi: 10.1042/BST20170506. PubMed PMID: 29802218; PMCID: PMC6008590.

286. Ghareeb H, Metanis N. The Thioredoxin System: A Promising Target for Cancer Drug Development. *Chemistry.* 2020;26(45):10175-84. Epub 2020/02/26. doi: 10.1002/chem.201905792. PubMed PMID: 32097513.

287. Harris IS, Treloar AE, Inoue S, Sasaki M, Gorrini C, Lee KC, Yung KY, Brenner D, Knobbe-Thomsen CB, Cox MA, Elia A, Berger T, Cescon DW, Adeoye A, Brustle A, Molyneux SD, Mason JM, Li WY, Yamamoto K, Wakeham A, Berman HK, Khokha R, Done SJ, Kavanagh TJ, Lam CW, Mak TW. Glutathione and thioredoxin antioxidant pathways synergize to drive cancer initiation and progression. *Cancer Cell.* 2015;27(2):211-22. Epub 2015/01/27. doi: 10.1016/j.ccell.2014.11.019. PubMed PMID: 25620030.

288. Combs JA, DeNicola GM. The Non-Essential Amino Acid Cysteine Becomes Essential for Tumor Proliferation and Survival. *Cancers (Basel).* 2019;11(5). Epub 2019/05/19. doi: 10.3390/cancers11050678. PubMed PMID: 31100816; PMCID: PMC6562400.

289. Wang Y, Yen FS, Zhu XG, Timson RC, Weber R, Xing C, Liu Y, Allwein B, Luo H, Yeh HW, Heissel S, Unlu G, Gamazon ER, Kharas MG, Hite R, Birsoy K. SLC25A39 is necessary for mitochondrial glutathione import in mammalian cells. *Nature.*

2021;599(7883):136-40. Epub 2021/10/29. doi: 10.1038/s41586-021-04025-w. PubMed PMID: 34707288; PMCID: PMC10981497.

290. Liu X, Olszewski K, Zhang Y, Lim EW, Shi J, Zhang X, Zhang J, Lee H, Koppula P, Lei G, Zhuang L, You MJ, Fang B, Li W, Metallo CM, Poyurovsky MV, Gan B. Cystine transporter regulation of pentose phosphate pathway dependency and disulfide stress exposes a targetable metabolic vulnerability in cancer. *Nat Cell Biol.* 2020;22(4):476-86. Epub 2020/04/02. doi: 10.1038/s41556-020-0496-x. PubMed PMID: 32231310; PMCID: PMC7194135.

291. Sullivan MR, Danai LV, Lewis CA, Chan SH, Gui DY, Kunchok T, Dennstedt EA, Vander Heiden MG, Muir A. Quantification of microenvironmental metabolites in murine cancers reveals determinants of tumor nutrient availability. *Elife.* 2019;8. Epub 2019/04/17. doi: 10.7554/eLife.44235. PubMed PMID: 30990168; PMCID: PMC6510537.

292. Koppula P, Zhang Y, Shi J, Li W, Gan B. The glutamate/cystine antiporter SLC7A11/xCT enhances cancer cell dependency on glucose by exporting glutamate. *J Biol Chem.* 2017;292(34):14240-9. Epub 2017/06/21. doi: 10.1074/jbc.M117.798405. PubMed PMID: 28630042; PMCID: PMC5572906.

293. Chen X, Kang R, Kroemer G, Tang D. Organelle-specific regulation of ferroptosis. *Cell Death Differ.* 2021;28(10):2843-56. Epub 2021/09/02. doi: 10.1038/s41418-021-00859-z. PubMed PMID: 34465893; PMCID: PMC8481335.

294. Bak DW, Bechtel TJ, Falco JA, Weerapana E. Cysteine reactivity across the subcellular universe. *Curr Opin Chem Biol.* 2019;48:96-105. Epub 2018/12/07. doi: 10.1016/j.cbpa.2018.11.002. PubMed PMID: 30508703; PMCID: PMC6382561.

295. Allocati N, Masulli M, Di Ilio C, Federici L. Glutathione transferases: substrates, inhibitors and pro-drugs in cancer and neurodegenerative diseases. *Oncogenesis.* 2018;7(1):8. Epub 2018/01/25. doi: 10.1038/s41389-017-0025-3. PubMed PMID: 29362397; PMCID: PMC5833873.

296. Zhang HF, Hughes CS, Li W, He JZ, Surdez D, El-Naggar AM, Cheng H, Prudova A, Delaidelli A, Negri GL, Li X, Orum-Madsen MS, Lizardo MM, Oo HZ, Colborne S, Shyp T, Scopim-Ribeiro R, Hammond CA, Dhez AC, Langman S, Lim JKM, Kung SHY, Li A, Steino A, Daugaard M, Parker SJ, Geltink RIK, Orentas RJ, Xu LY, Morin GB, Delattre O, Dimitrov DS, Sorensen PH. Proteomic Screens for Suppressors of Anoikis Identify IL1RAP as a Promising Surface Target in Ewing Sarcoma. *Cancer Discov.* 2021;11(11):2884-903. Epub 2021/05/23. doi: 10.1158/2159-8290.CD-20-1690. PubMed PMID: 34021002; PMCID: PMC8563374.

297. Zhu J, Berisa M, Schworer S, Qin W, Cross JR, Thompson CB. Transsulfuration Activity Can Support Cell Growth upon Extracellular Cysteine Limitation. *Cell Metab.* 2019;30(5):865-76 e5. Epub 2019/10/15. doi: 10.1016/j.cmet.2019.09.009. PubMed PMID: 31607565; PMCID: PMC6961654.

298. Zhang T, Bauer C, Newman AC, Uribe AH, Athineos D, Blyth K, Maddocks ODK. Polyamine pathway activity promotes cysteine essentiality in cancer cells. *Nat Metab.* 2020;2(10):1062-76. Epub 2020/08/05. doi: 10.1038/s42255-020-0253-2. PubMed PMID: 32747794; PMCID: PMC7614128.
299. Cao J, Chen X, Jiang L, Lu B, Yuan M, Zhu D, Zhu H, He Q, Yang B, Ying M. DJ-1 suppresses ferroptosis through preserving the activity of S-adenosyl homocysteine hydrolase. *Nat Commun.* 2020;11(1):1251. Epub 2020/03/08. doi: 10.1038/s41467-020-15109-y. PubMed PMID: 32144268; PMCID: PMC7060199.
300. Zielinska KA, Katanaev VL. The Signaling Duo CXCL12 and CXCR4: Chemokine Fuel for Breast Cancer Tumorigenesis. *Cancers (Basel).* 2020;12(10). Epub 2020/10/25. doi: 10.3390/cancers12103071. PubMed PMID: 33096815; PMCID: PMC7590182.
301. Khaled WT, Choon Lee S, Stingl J, Chen X, Raza Ali H, Rueda OM, Hadi F, Wang J, Yu Y, Chin SF, Stratton M, Futreal A, Jenkins NA, Aparicio S, Copeland NG, Watson CJ, Caldas C, Liu P. BCL11A is a triple-negative breast cancer gene with critical functions in stem and progenitor cells. *Nat Commun.* 2015;6:5987. Epub 2015/01/13. doi: 10.1038/ncomms6987. PubMed PMID: 25574598; PMCID: PMC4338552.
302. Seachrist DD, Hannigan MM, Ingles NN, Webb BM, Weber-Bonk KL, Yu P, Bebek G, Singh S, Sizemore ST, Varadan V, Licatalosi DD, Keri RA. The transcriptional repressor BCL11A promotes breast cancer metastasis. *J Biol Chem.* 2020;295(33):11707-19. Epub 2020/06/25. doi: 10.1074/jbc.RA120.014018. PubMed PMID: 32576660; PMCID: PMC7450125.
303. Brown MS, Abdollahi B, Wilkins OM, Lu H, Chakraborty P, Ognjenovic NB, Muller KE, Jolly MK, Christensen BC, Hassanpour S, Pattabiraman DR. Phenotypic heterogeneity driven by plasticity of the intermediate EMT state governs disease progression and metastasis in breast cancer. *Sci Adv.* 2022;8(31):eabj8002. Epub 2022/08/04. doi: 10.1126/sciadv.abj8002. PubMed PMID: 35921406; PMCID: PMC9348802.